Response to reviewers' comments #1

We thank the reviewers for the constructive comments and suggestions, which are very positive to improve scientific content of the manuscript. We have revised the manuscript appropriately and addressed all the reviewers' comments point-by-point for consideration as below. The remarks from the reviewers are shown in black, and our responses are shown in blue color. All the page and line numbers mentioned following are refer to the revised manuscript without change tracked.

Reviewer

The authors present measurements of a number of important atmospheric species, including O3, NOx, HONO, SO2, HCHO and VOCs, made in an urban environment in Shanghai during a five month period between May and September 2018. These measurements are used to constrain box model simulations, using the Master Chemical Mechanism (MCM), to study the atmospheric oxidising capacity (AOC, the sum of the rates of VOC oxidation reactions by OH, O3, and NO3), OH reactivity (the inverse of the OH lifetime), and the OH chain length (the ratio of OH recycling to OH termination). The authors focus on three short periods during the five month observation period, and determine that the main species contributing to ozone formation during these periods were formaldehyde, toluene, ethylene, and m/p-xylene, which have lower concentrations than other species but have greater contributions in terms of reactivity.

While the analysis and results reported in the paper will be of general interest to the atmospheric science community, the manuscript is somewhat limited in its scope. It is not entirely clear why the three short periods out of the full measurement period have been chosen for detailed study, or whether any of these three periods are representative of typical conditions. Some further discussion regarding the choice of these three periods is necessary, particularly since the authors comment several times on measurements made over five months but focus only on six days.

R: Thanks for the constructive comments. This study was aiming to explore the atmospheric oxidation capacity and photochemical reactivity during the summertime and their potential relationship with ozone pollution. Therefore, the main reason for three short periods out of the full five-months measurements for detailed study was that these three cases are selected to represent the typical similarities and differences of atmospheric photochemistry under different ambient O_3 levels, i.e. ozone pollution, moderate condition and non-pollution according to the Ambient Air Quality Standards of China (GB3095-2012).

As shown in Table 1, the ozone hourly mean values for the selected cases were 65.13±27.16 ppbv, 46.12±21.14 ppbv and 23.95±11.89 ppbv, respectively. Besides ozone pollution, other trace gases like NO_X, HONO, HCHO and the radiation were also showing different characteristics among these three cases. Figure R1 shows the mean diurnal profiles of O_3, other trace gases and J_{NO2} for three selected cases. The overall trace gases were at low levels without significant diurnal variation in Case 3 under the low O_3 level, while their mixing ratios increased strongly and exhibited distinct diurnal

profiles in Case 1 and Case 2 with relatively high O_3 levels. The differences in pollutant mixing ratios (Figure S1) and meteorological parameters (Figure S2) among the three cases manifest the three different atmospheric environments, which are helpful to explore the causes of changes in atmospheric oxidation capacity and photochemical reactivity.

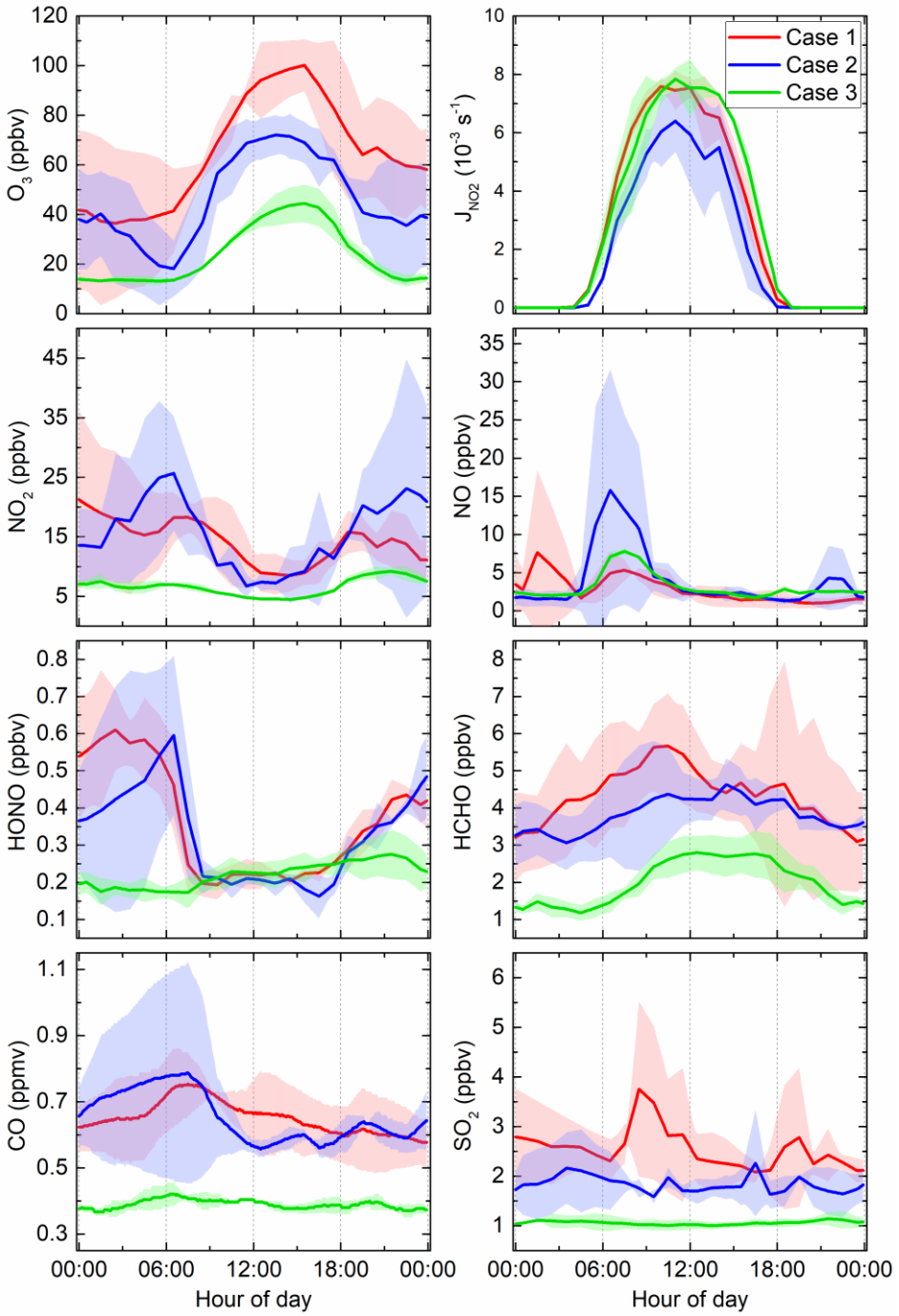

Figure R1. Mean diurnal profiles of measured trace gases mixing ratios for three cases. The shaded areas denote the standard deviation.

Details of the model simulations could also be expanded. How are model intermediates treated? Does the model include deposition terms to avoid build-up of high concentrations of model intermediates? If so, what were the deposition lifetimes and how do they impact the modelled AOC, OH reactivity and OH chain length? It would also be useful to include some discussion of the concentrations of modelled OH, HO2 and RO2 species.

R: Thanks for the suggestion. We have followed the comments to clearly describe the details of the model in the revised manuscript, such as whether to consider the deposition process and the boundary layer effect, and how they affect the model results. Please refer to Line 149-160.

Regarding to the deposition terms, it is regrettable that it was not taken into account previously, neither the accumulation of intermediates. Therefore, we have supplemented a simulation scenario considering the deposition process in order to discuss its impacts on intermediates. The loss of all unrestricted and model-generated species caused by the deposition is set as the accumulation of the deposition velocity of 0.01 m s^{-1} in the boundary layer (Santiago et al., 2016). Given that the boundary layer height (BLH) varied typically from 400 m at night to 1400 m in the afternoon during summer, which means that the lifetime of the model-generated species was ranged between ~11 h at night and ~40 h during the afternoon (Shi et al., 2015).

Afterwards, we have compared the simulated radical yields, AOC, OH reactivity, and OH chain length with or without considering the deposition process (see Table. R1). The simulated scenario without deposition is called Scenario N and the simulated scenario considering deposition is called Scenario Y. It can be clearly seen that the simulation results (OH, HO_2, RO_2, AOC, OH reactivity and OH chain length) without considering deposition term are enhanced to some extent compared with those with considering deposition term in three cases, especially for the intermediate (e.g. HO_2, RO_2), the results of Case 2 and Case 3 are increased by more than 50%. Therefore, it can be concluded that the deposition process has a great influence on the intermediates, which should be taken into account in the simulation.

Table R1. Summary of simulation results considering and not considering deposition process. All results are the average value of 06:00-18:00. N – Not considering deposition; Y – considering deposition.

Case 1	**OH** 10^6 mole cm^{-3}	**HO_2** 10^8 mole cm^{-3}	**RO_2** 10^8 mole cm^{-3}	**AOC** 10^8 mole cm^{-3} s^{-1}	**OH reactivity** s^{-1}	**OH chain length**
N	5.65±3.16	2.40±1.46	1.48±0.86	0.45±0.23	11.71±2.37	3.39±0.69
Y	5.27±3.13	1.99±1.29	1.09±0.70	0.42±0.22	11.48±2.16	3.17±0.63
(N-Y)/Y	7.21%	20.60%	35.78%	7.14%	2.00%	6.94%
Case 2	**OH** 10^6 mole cm^{-3}	**HO_2** 10^8 mole cm^{-3}	**RO_2** 10^8 mole cm^{-3}	**AOC** 10^8 mole cm^{-3} s^{-1}	**OH reactivity** s^{-1}	**OH chain length**
N	4.73±2.77	2.86±1.65	2.33±1.26	0.44±0.24	13.48±4.29	4.61±1.15
Y	4.05±2.68	1.87±1.18	1.34±0.82	0.37±0.22	12.86±3.80	3.75±0.90
(N-Y)/Y	16.79%	52.94%	73.88%	18.92%	4.82%	22.93%

Case 3	OH 10^6 mole cm^{-3}	HO_2 10^8 mole cm^{-3}	RO_2 10^8 mole cm^{-3}	AOC 10^8 mole cm^{-3} s^{-1}	OH reactivity s^{-1}	OH chain length
N	6.99±3.13	2.66±1.58	2.46±1.49	0.45±0.23	8.43±1.53	6.06±1.31
Y	6.12±3.37	1.76±1.22	1.51±1.08	0.40±0.23	8.41±1.21	4.96±1.08
(N-Y)/Y	14.22%	51.14%	62.91%	12.50%	0.24%	22.18%

Since the used deposition velocity and the BLH are empirical values from the previous literatures (Shi et al., 2015; Santiago et al., 2016), we have also carried out the sensitivity study on the deposition velocity and boundary layer height. The basic simulation scenario was set as deposition velocity of 0.01 m s^{-1} and the height of boundary layer varied from 400 m at night to 1400 m in the afternoon. Table R2 shows the settings of different simulation scenarios for the sensitivity study.

Table R2. Settings of simulation scenarios for sensitivity study.

Scenarios	deposition velocity (m s^{-1})	boundary layer-night (m)	boundary layer-noon (m)	Lifetime
Basic	0.01	400	1400	Night: 11 h; Day: 49 h
A	0.01	400	1000	Night: 11 h; Day: 28 h
B	0.01	400	2000	Night: 11 h; Day: 56 h
C	0.01	300	1400	Night: 8 h; Day: 39 h
D	0.01	500	1400	Night: 14 h; Day: 39 h
E	0.008	400	1400	Night: 14 h; Day: 49 h
F	0.012	400	1400	Night: 9 h; Day: 32 h

The sensitivity simulation results are summarized in Table R3, which demonstrated that the impacts of variations of deposition velocity and BLH on the modeling results could be negligible (i.e. < 3% in OH, HO_2, RO_2, AOC, OH reactivity and OH chain length).

Table R3. Summary of model sensitivity test results

Case 1	OH 10^6 mole cm^{-3}	HO_2 10^8 mole cm^{-3}	RO_2 10^8 mole cm^{-3}	AOC 10^8 mole cm^{-3} s^{-1}	OH reactivity s^{-1}	OH chain length
Basic	5.27±3.13	1.99±1.29	1.09±0.70	0.42±0.22	11.48±2.16	3.17±0.63
A	5.26±3.12	1.97±1.27	1.07±0.68	0.42±0.22	11.46±2.16	3.16±0.62
B	5.28±3.13	2.01±1.29	1.11±0.71	0.42±0.22	11.49±2.16	3.17±0.63
C	5.25±3.13	1.97±1.28	1.07±0.69	0.42±0.22	11.44±2.13	3.16±0.63
D	5.29±3.12	2.01±1.29	1.11±0.70	0.42±0.22	11.50±2.18	3.17±0.62
E	5.30±3.12	2.02±1.29	1.12±0.71	0.42±0.22	11.51±2.18	3.18±0.62
F	5.25±3.12	1.97±1.28	1.07±0.69	0.42±0.22	11.45±2.14	3.16±0.63
(A-Basic)/Basic	-0.23%	-0.90%	-1.87%	-0.48%	-0.17%	-0.22%
(B-Basic)/Basic	0.21%	0.79%	1.64%	0.43%	0.15%	0.20%
(C-Basic)/Basic	-0.42%	-0.92%	-1.78%	-0.84%	-0.29%	-0.30%
(D-Basic)/Basic	0.33%	0.74%	1.45%	0.67%	0.23%	0.24%

(E-Basic)/Basic	0.46%	1.26%	2.54%	0.95%	0.33%	0.37%
(F-Basic)/Basic	-0.39%	-1.05%	-2.10%	-0.79%	-0.27%	-0.31%
Case 2	**OH** 10^6 mole cm^{-3}	**HO_2** 10^8 mole cm^{-3}	**RO_2** 10^8 mole cm^{-3}	**AOC** 10^8 mole cm^{-3} s^{-1}	**OH reactivity** s^{-1}	**OH chain length**
basic	4.05±2.68	1.87±1.18	1.34±0.82	0.37±0.22	12.86±3.80	3.75±0.90
A	4.04±2.68	1.84±1.16	1.31±0.80	0.37±0.22	12.83±3.80	3.73±0.90
B	4.07±2.69	1.89±1.19	1.37±0.83	0.37±0.22	12.89±3.80	3.75±0.90
C	4.02±2.68	1.84±1.17	1.31±0.81	0.36±0.22	12.80±3.76	3.73±0.90
D	4.08±2.68	1.89±1.19	1.37±0.83	0.37±0.22	12.92±3.83	3.76±0.90
E	4.09±2.69	1.91±1.20	1.38±0.84	0.37±0.22	12.94±3.83	3.77±0.90
F	4.03±2.68	1.84±1.16	1.31±0.80	0.36±0.22	12.81±3.77	3.73±0.90
(A-Basic)/Basic	-0.38%	-1.30%	-2.06%	-0.67%	-0.23%	-0.28%
(B-Basic)/Basic	0.35%	1.17%	1.85%	0.63%	0.21%	0.26%
(C-Basic)/Basic	-0.76%	-1.52%	-2.22%	-1.38%	-0.50%	-0.49%
(D-Basic)/Basic	0.62%	1.26%	1.84%	1.12%	0.40%	0.40%
(E-Basic)/Basic	0.86%	2.08%	3.13%	1.57%	0.55%	0.57%
(F-Basic)/Basic	-0.68%	-1.63%	-2.47%	-1.22%	-0.44%	-0.46%
Case 3	**OH** 10^6 mole cm^{-3}	**HO_2** 10^8 mole cm^{-3}	**RO_2** 10^8 mole cm^{-3}	**AOC** 10^8 mole cm^{-3} s^{-1}	**OH reactivity** s^{-1}	**OH chain length**
basic	6.12±3.37	1.76±1.22	1.51±1.08	0.40±0.23	8.41±1.21	4.96±1.08
A	6.10±3.37	1.74±1.21	1.48±1.06	0.40±0.23	8.39±1.22	4.95±1.08
B	6.14±3.37	1.78±1.23	1.54±1.10	0.41±0.23	8.42±1.21	4.97±1.08
C	6.09±3.39	1.74±1.22	1.49±1.08	0.40±0.23	8.38±1.20	4.94±1.08
D	6.14±3.35	1.77±1.22	1.53±1.08	0.41±0.23	8.43±1.23	4.97±1.08
E	6.16±3.35	1.79±1.23	1.55±1.10	0.41±0.23	8.44±1.22	4.97±1.08
F	6.09±3.38	1.74±1.21	1.48±1.07	0.40±0.23	8.38±1.20	4.94±1.08
(A-Basic)/Basic	-0.30%	-1.44%	-2.08%	-0.59%	-0.25%	-0.20%
(B-Basic)/Basic	0.26%	1.22%	1.76%	0.52%	0.20%	0.18%
(C-Basic)/Basic	-0.47%	-0.93%	-1.30%	-0.85%	-0.37%	-0.28%
(D-Basic)/Basic	0.38%	0.79%	1.10%	0.70%	0.28%	0.23%
(E-Basic)/Basic	0.56%	1.60%	2.28%	1.05%	0.43%	0.35%
(F-Basic)/Basic	-0.46%	-1.33%	-1.90%	-0.85%	-0.36%	-0.28%

Finally, the basic simulation scenario of deposition velocity of 0.01 m s^{-1} and the height of boundary layer varied from 400 m at night to 1400 m in the afternoon were used in the simulation for the three cases study. And the relevant simulated results and discussion were replaced in the manuscript.

Minor comments are given below.
Page 1, line 19: 'Five months of observation' to 'Five months of observations'.
R: The 'observation' has been corrected to 'observations'. Please refer to Line 19.

Page 1, line 21: State clearly what the 92.2 % refers to, presumably of the observation

period?
R: Ambient Air Quality Index (AQI) was less than 100 for 141 days during the whole observation period, accounting for 92.2% of the total observational period. We have rewritten this sentence as 'Five months of observations from 1 May to 30 September 2018 showed that the air quality level is in lightly polluted and even worse (Ambient Air Quality Index, AQI>100) for 12 days, of which ozone is the primary pollutant for 10 days, indicating ozone pollution is the main challenge of air quality in Shanghai during summer of 2018.'. The detailed statement can be found on Line 19-22.

Page 1, line 28: '... of the OH lifetime'.
R: We have added 'the' before 'OH lifetime'. Please refer to Line 29.

Page 1, line 29: 'condition' to 'conditions'.
R: We have corrected it. Please refer to Line 30.

Page 1, line 31: 'the HONO photolysis' to 'HONO photolysis' and 'the O3 photolysis' to 'O3 photolysis'.
R: We have followed the comments and deleted both 'the'. Please refer to Line 32.

Page 1, line 32: The statement regarding the reaction with NO2 completely dominating seems over-exaggerated, there are surely some other contributions. 'radicals termination' to 'radical termination', and 'reactions of radical-radical' to 'radical-radical reactions'.
R: Thanks for the suggestion. According to the results in this study, the reaction with NO_2 accounts for 98% of the HO_x sinks during 05:30-11:00 in Case 1, and the contribution of reaction with NO_2 to the HO_x sinks reaches 98.9% and 99.7% during 05:30-09:00 in Case 2 and 3, respectively, suggesting that the cross-reactions between radicals contribute only nearly 1% in three cases at rush hour. Therefore, it can be concluded that the reaction with NO_2 are the most important sink of radicals during the morning rush hour. We have revised the over-exaggerated expression. Please refer to Line 32-33.

Page 2, line 56: Hydroperoxy is preferred over hydroperoxyl.
R: Thanks for the suggestion. The 'hydroperoxy' has been replaced with 'hydroperoxyl'. Please refer to Line 57.

Page 3, line 76: There are more recent measurements in London than those referenced.
R: Thanks for the information. We have reviewed the related literatures, e.g. Whalley et al. (2016; 2018). In these recent measurements in London, it is reported that OH reactivity was 15~27 s^{-1} and HONO photolysis dominated OH source in central London in the summer of 2012. We have also cited in the revised manuscript, please refer to Line 76.

Page 3, line 85: 'a emissions' to 'an emissions'.
R: We have corrected 'a' to 'an'. Please refer to Line 91.

Page 3, line 98: 'suburban' to 'suburban areas'.
R: The 'suburban' has been corrected to 'suburban areas'. Please refer to Line 104.

Page 4, line 111: ‘vehicle’ to ‘vehicles’.
R: We have made the revision. Please refer to Line 117.

Page 4, line 113: Please expand on what you mean by a clean environment. Clean air? Free of rubbish waste?
R: Thanks for the suggestion. We have rewritten this sentence as ‘The campus itself is relatively clean air condition without significant sources of air pollutants, mainly is affected by traffic emissions from viaducts and residential areas nearby.’. Please refer to Line 119-120.

Page 4, line 117: Please clarify what is analyzed further? How is the initial analysis performed? Why is further analysis necessary and what does it achieve?
R: We are apologized for the improper statements leading misunderstanding. Here we restructured this sentence like “O_3 and NO were measured by the short-path DOAS (Differential Optical Absorption Spectroscopy) instrument with a light path of 0.15 km and time resolution of 1 min. The fitting windows of them are 250-266 nm and 212-230 nm, respectively.” Please refer to line 122-124.

Page 4, line 122: ‘Photolysis frequency of...’ to ‘The photolysis frequency of...’.
R: We have added ‘the’ before ‘photolysis frequency of...’. Please refer to Line 128.

Page 5, line 135: How were deposition rates implemented in the model, if at all? What was the impact of these?
R: We have supplemented the discussion on the impacts of the deposition process on the simulation results and related sensitivity study. As shown in Tables R1 and R3, the results indicated that neglecting the deposition process can cause build-up of high concentrations of model intermediates. So we have re-simulated these three cases with consideration of the deposition process and further discussed atmospheric photochemistry for different ozone levels in Shanghai in the revised manuscript. Therefore, the corresponding figures and contents in the manuscript have been replaced. Please also refer to the Supplement.

Page 5, line 137: ‘last’ to ‘latest’.
R: We have corrected it and please refer to Line 143.

Page 5, line 144: How reliable is the use of measured JNO2 to scale calculated JO1D? They are known to be affected differently by cloud cover.
R: Thanks for the suggestion. The impacts of cloud cover on J_{NO_2} and J_{O^1D} are considerably complex. Crawford et al. (2003) reported that the observed UV actinic flux under cloudy conditions that unoccluded the sun disk is 40% higher than the clear sky value. When the solar disk is occluded, reductions in actinic flux appear to vary inversely with cloud fraction in some instances. In the broken cloud field, the fluctuation ranges of J_{O^1D} and J_{NO_2} are different, and the change of J_{NO_2} is larger than that of J_{O^1D}. Monks et al. (2004) research also revealed that the photolysis frequencies in the UVB and UVA do not vary linearly under different atmospheric conditions in a cloudy field. Cloud cover and its quantitative effects on UVA and UVB are important for the correction of J_{O^1D} from the measured J_{NO_2} scaling. Whalley et al. (2018) used the ratio of the model calculated J_{O^1D} in the clear sky to the observed J_{O^1D} to account

for clouds and to determine photolysis rates of other photolabile species.
Since we have not measured J_{O1D} but only for J_{NO2}, we are not able to use this method to determine cloud cover. However, we try to seek an approximate quantitative relationship between the fluctuation magnitude of J_{NO2} and J_{O1D} in cloudy days compared to clear sky:

$$\%\ \text{reduction or enhancement}\ in\ j(X) = \left(\frac{j(X)_{clear} - j(X)_{cloudy}}{j(X)_{clear}}\right) \times 100 \qquad \text{(E1)}$$

$$\%j(O^1D) \approx 1.08\%j(NO_2) - 0.12 \qquad \text{(E2)}$$

Where $\%j(O^1D)$ and $j(NO_2)$ is calculated by the equation (E1). Please note that the equation (E2) here is an approximate relationship between $\%j(O^1D)$ and $\%j(NO_2)$ on a certain summer day in the study by Monks et al. (2004).
In addition, it is also necessary to correct the cloudy day values of J_{O1D} considering the changes in overhead ozone column between the cloudy and clear day. The ratio of the overhead ozone column of clear sky day to that of cloudy day is used as the calibration coefficient *k*. The J_{O1D} of cloudy day can be calculated by equation (E3):

$$j(O^1D)_{cloud} = kj(O^1D)_{clear}\left(1 - \%j(O^1D)\right) \qquad \text{(E3)}$$

Table R4 lists the overhead total ozone column and calibration coefficient *k* for three cases, in which total ozone column data taken from OMI (download from https://disc.gsfc.nasa.gov/datasets/OMDOAO3_003/summary) and taken for 121.51°E, 31.34°N with a radius of 20 km at 13:45 local overpass time. The OMI data from September 2nd to 4th are missing due to no data available after the filtering (filtering conditions: solar zenith angles < 70°, cloud cover < 0.5, pixels were not affected by the row anomaly are used), and we took the mean value of available total ozone column from May to October as the reference data (294.262±18.240 DU). Considering that the total column concentration was relatively low in September, the final total ozone column of 290.000 DU was used.

Table R4. Daily ozone total column for three cases in Shanghai. Data taken from OMI. NOTE: Missing data on September 2, 3 and 4.

	Date	O_3 total column/DU	k
Case 1	11-Jun	341.955	0.874
	12-Jun	319.755	0.935
	13-Jun	321.510	0.929
Case 2	2-Sep	*290.000*	*1.030*
	3-Sep	*290.000*	*1.030*
	4-Sep	*290.000*	*1.030*
Case 3	12-Jul	277.529	1.077
	13-Jul	299.974	0.996
	14-Jul (clear sky)	298.841	1.000

In this study, we have used the observed J_{NO2} data and the J_{O1D} data scaled by J_{NO2}. As shown in Figure R2, it is a clear sky on July 14, 2018 in Case 3. The J_{NO2} on this day and the J_{O1D} obtained by scaling J_{NO2} can be considered as real or 'measured' $j(X)_{clear}$. The images of sky conditions for the remaining days of these three cases are shown in

Figure R3 (the images on July 12 are missing).

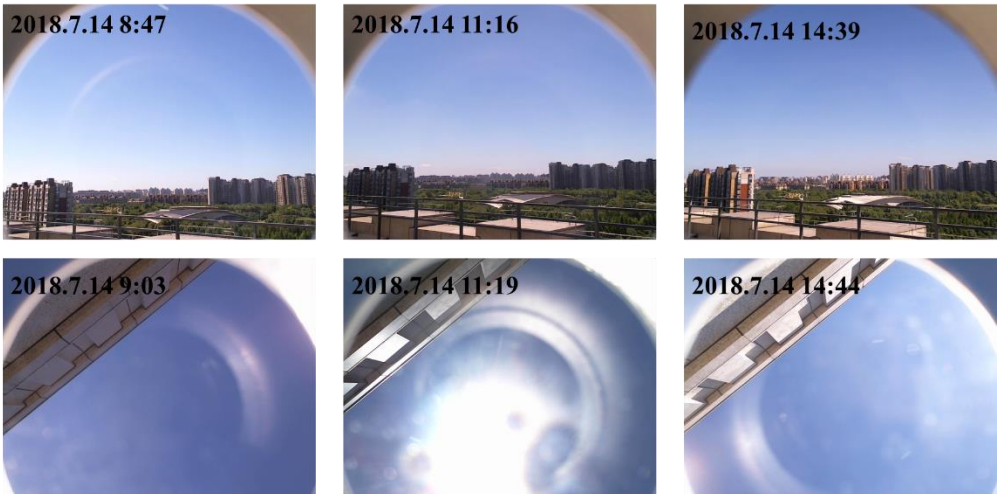

Figure R2. Sky images on July 14, 2018

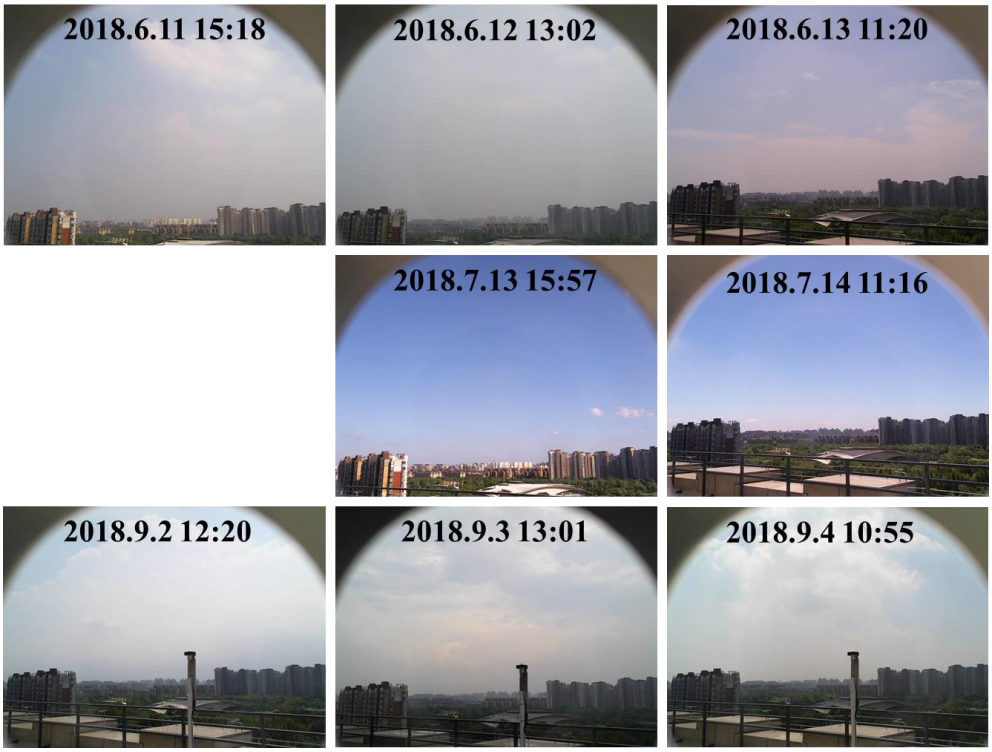

Figure R3. Representative sky images in three cases

Therefore, we can determine $\%j(NO_2)$ by the difference between J_{NO_2} on clear sky and cloudy days, and then calculate the $J_{O^1Dcloudy}$ via equation (E3). Figure R4 shows the difference of calibrated J_{O^1D} and J_{O^1D} without calibration for clouds in three cases. Compared with the J_{O^1D} scaled by the measured J_{NO_2} directly, the calibrated J_{O^1D} of the three cases changed by -0.75%, 32.22%, and 7.97%, respectively.

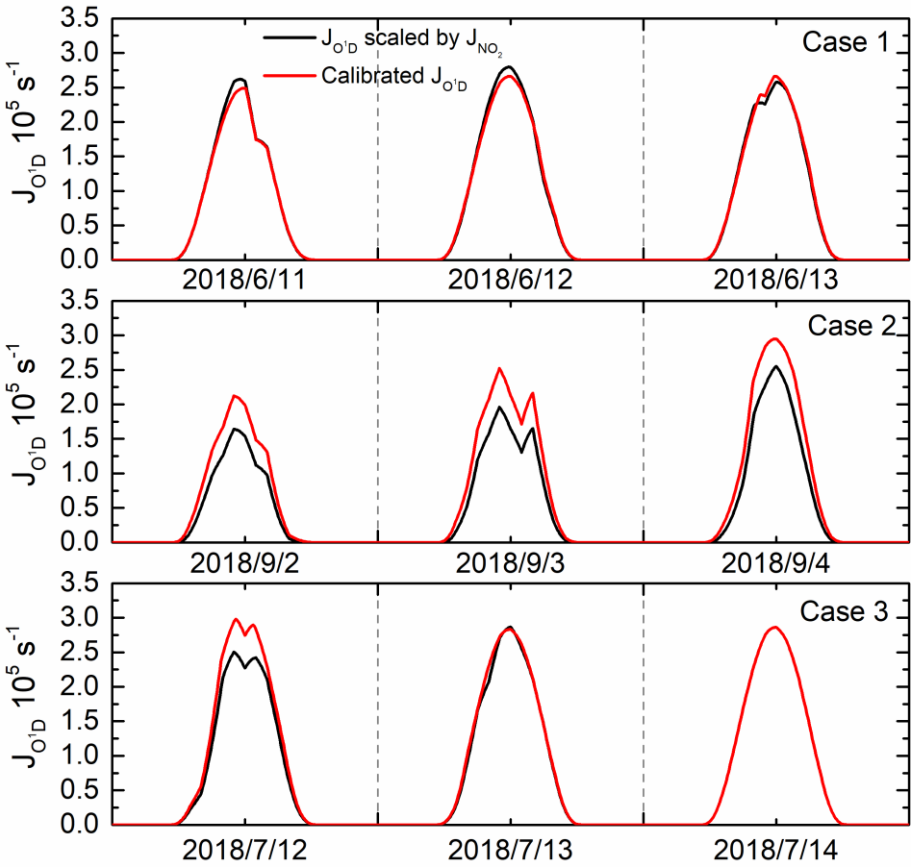

Figure R4. Comparison of calibrated J_{O1D} for cloud covers and J_{O1D} without calibration scaled directly by J_{NO_2} in three cases

Then, we have ran the simulation scenarios G with the calibrated J_{O1D} and compared the results with simulation scenarios Basic, as listed in Table R5. The impact of J_{O1D} on the simulation results of Case 1 was negligible, and the impact on the simulation results of Case 3 was less than 3%. In Case 2 with the largest change in J_{O1D}, the effects on radicals and AOC were less than 10%, and the effects on OH reactivity and OH chain length could be ignored.

Table R5. Summary of simulation results with or without J_{O1D} calibration

Case 1 Scenarios	J_{O1D} 10^{-5} s^{-1}	OH 10^6 mole cm^{-3}	HO_2 10^8 mole cm^{-3}	RO_2 10^8 mole cm^{-3}	AOC 10^8 mole cm^{-3} s^{-1}	OH reactivity s^{-1}	OH chain length
Basic	1.32±0.93	5.28±3.12	1.99±1.28	1.09±0.70	0.42±0.22	11.48±2.16	3.17±0.63
G	1.31±0.90	5.26±3.10	1.99±1.29	1.09±0.70	0.42±0.22	11.48±2.16	3.17±0.63
Discrepancy	-0.75%	-0.40%	0	0	0	0	0
Case 2 Scenarios	J_{O1D} 10^{-5} s^{-1}	OH 10^6 mole cm^{-3}	HO_2 10^8 mole cm^{-3}	RO_2 10^8 mole cm^{-3}	AOC 10^8 mole cm^{-3} s^{-1}	OH reactivity s^{-1}	OH chain length
Basic	0.90±0.72	4.06±2.68	1.88±1.18	1.35±0.82	0.37±0.22	12.96±3.89	3.77±0.89
G	1.19±0.89	4.41±2.94	2.03±1.29	1.46±0.89	0.40±0.24	12.84±3.80	3.74±0.89
Discrepancy	32.22%	8.62%	7.98%	8.15%	8.11%	-0.93%	-0.80%
Case 3 Scenarios	J_{O1D} 10^{-5} s^{-1}	OH 10^6 mole cm^{-3}	HO_2 10^8 mole cm^{-3}	RO_2 10^8 mole cm^{-3}	AOC 10^8 mole cm^{-3} s^{-1}	OH reactivity s^{-1}	OH chain length

Basic	1.40±0.97	6.13±3.36	1.76±1.22	1.51±1.08	0.40±0.23	8.41±1.21	4.96±1.08
G	1.49±0.97	6.22±3.44	1.78±1.23	1.53±1.09	0.41±0.24	8.41±1.21	4.95±1.08
Discrepancy	7.98%	1.47%	1.14%	1.32%	2.50%	0	-2.02%

Based on the discussion above, it is found that the calibrated J_{O^1D} considering clouds condition deviated from the J_{O^1D} directly scaled by the measured J_{NO_2} for -0.75%, 32.22%, and 7.97% during these three cases. Additionally, the modelling results shows the limited impacts of J_{O^1D} calibration for clouds on the results and has not changed the main conclusions for the three cases in this study.
Due to the particularity in the approximation method of equation (E2) and uncertainty on ozone column data, we think this calibration method is not an accurate way to calibrate J_{O^1D} for this study. Therefore, we decided to use the J_{O^1D} scaled by the measured J_{NO_2} as the O_3 photolysis frequency in three cases. We have also mentioned this impacts in the manuscript. Please refer to Line 152-153 and the Supplement.

Page 5, line 155: There are better references to provide for the definition of OH reactivity (similarly for OH chain length). The equation given could be generalized more widely instead of showing several species explicitly and 'other'.
R: We have found a better equation of OH reactivity from previous study (Whalley et al., 2016) and have cited it as $k_{OH} = \sum_i k_{OH+X_i}[X_i]$, where $[X_i]$ represents the concentration of species (VOC, NO_2, CO etc.) which react with OH and k_{OH+X_i} is the corresponding reaction rate coefficients. Please refer to Line 170-174.

Page 6, line 170: 'pollutants' to 'pollutant'.
R: Thanks for the suggestion. The 'pollutants' has been corrected to 'pollutant'. Please refer to Line 187.

Page 6, line 173: 'concentrations' to 'mean concentrations'. It would be helpful to include the standard deviation and median (and elsewhere where mean concentrations are referred to).
R: We have followed the suggestion and replaced 'concentrations' with 'mean mixing ratios' (also pointed by Reviewer #2 to change the concentration to mixing ratio), as well as added standard deviation and elsewhere in the manuscript. Please refer to Line 190 and elsewhere.

Page 7, Figure 1 caption: 'of Shanghai' to 'in Shanghai'.
R: Thanks for the suggestion. The 'of Shanghai' has been replaced with 'in Shanghai'. Please refer to Line 199.

Page 7: Are any of the cases chosen for detailed study representative of typical behavior?
R: Please also refer to the responses to the main comments #1. As shown in Table 1, the ozone hourly mean values for the selected cases were 65.13±27.16 ppbv, 46.12±21.14 ppbv and 23.95±11.89 ppbv, respectively, representing ozone pollution, moderate condition and non-pollution. Meanwhile, the five month observations shows that ozone is the primary air pollutant for the air quality degraded during summer of 2018 in Shanghai. So we have selected these three cases to explore the atmospheric oxidation capacity and photochemical reactivity during the summertime and their potential relationship with ozone pollution. In addition, the comparison of other trace gases is

shown in Figure R1, showing the different characteristics of the three cases.

Page 7, line 189/Figure 1: The differences in wind speed are difficult to see in the figure. 'the unfavourable diffusion condition is' to 'unfavourable diffusion conditions are'.
R: Thanks for the suggestion. We have redrawn the Figure 1 to ensure a clear view of the wind speed. And the 'the unfavourable diffusion condition is' has been corrected to 'unfavourable diffusion conditions are'. Please refer to Line 208.

Page 7, line 192: 'lead' to 'leads'. 'the JNO2' to 'when the JNO2'.
R: The 'the J_{NO_2}' have been corrected to 'when the J_{NO_2}'. The 'lead' does not need to be modified in the revised manuscript. Please refer to Line 212.

Page 8, line 204: 'an average total VOCs' to 'average total VOC'.
R: Thanks for the suggestion. We have corrected the 'an average total VOCs' to 'average total VOC'. Please refer to Line 223-224.

Page 9, line 213: 'highest concentrations in alkanes' to 'highest concentration alkanes' and 'the main species in alkenes' to 'the main alkene species'.
R: Thanks for the suggestion. The 'highest concentration in alkanes' and the 'the main species in alkenes' have been corrected to 'highest mixing ratio alkanes' and 'the main alkene species' (also pointed by Reviewer #2 to change the concentration to mixing ratio), respectively. Please refer to Line 230-231.

Page 9, line 215: Define the meaning of 'maximum incremental reactivity'.
R: Thanks for the suggestion. We have defined the MIR in the calculation formula of the OFP in Line 433. And we have followed the suggestion and added the definition of maximum incremental reactivity in the table caption here. Please refer to Line 234-236.

Page 10, line 220: 'due to acetylene is' to 'since acetylene is' or 'due to acetylene being'. Would it be more sensible to group as saturated aliphatic hydrocarbons and unsaturated aliphatic hydrocarbons?
R: Thanks for the suggestion. The 'due to acetylene is' has been corrected to 'due to acetylene being'. Considering that both acetylene and alkenes are unsaturated aliphatic hydrocarbons, which have unsaturated bonds, acetylene and other species with carbon-carbon double bonds are classified as alkenes category for the convenience of statistics. As pointed by the Reviewer #2, it should be clarified that the reactivity of acetylene with OH is far less than that of alkenes with OH, and be noted in the footnote of the table.
We have rewritten this sentence into 'Due to acetylene being similar in nature to alkenes, acetylene is classified into the alkenes category. It should be noted that the reactivity of acetylene with OH is far less than that of alkenes with OH'. Please refer to Line 238-239.

Page 10, section 3.2: What was the AOC in Berlin?
R: Geyer et al. (2001) reported that the maximum AOC value reached 1.4×10^{7} molecules cm^{-3} s^{-1} in Berlin and much lower than that of this study. And we have added relevant data in the revised manuscript. Please refer to Line 245.

Page 11, Figure 2: It would be interesting to be able to see the nighttime data as well,

perhaps a log scale for the y-axis or a separate plot?
R: We have followed the suggestion and drew a separate plot to show the nighttime data series clearly in the Supplement (see Figure S3).

Page 11, line 251: 'lower than that of Case 2 and Case 3' should be 'lower than that of Case 1 and Case 2'? Do the calculated losses of OH include reactions of OH with model generated oxidation intermediates or are the values reported given for observed concentrations only? If model generated oxidation intermediates are included, what are the impacts of deposition rates on the calculated reactivity? On page 12 it is stated that measured species are used to calculate OH reactivity, but intermediates from the model simulations could be included. If they haven't been, why not?
R: We are really sorry for the mistakes, which have been corrected. Please refer to Line 271. The calculated losses of OH just include reactions of OH with the species observed previously.
The influence of the deposition process on the simulation results was discussed in the response to main comments #1. After comparing the simulation results with or without consideration of the deposition process, it is definitely necessary to consider the deposition process in the simulation and re-discuss the corresponding results, which are updated in the revised manuscript. In the revised manuscript, the intermediates from the model simulations were included in the discussion on OH reactivity. Please refer to Line 265-287.

Page 12, line 258: There are also measurements of OH reactivity in urban regions in London.
R: Thanks for the information. We have reviewed the related reference presented by Whalley et al. (2018), in which the OH reactivity has been measured to be 15~27 s^{-1} in central London in the summer of 2012 during the Clean air for London project (ClearfLo). We have also cited it in Line 280.

Page 12, Figure 3: The y scale chosen is not ideal, the plots would be clearer if a smaller scale were used.
R: Thanks for the suggestion. We have chosen a smaller y-scale to redraw Figure 3.

Page 13, line 277: 'Case 1 about' to 'Case 1 was about'. The statement 'may be caused' could be strengthened – the data are there to show this either way without conjecture.
R: Thanks for the suggestion. The 'Case 1 about' has been corrected to 'Case 1 was about'. Please refer to Line 297-298. Data for trace gases and VOCs are shown in Table 1. We have rewritten this sentence into 'This is caused by the higher VOCs levels of 29.73±12.10 ppbv during Case 2 as compared to Case 1 of about 15% lower'. Please refer to Line 299-300.

Page 13, line 284: Do the authors mean to say that OVOCs are the main contribution or the second highest contribution? The use of 'predominant' indicates they are the main contributions, but the following discussion states alkenes represent the largest contribution.
R: As we have recalculated the OH reactivity including model-generated intermediate species, OVOCs were the highest contribution to OH reactivity for total NMVOCs. We still use this predominant to describe the important contribution of OVOC to OH reactivity, but to modify the description of the contribution of alkenes to OH reactivity.

Please refer to Line 303-309.

Line 13, line 290: Please quantify the statements 'similar' and 'negligible'.
R: Thanks for the suggestion. In three periods, the contributions of aromatics and alkanes to OH reactivity were comparable, both in the range of 0.3~0.6 s^{-1}, accounting for 10%~20%. And the contribution of other VOCs to OH reactivity was negligible, and the contribution ratio was only 0.4% or less. We have quantified the statement 'similar' and 'negligible' in Line 309-312.

Line 13, line 291: Are there any alcohol concentrations in similar locations? Do the authors expect significant contributions from these species?
R: The observed alcohol data are rarely reported in Shanghai and we have only found few useful data for reference. The data observed by Cai et al. (2010) showed that the mean mixing ratio of isopropyl alcohol is 0.27±1.08 ppbv and the fluctuation range is 0 ~ 14.32 ppbv from July 2006 to February 2010 in Shanghai. The mean mixing ratio of isopropyl alcohol measured by Zhang et al. (2018) reached 2.3 pbbv in Nantong, Jiangsu Province, situated to north of Shanghai, ranking third among the 105 VOCs measured. And the paper reported that the OFP of alcohols reached about 3.5 μg m^{-3}, which indicated that alcohols have high activity and contribute to OH reactivity.
We have re-calculated the OH reactivity including the simulated intermediate species. The contribution of OVOCs to OH reactivity was 1.77 s^{-1}, 2.05 s^{-1} and 1.26 s^{-1}, while the OH reactivity of OVOCs calculated by considering only the measured species was 1.28 s^{-1}, 1.43 s^{-1}, and 0.82 s^{-1} in three cases, respectively. So we expect that unmeasured species (e.g. alcohols) may cause underestimation the contribution of OVOCs to OH reactivity. In the revised manuscript, the model-calculated OH reactivity include the contribution of the simulated intermediate species to OH reactivity.

Page 14, line 305: 'evaluating the HOx' to 'evaluating HOx'.
R: We have deleted 'the' before 'HOx'. Please refer to Line 324.

Page 14, line 310: 'within' to 'less than'?
R: The 'within' has been replaced with 'less than'. Please refer to Line 329.

Page 15, line 322: Why were contributions from peroxides excluded?
R: The contribution of peroxides to HO_X is limited. For example, the rates of H_2O_2 to HO_x in three cases were 7.65×10^4 molecules cm^{-3} s^{-1}, 6.98×10^4 molecules cm^{-3} s^{-1} and 4.28×10^4 molecules cm^{-3} s^{-1}, which are two orders of magnitude smaller compared to O_3, HONO, HCHO photolysis, and alkenes ozonolysis. So there's no discussion here.

Page 15, line 324: 'sinks of HOx was' to 'sinks of HOx were'.
R: Thanks for the suggestion. The 'sinks of HO_x was' has been corrected to 'sinks of HO_x were'. Please refer to Line 345.

Page 15, line 331: 'generation rate of HOx was' to 'generation rates of HOx were'.
R: Thanks for the suggestion. The 'generation rate of HO_x was' has been corrected to 'generation rates of HO_x were'. Please refer to Line 352.

Page 15, line 332: 'loss rate was' to 'loss rates were'. Please include 'and' before the final value.

R: Thanks for the suggestion. The 'loss rate was' has been corrected to 'loss rates were'. And we have rewritten this sentence into 'while the average loss rates were $1.34\pm0.7\times10^7$ molecules cm^{-3} s^{-1}, $1.00\pm0.55\times10^7$ molecules cm^{-3} s^{-1} and $0.8\pm0.52\times10^7$ molecules cm^{-3} s^{-1}'. Please refer to Line 353-354.

Page 15, line 336: What were the concentrations of HONO and O3? Did the HONO concentration change significantly between cases?
R: As listed in Table 1, the mean mixing ratios of O_3 were 65.13±27.16 ppbv, 46.12±21.14 ppbv and 23.95±11.89 ppbv in three cases, respectively, while the mean mixing ratios of HONO were 0.36±0.16 ppbv, 0.32±0.17 ppbv and 0.22±0.05 ppbv, respectively. In addition, the mean diurnal profiles of O_3 and HONO are shown in figure R1. HONO were at low levels without significant diurnal variation in Case 3 under the low O_3 level, however, its mixing ratios increased strongly and exhibited distinct diurnal profiles in Case 1 and Case 2 of relatively high O_3 levels.

Page 16: It would be helpful to include some discussion of the concentrations of OH, HO2 and RO2, and any details of the main RO2 species in the model, with comparison to measured values in similar locations. Some discussion of the nighttime chemistry would also be of interest.
R: We have discussed the simulation results with deposition process in the revised manuscript instead of the previous simulation results without deposition process. Since the Sect 3.3 focuses on the discussion about sources and sinks of HO_x radicals, we have followed the suggestion and supplemented a discussion of the concentration of HO_x and their comparison with measured values from other sites in the revised manuscript, and won't discuss here for RO_2. Please refer to Line 387-398.
Since this article mainly discusses daytime photochemistry and there is no observation of NO_3 and N_2O_5 related to nighttime photochemistry, we have not discussed nighttime chemistry so much here. But we also mentioned the important contribution of NO_3 to AOC during nighttime in this study. Please refer to Line 254-256. In the future, we can strengthen the observations at night to better discussion on nighttime chemistry.

Page 17, line 373: 'VOCs concentrations' to 'VOC concentrations'.
R: The 'VOCs concentrations' has been corrected to 'VOC mixing ratios' (also pointed by Reviewer #2 to change the concentration to mixing ratio). Please refer to Line 410.

Page 18, line 386: 'VOC groups' to 'VOC group'.
R: The 'VOC groups' has been corrected to 'VOC group'. Please refer to Line 412.

Page 18, line 390: 'OVOCs shows its significant contribution' to 'OVOCs show significant contributions'.
R: Thanks for the suggestion. The 'OVOCs shows its significant contribution' has been corrected to 'OVOCs show significant contributions'. Please refer to Line 428.

Page 18, line 401: Is this 14.6 % of the total NMVOC concentration?
R: Yes, during Case 1, the mean mixing ratio of NMVOC was 25.31±6.16 ppbv, and the average mixing ratio of acetone was 3.69±0.78 ppbv, accounting for 14.6%. We have clarified, and please refer to Line 439-440.

Page 20, line 430: 'increase of radicals level' to 'increase of radical levels'.

R: The ‘increase of radicals level’ has been corrected to ‘increase of radical levels’. Please refer to Line 468.

Page 20, line 433: If each radical could generate more O3, why is the O3 level lower?
R: After in-depth relevant literature review, we try to explain the relationship between higher O_3 concentration and shorter chain length as following.
The ratio of the rate of HO_x cycling reactions to HO_x termination is called the chain length, as in equation (E4) (Martinez et al., 2003). When the termination reaction of HO_x is dominated by the reaction of NO_2 and OH, the definition can be simplified as equation (E6).

$$\text{Chain Length} = \frac{[OH]k_{OH} - L(HO_x)}{L(HO_x)} \quad \text{(E4)}$$

$$L(HO_x) = k_{OH+NO_2}[OH][NO_2] + 2k_{HO_2+HO_2}[HO_2]^2 + 2k_{OH+HO_2}[OH][HO_2] + 2k_{HO_2+RO_2}[HO_2][RO_2] + 2k_{RO_2+RO_2}[RO_2][RO_2] \quad \text{(E5)}$$

$$OH\ \ Chain\ \ Length = \frac{k_{OH}[OH] - k_{OH+NO_2+M}[OH][NO_2]}{k_{OH+NO_2+M}[OH][NO_2]} \quad \text{(E6)}$$

During daytime, the greater the chain length, the greater the amount of O_3 produced per NO_X molecule converted to HNO_3, rather than the more ozone produced per OH radical. In the profile of OH chain length in Figure 5, the OH chain length in Case 3 with the lowest ozone mixing ratio is the largest, meaning that per NO_X converted into HNO_3 produces more O_3, but the daytime NO_X mixing ratio in Case 3 is almost half that of Case 1 and 2 (see Figure R1), causing ozone mixing ratios to be lower than Case 1 and 2. In addition, we found that the OH chain length was opposite to the ozone level, and the explanation given was also due to the lower NO_X mixing ratios in previous studies (Mao et al., 2010; Ling et al., 2014).

Data availability: It would be preferable to host the data at a secure and available site/database rather than needing to contact the corresponding author.
R: Since the measured VOC data were provided by another group, it is not suitable to be published by us. We are very willing to provide the data of DOAS measurements and modelling simulation for scientific aims with contacts from others, and the communication for the VOCs data availability.

References

Cai, C. J., Geng, F. H., Tie, X. X., Yu, Q., Peng, L., and Zhou, G. Q.: Characteristics of ambient volatile organic compounds (VOCs) measured in Shanghai, China, Sensors (Basel), 10, 7843-7862, https://doi.org/10.3390/s100807843, 2010.

Crawford, J., Shetter, R. E., Lefer, B., Cantrell, C., Junkermann, W., Madronich, S., and Calvert, J.: Cloud impacts on UV spectral actinic flux observed during the International Photolysis Frequency Measurement and Model Intercomparison (IPMMI), J. Geophys. Res., 108, https://doi.org/10.1029/2002jd002731, 2003.

Geyer, A., Alicke, B., Konrad, S., Schmitz, T., Stutz, J., and Platt, U.: Chemistry and oxidation capacity of the nitrate radical in the continental boundary layer near Berlin, J. Geophys. Res.-Atmos., 106, 8013-8025, https://doi.org/10.1029/2000jd900681, 2001.

Ling, Z. H., Guo, H., Lam, S. H. M., Saunders, S. M., and Wang, T.: Atmospheric photochemical reactivity and ozone production at two sites in Hong Kong: Application of a Master Chemical Mechanism-photochemical box model, J. Geophys. Res.-Atmos., 119, 10567-10582, https://doi.org/10.1002/2014jd021794, 2014.

Mao, J., Ren, X., Shuang, C., Brune, W. H., Zhong, C., Martinez, M., Harder, H., Lefer, B., Rappenglück, B., and Flynn, J.: Atmospheric oxidation capacity in the summer of Houston 2006: Comparison with summer measurements in other metropolitan studies, Atmos. Environ., 44, 4107-4115, https://doi.org/10.1016/j.atmosenv.2009.01.013, 2010.

Martinez, M., Harder, H., Kovacs, T. A., Simpas, J. B., Bassis, J., Lesher, R., Brune, W. H., Frost, G. J., Williams, E. J., and Stroud, C. A.: OH and HO_2 concentrations, sources, and loss rates during the Southern Oxidants Study in Nashville, Tennessee, summer 1999, J. Geophys. Res.-Atmos., 108, 4617, https://doi.org/10.1029/2003JD003551, 2003.

Monks, P. S., Rickard, A. R., and Hall, S. L.: Attenuation of spectral actinic flux and photolysis frequencies at the surface through homogenous cloud fields, J. Geophys. Res., 109, https://doi.org/10.1029/2003jd004076, 2004.

Santiago, J.-L., Martilli, A., and Martin, F.: On dry deposition modelling of atmospheric pollutants on vegetation at the microscale: Application to the impact of street vegetation on air quality, Boundary Layer Meteorol., 162, 451-474, https://doi.org/10.1007/s10546-016-0210-5, 2016.

Shi, C., Wang, S., Liu, R., Zhou, R., Li, D., Wang, W., Li, Z., Cheng, T., and Zhou, B.: A study of aerosol optical properties during ozone pollution episodes in 2013 over Shanghai, China, Atmos. Res., 153, 235-249, https://doi.org/10.1016/j.atmosres.2014.09.002, 2015.

Whalley, L. K., Stone, D., Bandy, B., Dunmore, R., Hamilton, J. F., Hopkins, J., Lee, J. D., Lewis, A. C., and Heard, D. E.: Atmospheric OH reactivity in central London: observations, model predictions and estimates of in situ ozone production, Atmos. Chem. Phys., 16, 2109-2122, https://doi.org/10.5194/acp-16-2109-2016, 2016.

Whalley, L. K., Stone, D., Dunmore, R., Hamilton, J., Hopkins, J. R., Lee, J. D., Lewis, A. C., Williams, P., Kleffmann, J., Laufs, S., Woodward-Massey, R., and Heard, D. E.: Understanding in situ ozone production in the summertime through radical observations and modelling studies during the Clean air for London project (ClearfLo), Atmos. Chem. Phys., 18, 2547-2571, https://doi.org/10.5194/acp-18-2547-2018, 2018.

Zhang, J., Zhao, Y., Zhao, Q., Shen, G., Liu, Q., Li, C., Zhou, D., and Wang, S.: Characteristics and source apportionment of summertime volatile organic compounds in a fast developing city in the Yangtze River Delta, China, Atmosphere, 9, https://doi.org/10.3390/atmos9100373, 2018.

Response to reviewers' comments #2

We thank the reviewers for the constructive comments and suggestions, which are very positive to improve scientific content of the manuscript. We have revised the manuscript appropriately and addressed all the reviewers' comments point-by-point for consideration as below. The remarks from the reviewers are shown in black, and our responses are shown in blue color. All the page and line numbers mentioned following are refer to the revised manuscript without change tracked.

Reviewer

This paper presents a set of recent (2018) measurements of trace gases from a ground site in Shanghai to assess the factors that lead to photochemical ozone pollution in that region of China. The measurements span five months of nearly continuous measurements. They include NOx and speciated VOCs, among other chemical measurements, together with standard meteorological data (but not including boundary layer dynamics).

The results are analyzed in the context of three different case studies of high, medium and low ozone. Several different standard metrics of photochemistry and ozone production are used to analyze the data using both observationally derived quantities as well as box modeling.

While the overall measurements and analysis are standard and do not present any novel data or analysis methods, they do represent a comprehensive analysis from a particular year and location in China, a highly polluted region that is currently undergoing a transition from recent high emissions to somewhat lower and more controlled emissions of common air pollutants. They will therefore represent a useful data point and analysis of factors that control ozone pollution in a Chinese megacity.

The manuscript is generally well written and easy to follow.

I recommend publication following attention to the minor comments and technical corrections below.

R: Thanks very much for the comments. This paper focuses on comparing atmospheric photochemistry and radical chemistry at different ozone levels in Shanghai in summer 2018. Although the traditional data and analysis methods are used, we did a comprehensive analysis of atmospheric photochemistry in specific years and locations in China. Since ozone pollution is the big challenge for the air quality during summer and the long-term observations show that the mean mixing ratio of O_3 concentration in Shanghai increased 67% from 2006 to 2015 at a growth rate of 1.1 ppbv/year (Gao et al., 2017), it is necessary to study the atmospheric photochemical behavior under different ozone levels and explore the contribution of precursor VOCs to ozone generation.

Minor comments are given below.

Line 21, Abstract: AQI is not defined here nor referenced further in the text. The wording is also not clear. 92.2% of all the days in the observation period? Or some fraction of the AQI?

R: Thanks for the suggestion. AQI, Air Quality Index, comes from 'Technical

Regulation on Ambient Air Quality Index' formulated by Ministry of Environmental Protection of China (now called Ministry of Ecology and Environment of China) to regulate the daily and real-time report on air quality index.
92.2% refers to the ratio of the days without air pollution to the total days during the observation period. And we have rewritten this sentence to 'Five months of observations from 1 May to 30 September 2018 showed that the air quality level is in lightly polluted and even worse (Ambient Air Quality Index, AQI>100) for 12 days, of which ozone is the primary pollutant for 10 days, indicating that ozone is the main challenge of air quality in Shanghai in the summer of 2018.'. Please refer to Line 19-22.

Line 34, Abstract: "Concentration ratio" should be defined. This is the summed mixing ratio of these species relative to what? Total NMVOC? Or total carbon? Also, the statement that follows implies that these four compounds could be controlled, but since HCHO is not a direct emission, it would result from control of all VOC and could not be targeted individually.
R: Thanks for the suggestion. 'Concentration ratio' means the ratio of certain NMVOC concentration to total NMVOC concentration. We have rewritten this sentence as 'The concentration ratio (~23%) of these four species to total NMVOCs is not proportional to their contribution (~55%) to OFP'. Please refer to Line 35-36.
In general, the sources of HCHO can be attributed to the primary and secondary contribution, as well as the background. The primary sources of HCHO are mainly from fossil fuels, industrial and vehicular emissions (Lui et al., 2017). Previous studies have shown that the contribution of primary source to HCHO in Summer in Wuhan, China reached 32.4 ± 6.5%, primary source contributed 40% to HCHO in Houston in Summer, and the annual average contribution of primary source to HCHO were 42.52% in Shanghai in 2016 (Buzcu Guven and Olaguer, 2011; Su et al., 2019; Yang et al., 2019). This indicates that the primary source of HCHO cannot be ignored, and the controlling of the primary emission of HCHO also make sense. In addition, the secondary formation of formaldehyde is also indeed important, which means that the level of precursors of formaldehyde needs to be controlled. So we prefer to keep the current statements.

Line 73: The differences described are not all a function of metropolitan areas but also of the season in which the measurements took place. The Ren 2003 reference, for example, was in winter, one of the main reasons that HONO photolysis is listed as important. The list is also not a comprehensive literature review, which should be stated, as there are numerous similar analyses in addition to those listed here.
R: Thanks for the suggestion. The literature review should be more comprehensive and detailed. We have introduced the HO_x sources among different places and also highlighted its change due to the observational periods/seasons, as following 'For example, ozone photolysis is the dominant OH source in Nashville (Martinez et al., 2003); HONO photolysis has a more important role in New York City (Ren et al., 2003), Paris (Michoud et al., 2012) and Santiago (Elshorbany et al., 2009), Wangdu, China

(Tan et al., 2017) and London (Whalley et al., 2016; Whalley et al., 2018); HCHO photolysis is a significant source of OH in Milan (Alicke et al., 2002); while OVOCs photolysis plays a more critical role in Mexico City (Sheehy et al., 2010), Beijing (Liu et al., 2012), London (Emmerson et al., 2007) and Hong Kong (Xue et al., 2016). However, it also should be noted that the sources of HO_x also changed with different observational seasons/periods even in the same place. The HO_x production in New York City was reported to be dominated by HONO photolysis during daytime but O_3 reactions with alkenes at night in winter (Ren et al., 2006). The main source of radicals was the reaction of O_3 and alkenes during whole day in winter, while HONO photolysis dominated the source of radicals in the morning but photolysis of carbonyls at noon of summer in Tokyo (Kanaya et al., 2007).' Please refer to Line 74-83.

Line 89: Remove "the of". What does the growth rate refer to? Average O3? Maximum O3? Number of air quality exceedances?
R: Thanks for the suggestion. The imprecise expression may lead misunderstanding. The growth rate here refers to the mean concentration of O_3. So we have rewritten this sentence into "The long-term observations show that the mean mixing ratio of O_3 at the downtown urban site in Shanghai increased 67% from 2006 to 2015 at a growth rate of 1.1 ppbv/year". Please refer to Line 94-96.

Line 125: Define "ultra-low temperature"
R: The ultra-low temperature freezing collection device adopted electronic refrigeration, and the internal temperature of the cold trap could reach -150 °C, which can completely capture the target compound. Please refer to Line 131.

Line 141: PAN is not technically defined as an oxidant, but is co-produced with O3.
R: Thanks for the suggestion. PAN does not belong to oxidants, it is the same photochemical product as O_3. What we want to say here is that O_3 and PAN are secondary products. The 'oxidant formation' has been corrected to 'secondary products formation'. Please refer to Line 147.

Line 145-146: The model procedure is not clear. A seven-day run is constrained to data throughout, with seven days of continuous measurements? Or is the run constrained to some sort of diel average? Why does it require four days to reach a steady state? Which species require this spin up time?
R: Thanks for the suggestion, we have introduced the model procedure and describe it accurately and specifically. Please refer to Line 149-160. A seven-day run is constrained by seven-day continuous measurements, where the first four days of pre-simulation are for unmeasured, model-generated intermediate species (HO_2, RO_2, PAN, etc.) to reach steady-state concentrations during the last three days of simulation. Previous literature reported that the pre-simulation time was set to 4 day, 5 days or 9 days (Xue et al., 2014; Xue et al., 2016; Li et al., 2018). Considering the lifetime of the model-generated intermediate species and the simulation time cost, the pre-simulation time is set to four days in this study.

Line 150, AOC: The definition of AOC does not include NOx, notably not the reaction of OH with NO2, but also not RO2 + NO reactions (i.e., producing organic nitrates). These are chain termination steps and so perhaps are excluded for that reason, but the exclusion would not then fit the definition that follows of defining the "removal rate of most pollutants", since NOx (as well as SOx) is excluded. Some comment or caveat to this effect is warranted, even if the definition is simply following prior literature. The quantity as defined is not as commonly used as other metrics in this paper.

R: Thanks for the suggestion. Indeed the definition of AOC is to follow the previous literature, and the "removal rate of most pollutants" does not conform exactly to AOC definition. According to the definition of AOC, AOC actually determines the removal rate of VOC, CO and CH_4.

We have modified this part to 'According to the definition of AOC, it can be calculated by the equation (E1) (Elshorbany et al., 2009; Xue et al., 2016):

$$AOC = \sum_i k_{Yi}[Y_i]\,[X] \qquad \text{(E1)}$$

Where Y_i are VOCs, CO, and CH_4, X are oxidants (OH, O_3, and NO_3), and k_{Yi} is the bi-molecular rate constant for the reaction of Y_i with X. Atmospheric oxidation capacity determines the rate of Y_i removal (Prinn and Resources, 2003).'. Please refer to Line 163-166.

Line 162, OH chain length: This is one of several available definitions. The assumption in this formulation appears to be that OH + NO2 is the major chain termination reaction. This is shown in the later analysis but not justified here. The later analysis needs to be referenced to justify this equation. In some instances, RO2 + NO producing organic nitrates is competitive with OH + NO2. No mention is made of this chain termination step, nor is its importance ever assessed in the context of other metrics. This chain termination reaction needs to be included in the metrics of ozone photochemistry somewhere in this paper.

R: After in-depth reading of relevant literature, we have a deeper understanding of chain length. The ratio of the rate of HO_x cycling reactions to HO_x termination is called the chain length, as in Equation 1 (Martinez et al., 2003). When the termination reaction of HO_x is dominated by the reaction of NO_2 and OH, the definition can be simplified as equation (E4). When we use the simplified equation (E4), we need to declare that the reaction between OH and NO_2 is the main termination reaction of radicals.

$$\text{Chain Length} = \frac{[OH]k_{OH} - L(HO_x)}{L(HO_x)} \qquad \text{(E2)}$$

$$L(HO_x) = k_{OH+NO_2}[OH][NO_2] + 2k_{HO_2+HO_2}[HO_2]^2 + 2k_{OH+HO_2}[OH][HO_2] + 2k_{HO_2+RO_2}[HO_2][RO_2] + 2k_{RO_2+RO_2}[RO_2][RO_2] \qquad \text{(E3)}$$

$$OH\ \ Chain\ \ Length = \frac{k_{OH}[OH] - k_{OH+NO_2+M}[OH][NO_2]}{k_{OH+NO_2+M}[OH][NO_2]} \qquad \text{(E4)}$$

This is one of several definitions available based on the assumption that OH + NO_2 is the main chain termination reaction, which is further discussed in Sect 3.3. Please refer to Line 180-181 and Line 376-383.

Line 191-192: Is radiation the only factor? From Figure 1, it appears that meteorology and transport could also easily have been important. The temperature, relative humidity, and distribution of wind vectors were also different between the two periods.

R: Thanks for the suggestion. After comparing other meteorological parameters, it can be seen that not only the radiation of Case 1 was higher than that of Case 2, but also the temperature, humidity and pressure of Case 1 are different from Case 2. The temperature difference between day and night in Case 1 was greater than Case 2, and the humidity and air pressure were lower than Case 2 (see Figure R1). These meteorological conditions are conducive to photochemical reactions. We have revised it. Please refer to Line 209-212.

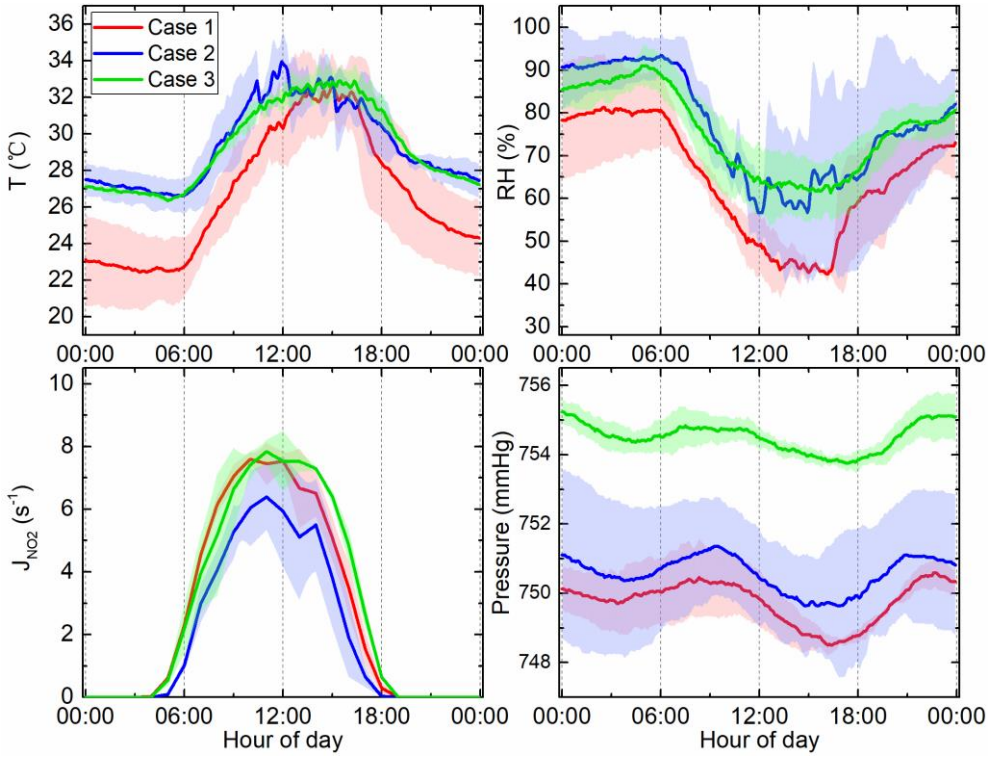

Figure R1. Mean diurnal profiles of meteorological parameters for three cases. The shaded areas denote the standard deviation.

Line 212: Acetylene is not technically an alkene but rather an alkyne. It is much less reactive than alkenes towards OH. This is described in footnote c of table 2, but would be better also in the text. The lumping of acetylene with alkenes is not really appropriate, but if it is done, the statement that this compounds is far less reactive with alkenes toward OH needs to be explicit.

R: Acetylene is indeed not technically an alkene, but an alkyne. Considering that both acetylene and alkenes are unsaturated aliphatic hydrocarbons, which have unsaturated bonds, acetylene and other species with carbon-carbon double bonds are classified as alkenes category for the convenience of statistics. We have followed the comment and made the description clearly that the reactivity of acetylene with OH is far less than that

of alkenes with OH and need to be explicit. Please refer to Line 238-239.

Line 215, Table 2: Units are given in footnote (b) but are otherwise difficult to find. Suggest moving this description to the table caption.
R: We have followed the comments and move this description to the table caption. Please refer to Line 233-235.

Line 229-230, and 235-239: Were there NO3 measurements to define nighttime AOC? The NO3 measurement (by DOAS?) is not specified in the experimental techniques. Was this a calculated quantity? Was there nighttime NO at the surface level measurement site that limited NO3?
R: We have not measured the NO_3 concentration in this study. The presented NO_3 data and its contribution to nighttime AOC were the simulated results.

Line 238: Numbers given for NO3 do not match the figure, which always shows much larger AOC due to OH. Do these percentages refer to nighttime data only?
R: These percentages of NO_3 to AOC refer to nighttime only. The time periods that these percentages refer to should be indicated clearly in the manuscript. Please refer to Line 256-257.

Line 310: Clarify what is meant by "all within 10". This could imply a factor of 10 difference between chain lengths, which is likely not what is intended.
R: Thanks for the suggestion. As Reviewer #1 commented on this, I have changed 'within 10' to 'less than 8'. Please refer to Line 329.

Line 312: This is not "probably" due to higher NOx, but rather simply "due to higher NOx", correct? The dependence should not be difficult to infer.
R: Thanks for the suggestion. As shown in Figure R2 and Table 1, the high mixing ratio of NO_X in Case 1 during the 09:00-14:00 results in a relatively larger sink of OH + NO_2. We have followed the comment and remove 'probably'. Please refer to Line 331-332.

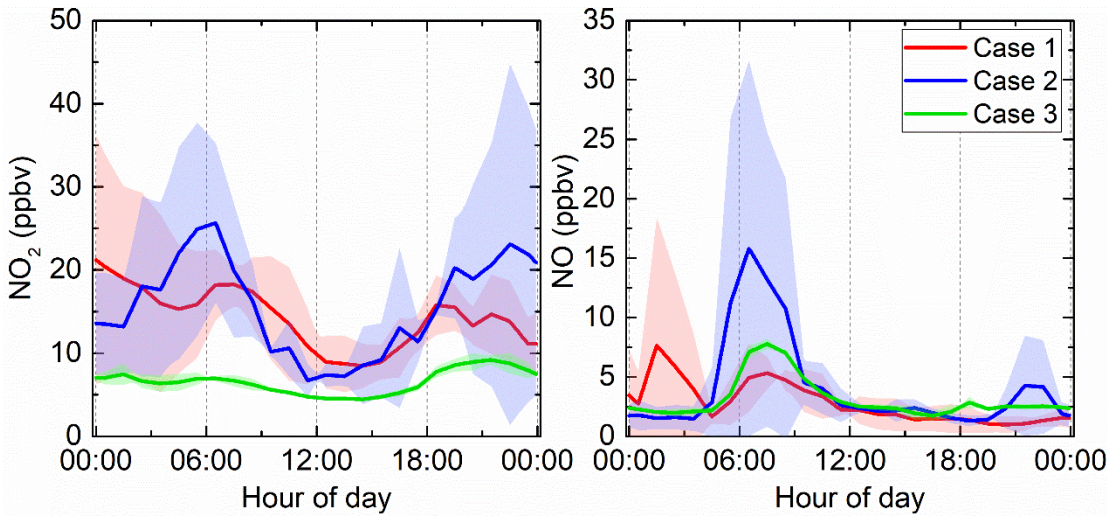

Figure R2. Mean diurnal profiles of NO_2 and NO for three cases. The shaded areas denote the

standard deviation.

Line 313-315: The OH chain length is described at the beginning of the paragraph as being similar to ozone production efficiency, yet here trend in OH chain length is show to be opposite to ozone abundance. Can the authors reconcile these statements?
R: During the daytime, the greater the chain length, the greater the amount of O_3 produced per NO_X molecule converted to HNO_3. Thus, the chain length is related to ozone production efficiency (OPE), which is given by $\Delta O_3/\Delta(NO_y - NO_X)$ (note: NOy = NO_X + HNO_3 +NO_3 + PAN) (Wang et al., 2018). In the profile of OH chain length in Figure 5, the OH chain length in Case 3 is longer accompanied with the lowest ozone mixing ratio, meaning that per NO_X converted into HNO_3 produces more O_3 whereas the daytime NO_X mixing ratio in Case 3 is almost half that of Case 1 and 2 (see Figure R1), causing ozone mixing ratios to be lower than Case 1 and 2. In addition, we found that the OH chain length was opposite to the ozone level, and the explanation given was also due to the lower NO_X mixing ratios in previous studies (Mao et al., 2010; Ling et al., 2014).

Line 344-350: The photolysis of ClNO2 was noted in an earlier section and should be noted here again as previous studies have shown it to be as important as HONO during the morning hours (e.g., Young, ES&T, v 46, p10965, 2012)
R: Thanks for the suggestion. We have followed the comments and stated the importance of $ClNO_2$ photolysis to OH sources in the morning. Please refer to Line 369-370.

Line 367: Where do the calculated MIR coefficients come from in this equation? How are they determined?
R: MIR coefficients come from Carter (2010) research, as listed in Table 1. The Maximum Incremental Reactivity (MIR) scale is determined by adjusting the input ratio of VOC to NO_X in model (built on the SAPRC atmospheric chemical mechanisms) to maximize the incremental reactivity of a base VOC mixture. Please refer to Carter (2010) research for details.

Line 412-414: Same comment as in the abstract. While three of the four NMVOC can in fact be controlled, formaldehyde is mainly the secondary oxidation product from a wide range of other compounds and cannot be controlled directly.
R: Please also refer to the responses to the minor comments #2. Many studies have reported that the primary source is a non-negligible source of formaldehyde (Buzcu Guven and Olaguer, 2011; Lui et al., 2017; Su et al., 2019; Yang et al., 2019). So we consider that the regulating on the primary sources of HCHO also can make sense.

Technical Corrections
Line 23, Abstract: The word “premise” is not properly used here.
R: Thanks for the suggestion. Now we are using ‘precondition’. Please refer to Line 23.

Line 32, Abstract: “radical” rather than “radicals”
R: We have corrected it. Please refer to Line 33.

Line 83: Replace “even more” with “increasingly”; Line 86: remove the word “around”
R: Thanks for the suggestion. The ‘even more’ has been corrected to ‘increasingly’. And we have removed the word ‘around’. Please refer to Line 89 and Line 92.

Line 104, 123, 153, 336, 409: Replace “Besides” with “Additionally”
R: We have followed the suggestions and replaced ‘Additionally’ with ‘Besides’. Please refer to Line 112, 130, 168, 358 and 447.

Line 143: “input” rather than “inputted”
R: We have corrected ‘inputted’ to ‘input’. Please refer to Line 150.

Line 170: Pollutants shown in Figure 1 are given in mixing ratio, not concentration units.
R: We have followed the suggestion and replaced ‘concentrations’ with ‘mixing ratios’ and elsewhere in the manuscript. Please refer to Line 199 and other places.

Line 223: “based” rather than “base”
R: Thanks for the suggestion. The ‘base’ has been replaced with ‘based’. Please refer to Line 242.

Line 289: Eliminate the word “besides”
R: We have been removed the ‘besides’. Please refer to Line 309.

Line 373: Figure gives mixing ratios rather than concentrations. Specify mixing ratio in text.
R: We have followed the suggestion and replaced ‘concentrations’ with ‘mixing ratios’ and elsewhere in the manuscript. Please refer to Line 411 and other places.

References

Alicke, B., Platt, U., and Stutz, J.: Impact of nitrous acid photolysis on the total hydroxyl radical budget during the Limitation of Oxidant Production/Pianura Padana Produzione di Ozono study in Milan, J. Geophys. Res.-Atmos., 107, 8196, https://doi.org/10.1029/2000jd000075, 2002.

Buzcu Guven, B., and Olaguer, E. P.: Ambient formaldehyde source attribution in Houston during TexAQS II and TRAMP, Atmos. Environ., 45, 4272-4280, https://doi.org/10.1016/j.atmosenv.2011.04.079, 2011.

Carter, W. P.: Updated maximum incremental reactivity scale and hydrocarbon bin reactivities for regulatory applications, California Air Resources Board Contract, 07-339, 2010.

Elshorbany, Y. F., Kurtenbach, R., Wiesen, P., Lissi, E., Rubio, M., Villena, G., Gramsch, E., Rickard, A. R., Pilling, M. J., and Kleffmann, J.: Oxidation capacity of the city air of Santiago, Chile, Atmos.

Chem. Phys., 9, 2257-2273, https://doi.org/10.5194/acp-9-2257-2009, 2009.

Emmerson, K. M., Carslaw, N., Carslaw, D., Lee, J. D., McFiggans, G., Bloss, W. J., Gravestock, T., Heard, D. E., Hopkins, J., and Ingham, T.: Free radical modelling studies during the UK TORCH Campaign in Summer 2003, Atmos. Chem. Phys., 7, 167-181, https://doi.org/10.1016/j.atmosenv.2006.07.023, 2007.

Gao, W., Tie, X., Xu, J., Huang, R., Mao, X., Zhou, G., and Chang, L.: Long-term trend of O_3 in a mega City (Shanghai), China: Characteristics, causes, and interactions with precursors, Sci. Total Environ., 603, 425-433, https://doi.org/10.1016/j.scitotenv.2017.06.099, 2017.

Kanaya, Y., Cao, R., Akimoto, H., Fukuda, M., Komazaki, Y., Yokouchi, Y., Koike, M., Tanimoto, H., Takegawa, N., and Kondo, Y. J. J. o. G. R. A.: Urban photochemistry in central Tokyo: 1. Observed and modeled OH and HO_2 radical concentrations during the winter and summer of 2004, 112, 2007.

Li, Z., Xue, L., Yang, X., Zha, Q., Tham, Y. J., Yan, C., Louie, P. K., Luk, C. W., Wang, T., and Wang, W.: Oxidizing capacity of the rural atmosphere in Hong Kong, Southern China, Sci. Total Environ., 612, 1114-1122, https://doi.org/10.1016/j.scitotenv.2017.08.310, 2018.

Ling, Z. H., Guo, H., Lam, S. H. M., Saunders, S. M., and Wang, T.: Atmospheric photochemical reactivity and ozone production at two sites in Hong Kong: Application of a Master Chemical Mechanism-photochemical box model, J. Geophys. Res.-Atmos., 119, 10567-10582, https://doi.org/10.1002/2014jd021794, 2014.

Liu, Z., Wang, Y., Gu, D., Zhao, C., Huey, L. G., Stickel, R., Liao, J., Shao, M., Zhu, T., Zeng, L., Amoroso, A., Costabile, F., Chang, C. C., and Liu, S. C.: Summertime photochemistry during CAREBeijing-2007: RO_x budgets and O_3 formation, Atmos. Chem. Phys., 12, 7737-7752, https://doi.org/10.5194/acp-12-7737-2012, 2012.

Lui, K. H., Ho, S. S. H., Louie, P. K. K., Chan, C. S., Lee, S. C., Hu, D., Chan, P. W., Lee, J. C. W., and Ho, K. F.: Seasonal behavior of carbonyls and source characterization of formaldehyde (HCHO) in ambient air, Atmos. Environ., 152, 51-60, https://doi.org/10.1016/j.atmosenv.2016.12.004, 2017.

Mao, J., Ren, X., Shuang, C., Brune, W. H., Zhong, C., Martinez, M., Harder, H., Lefer, B., Rappenglück, B., and Flynn, J.: Atmospheric oxidation capacity in the summer of Houston 2006: Comparison with summer measurements in other metropolitan studies, Atmos. Environ., 44, 4107-4115, https://doi.org/10.1016/j.atmosenv.2009.01.013, 2010.

Martinez, M., Harder, H., Kovacs, T. A., Simpas, J. B., Bassis, J., Lesher, R., Brune, W. H., Frost, G. J., Williams, E. J., and Stroud, C. A.: OH and HO_2 concentrations, sources, and loss rates during the Southern Oxidants Study in Nashville, Tennessee, summer 1999, J. Geophys. Res.-Atmos., 108, 4617, https://doi.org/10.1029/2003JD003551, 2003.

Michoud, V., Kukui, A., Camredon, M., Colomb, A., Borbon, A., Miet, K., Aumont, B., Beekmann, M., Durand-Jolibois, R., and Perrier, S.: Radical budget analysis in a suburban European site during the MEGAPOLI summer field campaign, Atmos. Chem. Phys., 12, 11951-11974, https://doi.org/10.5194/acp-12-11951-2012, 2012.

Prinn, R. G. J. A. R. o. E., and Resources: The cleansing capacity of the atmosphere, 28, 29-57, 2003.

Ren, X., Harder, H., Martinez, M., Lesher, R. L., Oliger, A., Shirley, T., Adams, J., Simpas, J. B., and Brune, W. H.: HO_x concentrations and OH reactivity observations in New York City during PMTACS-NY2001, Atmos. Environ., 37, 3627-3637, https://doi.org/10.1016/S1352-2310(03)00460-6, 2003.

Ren, X., Brune, W. H., Mao, J., Mitchell, M. J., Lesher, R. L., Simpas, J. B., Metcalf, A. R., Schwab, J. J., Cai, C., and Li, Y.: Behavior of OH and HO_2 in the winter atmosphere in New York City, Atmos. Environ., 40, 252-263, https://doi.org/10.1016/j.atmosenv.2005.11.073, 2006.

Sheehy, P. M., Volkamer, R., Molina, L. T., and Molina, M. J.: Oxidative capacity of the Mexico City atmosphere – Part 2: A RO_x radical cycling perspective, Atmos. Chem. Phys., 10, 6993-7008, https://doi.org/10.5194/acp-10-6993-2010, 2010.

Su, W., Liu, C., Hu, Q., Zhao, S., Sun, Y., Wang, W., Zhu, Y., Liu, J., and Kim, J.: Primary and secondary sources of ambient formaldehyde in the Yangtze River Delta based on Ozone Mapping and Profiler Suite (OMPS) observations, Atmos. Chem. Phys., 19, 6717-6736, https://doi.org/10.5194/acp-19-6717-2019, 2019.

Tan, Z., Fuchs, H., Lu, K., Hofzumahaus, A., Bohn, B., Broch, S., Dong, H., Gomm, S., Häseler, R., He, L., Holland, F., Li, X., Liu, Y., Lu, S., Rohrer, F., Shao, M., Wang, B., Wang, M., Wu, Y., Zeng, L., Zhang, Y., Wahner, A., and Zhang, Y.: Radical chemistry at a rural site (Wangdu) in the North China Plain: observation and model calculations of OH, HO2 and RO2 radicals, Atmos. Chem. Phys., 17, 663-690, https://doi.org/10.5194/acp-17-663-2017, 2017.

Wang, J., Ge, B., and Wang, Z.: Ozone Production Efficiency in Highly Polluted Environments, Current Pollution Reports, 4, 198-207, https://doi.org/10.1007/s40726-018-0093-9, 2018.

Whalley, L. K., Stone, D., Bandy, B., Dunmore, R., Hamilton, J. F., Hopkins, J., Lee, J. D., Lewis, A. C., and Heard, D. E.: Atmospheric OH reactivity in central London: observations, model predictions and estimates of in situ ozone production, Atmos. Chem. Phys., 16, 2109-2122, https://doi.org/10.5194/acp-16-2109-2016, 2016.

Whalley, L. K., Stone, D., Dunmore, R., Hamilton, J., Hopkins, J. R., Lee, J. D., Lewis, A. C., Williams, P., Kleffmann, J., Laufs, S., Woodward-Massey, R., and Heard, D. E.: Understanding in situ ozone production in the summertime through radical observations and modelling studies during the Clean air for London project (ClearfLo), Atmos. Chem. Phys., 18, 2547-2571, https://doi.org/10.5194/acp-18-2547-2018, 2018.

Xue, L. K., Wang, T., Gao, J., Ding, A. J., Zhou, X. H., Blake, D. R., Wang, X. F., Saunders, S. M., Fan, S. J., Zuo, H. C., Zhang, Q. Z., and Wang, W. X.: Ground-level ozone in four Chinese cities: precursors, regional transport and heterogeneous processes, Atmos. Chem. Phys., 14, 13175-13188, https://doi.org/10.5194/acp-14-13175-2014, 2014.

Xue, L. K., Gu, R. G., Wang, T., Wang, X. F., Saunders, S., Blake, D., Louie, P. K. K., Luk, C. W. Y., Simpson, I., and Xu, Z.: Oxidative capacity and radical chemistry in the polluted atmosphere of Hong Kong and Pearl River Delta region: analysis of a severe photochemical smog episode, Atmos. Chem. Phys., 9891-9903, https://doi.org/10.5194/acp-16-9891-2016, 2016.

Yang, Z., Cheng, H. R., Wang, Z. W., Peng, J., Zhu, J. X., Lyu, X. P., and Guo, H.: Chemical characteristics of atmospheric carbonyl compounds and source identification of formaldehyde in Wuhan, Central China, Atmos. Res., 228, 95-106, https://doi.org/10.1016/j.atmosres.2019.05.020, 2019.

Observationally constrained modelling of atmospheric oxidation capacity and photochemical reactivity in Shanghai, China

Jian Zhu[1], Shanshan Wang[1,2,*], Hongli Wang[3], Shengao Jing[3], Shengrong Lou[3], Alfonso Saiz-Lopez[1,5], Bin Zhou[1,2,4]

[1] Shanghai Key Laboratory of Atmospheric Particle Pollution and Prevention (LAP[3]), Department of Environmental Science and Engineering, Fudan University, Shanghai, China
[2] Institute of Eco-Chongming (IEC), No.20 Cuiniao Road, Shanghai 202162, China
[3] State Environmental Protection Key Laboratory of the Formation and Prevention of Urban Air Pollution Complex, Shanghai Academy of Environmental Sciences, Shanghai 200233, China
[4] Institute of Atmospheric Sciences, Fudan University, Shanghai, 200433, China
[5] Department of Atmospheric Chemistry and Climate, Institute of Physical Chemistry Rocasolano (CSIC), Madrid 28006, Spain

Correspondence to: Shanshan Wang (shanshanwang@fudan.edu.cn)

Abstract.

An observation-based model coupled to the Master Chemical Mechanism (V3.3.1) and constrained by a full suite of observations was developed to study atmospheric oxidation capacity (AOC), OH reactivity, OH chain length, and HO_x (= OH + HO_2) budget for three different ozone (O_3) concentration levels in Shanghai, China. Five months of observations from 1 May to 30 September 2018 showed that the air quality level is in lightly polluted and even worse (Ambient Air Quality Index, AQI>100) for 12 days, of which ozone is the primary pollutant for 10 days, indicating ozone pollution is the main challenge of air quality in Shanghai during summer of 2018. ~~with ozone as the primary pollutant occurred and the days with good air quality (AQI < 100) accounted for 92.2% during this spring-summer time.~~ The levels of ozone and its precursors, as well as meteorological parameters revealed the significant differences among different ozone levels, indicating that the high level of precursors is the precondition~~premise~~ of ozone pollution, and strong radiation is an essential driving force. By increasing the input J_{NO2} value by 40%, the simulated O_3 level increased by 30-40% correspondingly under the same level of precursors. The simulation results show that AOC, dominated by reactions involving OH radical during the daytime, has a positive correlation with ozone levels. The reactions with non-methane volatile organic compounds (NMVOCs) (30%-36%), carbon monoxide (CO) (26%-31%), and nitrogen dioxide (NO_2) (21%-29%) dominated the OH reactivity under different ozone levels in Shanghai. Among the NMVOCs, alkenes and oxygenated VOCs (OVOCs) played a key role in OH reactivity defined as the inverse of the OH lifetime. A longer OH chain length was found in clean conditions primarily due to low NO_2 in the atmosphere. The high level of radical precursors (e.g., O_3, HONO, and OVOCs) promotes the production and cycling of HO_x, and the daytime HO_x primary source shifted from ~~the~~ HONO photolysis in the morning to ~~the~~ O_3 photolysis in the afternoon. For the sinks of radicals, the reaction with NO_2 ~~completely~~ dominated radical~~s~~ termination during the morning rush hour, while the reactions of radical-radical also contributed to the sinks of HO_x in the afternoon. Furthermore, the top four species contributing

to ozone formation potential (OFP) were HCHO, toluene, ethylene, and m/p-xylene. The concentration ratio (~23%) of these four species to total NMVOCs is not proportional to their contribution (~55%) to OFP, implying that controlling key VOC species emission is more effective than limiting the total concentration of VOC in preventing and controlling ozone pollution.

1 Introduction

Air quality in urban areas has received increasing attention in recent years, especially photochemical smog pollution during summer. It is well known that high concentrations of ozone (O_3), an essential product of atmospheric photochemistry and free radical chemistry, have adverse effects on human health, plants and crop (National Research Council, 1992; Seinfeld and Pandis, 2016). The abundance of tropospheric O_3 is primarily determined by the external transport (transport down from the stratosphere, dry deposition to the earth surface) and in situ photochemical generation through a series of reactions involving volatile organic compounds (VOCs) and nitrogen oxides (NO_x) under sunlight (Jenkin and Clemitshaw, 2000; Seinfeld and Pandis, 2016). Both the removal of these O_3 precursors, such as methane (CH_4), non-methane volatile organic compounds (NMVOCs), carbon monoxide (CO) and NO_x, and the formation of secondary pollutants like ozone and secondary organic/inorganic aerosols are controlled by the oxidation capacity of the atmosphere (Prinn, 2003; Hofzumahaus et al., 2009; Ma et al., 2010; Ma et al., 2012; Feng et al., 2019). The term "atmospheric oxidation capacity (AOC)" is defined as the sum of the respective oxidation rates of primary pollutants (CH_4, NMVOCs, CO) by the oxidants (OH, O_3 and NO_3) (Elshorbany et al., 2009; Xue et al., 2016). Therefore, understanding the processes and rates under which these species are oxidized in the atmosphere is critical to identify the controlling factors of secondary pollution in the atmosphere.

As the most reactive species in the atmosphere, hydroxyl (OH) poses a significant role in atmospheric chemistry, driving AOC (Li et al., 2018). OH is removed by reactions with primary pollutants and with intermediate products of these oxidation reactions. The OH loss frequency (referred as OH reactivity) is defined as the inverse of the OH lifetime and has been widely used to evaluate the oxidation intensity of the atmosphere (Kovacs et al., 2003; Li et al., 2018). The OH and hydroperoxyl radical (HO_2), collectively called HO_x, in which OH initiates a series of oxidation reactions, while HO_2 is the primary precursor of ozone generation in the presence of NO_x. OH can react with many species in the atmosphere such as CO, CH_4, and NMVOCs, which directly produce HO_2 in some cases, and initiate a reaction sequence that produces HO_2 in other cases, e.g., OH → RO_2 → RO → HO_2. Meanwhile, HO_2 can react with NO or O_3 to produce OH. High temperature and high radiation promote HO_x cycling reactions, which is also affected by the abundance of other atmospheric compounds (Coates et al., 2016; Xing et al., 2017). This cycling is closely related to atmospheric photochemical reactivity, especially the generation of ozone, secondary aerosols, and other pollutants (Mao et al., 2010; Xue et al., 2016). The radical cycling is terminated by their cross-reactions with NO_x under high-NO_x conditions (e.g., OH + NO_2, RO_2 + NO and RO_2 + NO_2) and RO_x under low-NO_x conditions (e.g., HO_2 + HO_2, RO_2 + HO_2 and RO_2 + RO_2), which results in the formation of nitric acid, organic nitrates and peroxides (Wood

et al., 2009; Liu et al., 2012; Xue et al., 2016).

To further understand the atmospheric oxidation capacity and radical chemistry, it is necessary to explore the HO_x budget. In general, significant sources of HO_x include the photolysis of ozone ($O(^1D) + H_2O$), HONO, HCHO and other oxygenated VOCs (OVOCs), as well as other non-photolytic sources such as the reactions of ozone with alkenes and the reactions of NO_3 with unsaturated VOCs (Xue et al., 2016). During the past decades, research on the sources of HO_x has shown that although air pollution problems are visually very similar, radical chemistry, especially the relative importance of primary radical sources, is unique in different metropolitan areas. For example, ozone photolysis is the dominant OH source in Nashville (Martinez et al., 2003); HONO photolysis has a more important role in New York City (Ren et al., 2003), Paris (Michoud et al., 2012) and Santiago (Elshorbany et al., 2009), Wangdu, China (Tan et al., 2017) and London (Whalley et al., 2016; Whalley et al., 2018); HCHO photolysis is a significant source of OH in Milan (Alicke et al., 2002); while OVOCs photolysis plays a more critical role in Mexico City (Sheehy et al., 2010), Beijing (Liu et al., 2012), London (Emmerson et al., 2007) and Hong Kong (Xue et al., 2016). However, it also should be noted that the sources of HO_x also changed with different observational seasons/periods even in the same place. The HO_x production in New York City was reported to be dominated by HONO photolysis during daytime but O_3 reactions with alkenes at night in winter (Ren et al., 2006). The main source of radicals was the reaction of O_3 and alkenes during whole day in winter, while HONO photolysis dominated the source of radicals in the morning but photolysis of carbonyls at noon of summer in Tokyo (Kanaya et al., 2007). Previous studies reported that for HO_x sinks, the reaction of OH with NO_2 dominates HO_x sinks all day, and the reactions between radicals themselves, e.g. $HO_2 + HO_2$ and $HO_2 + RO_2$, start to be important for the contribution of HO_x sinks in the afternoon (Guo et al., 2013; Ling et al., 2014; Mao et al., 2010). Overall, atmospheric oxidation capacity, OH reactivity, and HO_x budget are three crucial aspects for understanding the complex photochemistry of an urban atmosphere.

As a photochemical product, ozone pollution has been ~~even more~~increasingly severe during the past few years in China (Wang et al., 2017). At a rural site 50 km north of Beijing city center, a six-week observation experiment in June and July 2005 reported the maximum average hourly ozone reaching 286 ppbv (Wang et al., 2006). Even in the first two weeks under an emissions control scenario, for the Beijing Olympic Games, the hourly ozone level was ~~around~~ 160-180 ppbv in urban Beijing (Wang et al., 2010). In comparison, the highest hourly ozone also frequently exceeded 200 ppbv in the Pearl River Delta region and Hong Kong (Zhang et al., 2007; Guo et al., 2009; Cheng et al., 2010; Xue et al., 2016; Zhang et al., 2016). The long-term observations show that the mean mixing ratio of O_3 ~~concentration~~ at the downtown urban site in Shanghai increased 67% from 2006 to 2015 at a growth rate of 1.1 ppbv/year (Gao et al., 2017). Most of the previous studies on ozone pollution in Shanghai had a focus on the precursor-O_3 relationships, cause of O_3 formation, and local or regional contributions (Gao et al., 2017; Wang et al., 2018; Li et al., 2008). The NCAR Master Mechanism model and measurement results between 2006 and 2007 indicated that the O_3 formation is clearly under VOC-sensitive regime in Shanghai, pointing to the essential role of aromatics and alkenes in O_3 formation (Geng et al., 2008). A regional modelling study using the Weather Research and Forecasting

Chemical (WRF-Chem) model suggested that the variations of ambient O_3 levels in 2007 in Shanghai were mainly driven by the ozone precursors, along with regional transport (Tie et al., 2009). The sensitivity study of the WRF-Chem model quantified the threshold value of the emission ratio of NO_x/VOCs for switching from a VOC-limited to a NO_x-limited regime in Shanghai (Tie et al., 2013). Another study has estimated that future ozone will be reduced by 2-3 ppbv in suburban areas, and more than 4 ppbv in rural areas in Shanghai after 2020 (Xu et al., 2019). However, few of these earlier studies investigated atmospheric oxidation capacity and radical chemistry in Shanghai with an observation-constrained model.

In this study, a spring-summer observational experiment was conducted from 1 May to 30 September in 2018 in Shanghai that helped to construct a detailed observation-based model (OBM) to quantify atmospheric oxidation capacity, OH reactivity, OH chain length, and HO_x budget. Here we selected three cases with different ozone mixing ratio~~concentration~~ levels to better illustrate the characteristics of atmospheric oxidation and radical chemistry in this megacity. The AOC, OH reactivity, OH chain length, and HO_x budget in three cases were analyzed and compared to investigate their relationships with ozone pollution. Additionally~~Besides~~, some major VOCs species are identified to contribute significantly to ozone formation potential (OFP).

2 Methodology

2.1 Measurement site and techniques

Shanghai, China, is one of the largest cities in the world, located at the estuary of the Yangtze River, with more than 24 million people and more than 3 million motor vehicles (National Bureau of Statistics, 2018). The measurements were conducted at the Jiangwan campus of Fudan University in the northeast of Shanghai (121.5°E, 31.33°N). It is a typical urban environment, surrounded by commercial and residential areas. The campus ~~environment~~ itself is relatively clean air condition without~~and has no~~ significant sources of air pollutants~~ion~~, mainly is affected by ~~anthropogenic~~ traffic emissions from viaducts and residential areas nearby.

O_3, HONO, NO_2, NO, SO_2, and HCHO were monitored in real-time. O_3 and NO were measured by the short-path DOAS (Differential Optical Absorption Spectroscopy) instrument with a light path of 0.15 km and time resolution of 1 min. ~~and further analyzed in the~~ The fitting windows of them are 250-266 nm and 212-230 nm, respectively. HONO, NO_2, SO_2, and HCHO were measured by the long-path DOAS apparatus with a light path of 2.6 km and time resolution of 6 min. The spectral fitting intervals are 339-371 nm, 341-382 nm, 295-309 nm, and 313-341 nm, respectively. Meteorological parameters, including temperature, relative humidity, wind direction, and wind speed, were recorded by the collocated automatic weather station (CAMS620-HM, Huatron Technology Co. Ltd). The p~~P~~hotolysis frequency of NO_2 (J_{NO_2}) was measured with a filter radiometer (Meteorologie Consult Gmbh). CO was measured by a Gas Filter Correlation CO Analyzer (Thermo-Model 48i) with a time resolution of 1 h. Additionally~~Besides~~, NMVOCs were monitored using the TH-300B online VOCs Monitoring system that includes ultralow-temperature (-150 °C) preconcentration combined with gas chromatography and mass

spectrometry (GC/MS). Under the ultralow-temperature condition, the volatile organic compounds in the atmosphere are frozen and captured in the empty capillary trap column; then a rapid heating analysis is performed to make the mixture enter the GC/MS analysis system. After separation by chromatography, NMVOCs are detected by FID (flame ionization detector) and MS detectors. Typically, the complete detection cycle was one hour. CH_4 was measured by a Methane and Non-Methane hydrocarbon analyzer (Thermo-Model 55i) with a time resolution of 1 h.

All of the above techniques have been validated and applied in many previous studies, and their measurement principles, quality assurance, and control procedures were described in detail (Wang et al., 2015; Hui et al., 2018; Shen et al., 2016; Zhao et al., 2015; Nan et al., 2017; Hui et al., 2019).

2.2 Observation-based model

In this study, the in-situ atmospheric photochemistry was simulated using an observation-based model (OBM) incorporating the la~~s~~test version of Master Chemical Mechanism (MCM, v3.3.1; http://mcm.leeds.ac.uk/MCM/), a near-explicit chemical mechanism which describes the degradation of methane and 142 non-methane VOCs and over 17000 elementary reactions of 6700 primary, secondary and radical species (Jenkin et al., 2003; Saunders et al., 2003). The model can simulate the concentration of highly active radicals, so that the critical aspects of atmospheric chemistry can be quantitatively evaluated, including secondary products~~oxidant~~ formation (e.g., O_3 and PAN), VOC oxidation and radical budgets.

The observed data of O_3, NO_2, NO, CO, SO_2, HONO, CH_4, 54 species of NMVOCs, J_{NO_2}, water vapor (converted from relative humidity) and temperature were interpolated to a time resolution of 5 minutes and then input~~ted~~ into the model as constraints. The photolysis rates of other molecules such as O_3, HCHO, HONO, and OVOCs were driven by solar zenith angle and scaled by measured J_{NO_2} (Jenkin et al., 1997; Saunders et al., 2003). Considering the potential impact of cloud cover on the frequency of photolysis, we have discussed the impacts of cloud cover on the scaled photolysis rates in the Supplement. In addition to the chemistry, deposition process within the boundray layer height is also included in the model. The loss of all unrestricted and model-generated species caused by the deposition is set as the accumulation of the deposition velocity of 0.01 m s^{-1} in the boundary layer (Santiago et al., 2016). Given that the boundary layer height (BLH) varied typically from 400 m at night to 1400 m in the afternoon during summer (Shi et al., 2015), which means that the lifetime of the model-generated species was ranged between ~ 11 h at night and ~ 40 h during the afternoon. We have also carried out the sensitivity study on the deposition velocity and boundary layer height, as referred to the Supplement. The model simulation period for three different ozone levels is seven days, including four days of pre-simulation to make unconstrained compounds to reach steady state.

2.3 Evaluation of AOC and photochemical reactivity

According to the definition of AOC, it can be calculated by the equation (1) (Elshorbany et al., 2009; Xue et al., 2016):

$$AOC = \sum_i k_{Yi}[Y_i]\,[X] \sum k_{OH+VOC_i}[OH][VOC_i] + \sum k_{OH+CO}[OH][CO] + \sum k_{O_3+VOC_i}[O_3][VOC_i] + \sum k_{NO_3+VOC_i}[NO_3][VOC_i] \quad (1)$$

Where Y_i are VOCs, CO, and CH_4, X are oxidants (OH, O_3, and NO_3), and k_{Yi} is the bi-molecular rate constant for the reaction of Y_i with X. Atmospheric oxidation capacity determines the rate of Y_i removal (Prinn and Resources, 2003).~~The higher the AOC, the higher the removal rate of most pollutants.~~

Additionally~~Besides~~, another widely used indicator of atmospheric oxidation intensity is the OH reactivity, which is defined as the sum of the reaction rate coefficients multiplied by the concentrations of the reactants with OH and depends on the abundances and compositions of primary pollutants. As the inverse of the OH lifetime, OH reactivity is calculated by equation (2) (Mao et al., 2010) :

$$k_{OH} = \sum_i k_{OH+X_i}[X_i] \sum k_{OH+VOC_i}[VOC_i] + k_{OH+CO}[CO] + k_{OH+NO}[NO] + k_{OH+NO_2}[NO_2] + k_{OH+other}[other] \quad (2)$$

Where $[X_i]$ represents the concentration of species (VOC, NO_2, CO etc.) which react with OH and k_{OH+X_i} is the corresponding reaction rate coefficients~~The term 'other' represents other species that can react with OH, such as HNO_3. And the calculation of OH reactivity in this study only included the measured species~~.

Moreover, the ratio of the OH cycling to OH terminal loss, known as the OH chain length, can characterize atmospheric photochemical activity. The OH chain length can be calculated by equation (3) when the reaction between OH and NO_2 is the main termination reaction of radicals (Martinez et al., 2003; Mao et al., 2010)~~ (Mao et al., 2010)~~:

$$OH\ \ Chain\ \ Length = \frac{k_{OH}[OH] - k_{OH+NO_2+M}[OH][NO_2]}{k_{OH+NO_2+M}[OH][NO_2]} \quad (3)$$

This is one of several definitions available based on the assumption that OH + NO_2 is the main chain termination reaction, which is further discussed in Sect 3.3.~~Longer chain length means more HO_x cycling and more O_3 generation efficiency for each radical.~~

The AOC, OH reactivity, and OH chain length, as well as HO_x budget, can be quantitatively assessed by tracking the relative reactions and corresponding rates of the reactions in the OBM simulation.

3 Results and Discussion

3.1 Overview of O_3 and its precursors

All the measured data were hourly averaged. Figure 1 shows the observed time series of major pollutant~~s~~ mixing ratios~~concentrations~~ and meteorological parameters during the campaign from 1 May to 30 September 2019 at Jiangwan

campus in Shanghai. During the five-month observation period, the average temperature and humidity levels were 26.4 ℃ and 78.78%, respectively, while the mean mixing ratios~~concentrations~~ of O_3, NO_2, NO, HONO, and HCHO were 35.14±18.72 ppbv, 13.0±4.31 ppbv, 5.30±9.26 ppbv, 0.29±0.18 ppbv and 2.78±1.33 ppbv, respectively. According to the air quality index (AQI) data released by the Shanghai Environmental Monitoring Center (SEMC) and the ozone mixing ratio~~concentration~~ data observed, the overall air quality in Shanghai was good in the spring-summer season of 2018. The days with good air quality (AQI < 100) accounted for 92.2% during the experiment. However, there were occasionally high ozone pollution days, during which the primary pollutant of 10 days of the residual 12 polluted days is ozone (the average hourly ozone exceeded the Class 2 standard 93 ppbv, GB 3095-2012, China) (Ambient air quality standards, 2012).

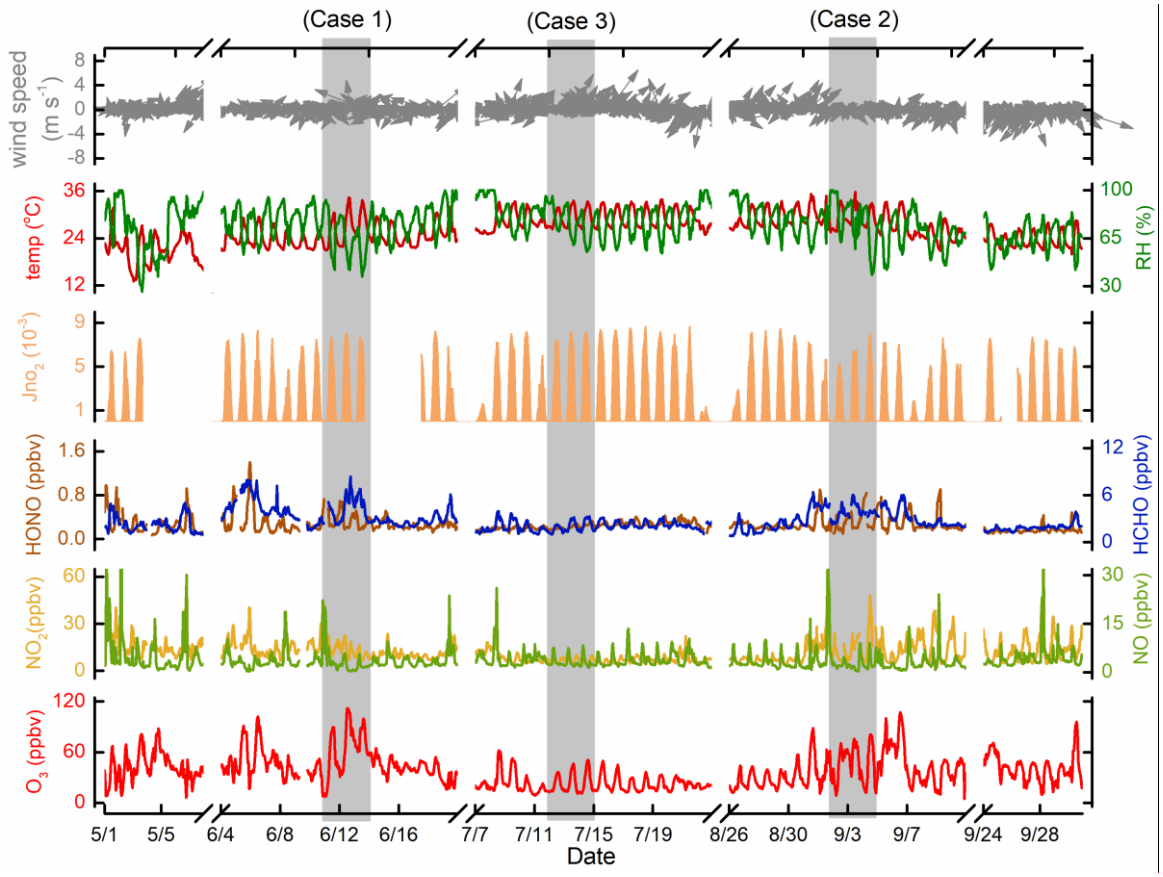
(Case 1)
(Case 3)
(Case 2)
wind speed (m s-1)
temp (°C)
RH (%)
Jno2 (10-3)
HONO (ppbv)
HCHO (ppbv)
NO2(ppbv)
NO (ppbv)
O3 (ppbv)
5/1
5/5
6/4
6/8
6/12
6/16
7/7
7/11
7/15
7/19
8/26
8/30
9/3
9/7
9/24
9/28
Date

205

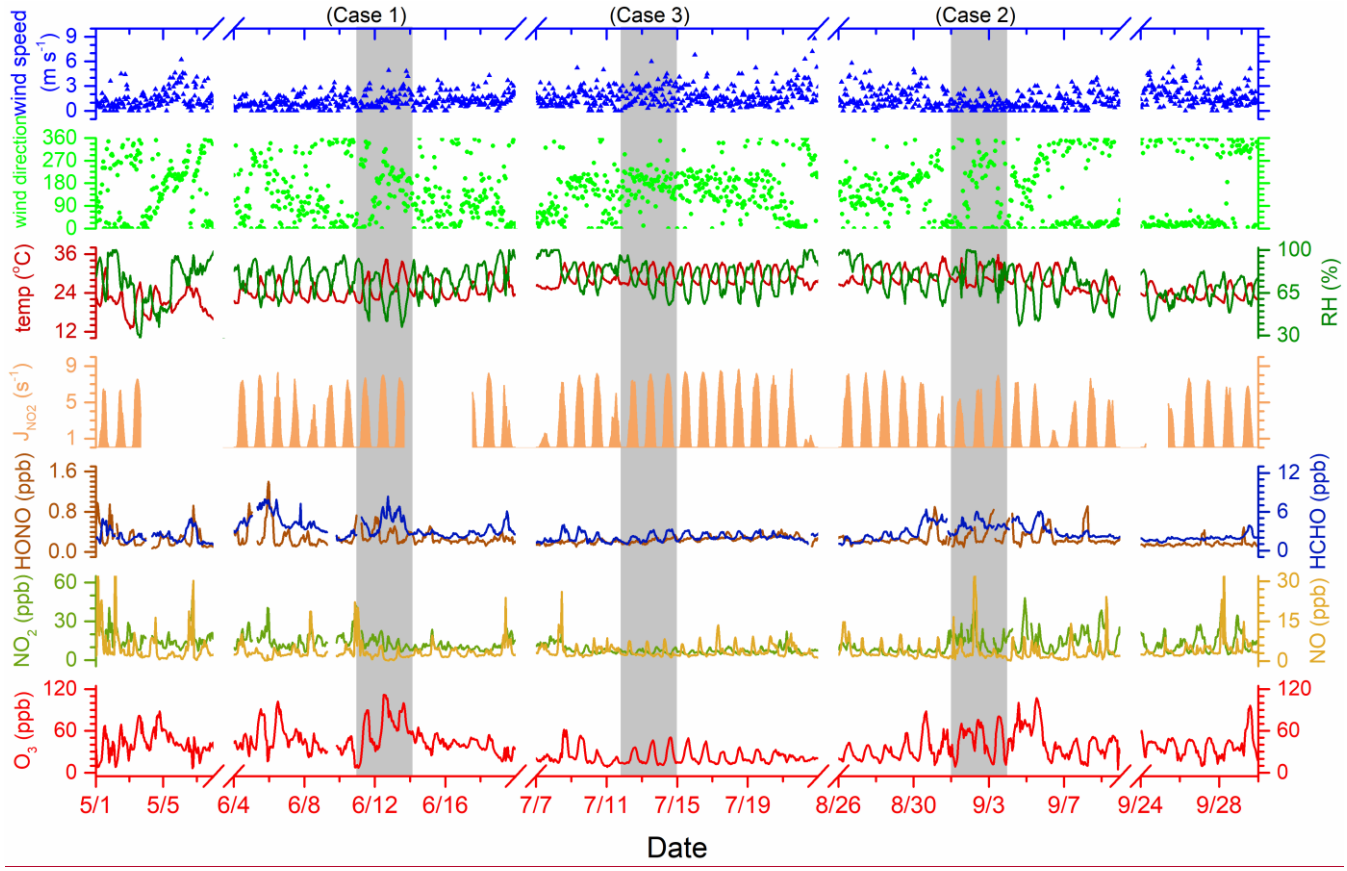

Figure 1. Time series of major pollutants mixing ratios~~concentrations~~ and meteorological parameters at an urban site ~~of~~ in Shanghai from 1 May to 30 September 2018, with three cases highlighted.

As indicated with the gray rectangle in Fig. 1, three cases of different ozone levels were selected to study atmospheric oxidation and free radical chemistry. These are the polluted case (Case 1) between 11 and 13 June, the semi-polluted case (Case 2) from 2 to 4 September and the non-polluted period (Case 3) of 12 to 14 July, respectively. As can be seen in Table 1 (also refer to Figure S1), the averaged O_3 mixing ratios~~concentrations~~ in Case 1, Case 2 and Case 3 were 65.13±27.16~~57.39~~ ppbv, 46.12±21.14~~43.92~~ ppbv and 23.95±11.89~~24.39~~ ppbv, during which the maximum mixing ratios~~concentrations~~ reached 111.87 ppbv, 80.76 ppbv, and 50.74 ppbv, respectively. By comparing the meteorological parameters, the wind speed of Case 3 was highest, followed by Case 2 and Case 1, indicating that the unfavorable diffusion conditions ~~is~~are one of the causes of ozone pollution. Although the ozone mixing ratio~~concentration~~ of Case 2 was much lower than that of Case 1, the levels of NO_x, CO, HONO in Case 2 were also high or close to Case 1. This is explained by the fact that meteorological parameters of Case 1 and Case 2 were quite different (Figure S2)~~the radiation of Case 1 was higher than Case 2~~, i.e. higher radiation, greater differences in temperature during day and night, and lower humidity and air pressure during Case 1 are conductive to~~which~~ enhance~~s~~ atmospheric photochemistry and lead to ozone formation. In addition, when the J_{NO_2} value input to the OBM was artificially

increased by 40% for Case 2, and the simulation result showed that the peak value of ozone increased by 30-40% as a consequence. The observations and simulations suggested that high radiation is an influencing factor in ozone pollution. However, ozone levels were lowest, during the most intensive radiation in Case 3. Under such favorable meteorological conditions, the low ozone mixing ratio~~concentration~~ was attributed to the low mixing ratios~~concentrations~~ of O_3 precursors NO_x and VOCs. Therefore, it can be inferred that ozone pollution was caused by the combination of high levels of O_3 precursors and strong radiation.

Table 1. Summary of pollutants mixing ratios~~concentrations~~ (unit: ppbv) and meteorological parameters for three cases of different ozone levels.

	Case 1 (11 to 13 June)		Case 2 (2 to 4 September)		Case 3 (12 to 14 July)	
	Average ± S.D.	Maximum	Average ± S.D.	Maximum	Average ± S.D.	Maximum
O_3	65.13 ± 27.16	111.87	46.12 ± 21.14	80.76	23.95 ± 11.89	50.74
NO_2	14.20 ± 6.13	38.25	15.62 ± 9.41	47.87	6.54 ± 1.52	10.17
NO	3.38 ± 4.27	34.27	4.37 ± 6.88	51.65	3.13 ± 1.82	10.51
CO	652 ± 93	860	654 ± 152	1170	390 ± 21	460
HONO	0.36 ± 0.16	0.72	0.32 ± 0.17	0.84	0.22 ± 0.05	0.34
J_{NO_2} (10^{-3} s^{-1})	2.78 ± 3.06	8.00	2.03 ± 2.50	7.96	2.94 ± 3.17	8.13
Wind speed (m s^{-1})	1.40 ± 1.11	4.90	0.83 ± 0.70	2.60	2.93 ± 1.21	6.00
RH (%)	64.37 ± 14.91	93.00	76.65 ± 16.49	100.00	75.45 ± 11.05	96.00
Alkanes	9.21 ± 2.81	16.74	10.57 ± 5.62	26.55	3.66 ± 0.93	5.95
Alkenes	3.24 ± 2.15	10.60	3.61 ± 1.70	9.68	1.41 ± 0.63	3.09
Aromatics	1.48 ± 0.69	4.09	2.88 ± 2.63	13.33	1.23 ± 1.17	11.52
OVOCs	9.20 ± 2.33	15.15	9.39 ± 2.75	18.76	4.12 ± 2.06	8.82
Haloalkanes	2.19 ± 0.60	5.37	3.29 ± 1.40	8.28	1.75 ± 1.34	5.90
NMVOCs	25.31 ± 6.16	41.68	29.73 ± 12.10	66.73	12.18 ± 3.69	21.98

The statistical information of each species groups of VOCs classified based on their chemical nature and composition is also shown in Table 1. In general, the mixing ratios of VOCs were highest in Case 2, followed by Case 1 and Case 3, with ~~an~~ average total VOC~~s~~ mixing ratios~~concentrations~~ of 25.31±6.16 ppbv, 29.73±12.10 ppbv, and 12.18±3.69 ppbv, respectively. During Case 1, OVOCs and alkanes accounted for the vast majority of total NMVOCs, reaching 36.3% and 36.4%, followed by alkenes (12.8%), other VOCs (8.7%) and aromatics (5.8%). For Case 2, alkanes and OVOCs also dominated total NMVOCs (35.5% and 31.6%), followed by alkenes (12.1%), other VOCs (11.1%) and aromatics (9.7%). During Case 3, OVOCs represented the largest contribution to total NMVOCs (33.8%), followed by alkanes (30.1%), other VOCs (14.4%), alkenes

(11.6%) and aromatics (10.1%). Table 2 shows the average mixing ratios and standard deviation of 54 VOCs including methane during the three cases. The key species in different groups were consistent in three cases, for example, ethane and propane were the two highest mixing ratio~~concentrations in~~ alkanes; the main alkene species ~~in alkenes~~ were ethylene and acetylene; the highest concentrations in aromatics were benzene and toluene; while HCHO and acetone were the dominant fraction in OVOCs.

Table 2. Summary of the mixing ratios of measured VOCs (unit: pptv, except for ppbv of methane) in three cases and their maximum incremental reactivity (MIR) (unit: g O_3/ g VOC, the ozone formation coefficient for VOC species in the maximum increment reactions of ozone.).

Species	MIR[a]	Case 1	Case 2	Case 3
Methane[b]	0.00144	2181 ± 164	2178 ± 189	1812 ± 55
		Alkanes		
Ethane	0.28	3838 ± 1181	3654 ± 1861	1100 ± 182
Propane	0.49	1954 ± 601	1860 ± 947	560 ± 93
n-Butane	1.15	1132 ± 439	1535 ± 938	499 ± 169
i-Butane	1.23	715 ± 266	883 ± 440	300 ± 93
n-Pentane	1.31	414 ± 185	716 ± 697	193 ± 126
i-Pentane	1.45	670 ± 236	1267 ± 1116	305 ± 129
n-Hexane	1.24	138 ± 116	222 ± 168	46 ± 20
2-Methylpentane	1.50	127 ± 41	133 ± 130	59 ± 18
3-Methylpentane	1.80	96 ± 40	197 ± 140	35 ± 10
n-Heptane	1.07	54 ± 27	15 ± 13	5 ± 1
n-Octane	0.90	32 ± 13	37 ± 26	186 ± 220
n-Nonane	0.78	21 ± 10	28 ± 13	208 ± 255
n-Decane	0.58	14 ± 8	23 ± 14	170 ± 222
		Alkenes		
Ethylene	9.00	1070 ± 747	1093 ± 711	439 ± 232
Propylene	11.66	541 ± 1130	251 ± 229	150 ± 127
1-Butene	9.73	63 ± 68	88 ± 55	62 ± 43
2-methylpropene	6.29	222 ± 88	386 ± 219	192 ± 98
Trans-2-Butene	15.16	58 ± 43	98 ± 42	37 ± 15
Cis-2-Butene	14.24	6 ± 0	28 ± 36	14 ± 8
1,3-Butadiene	12.61	10 ± 11	24 ± 12	20 ± 14
1-Pentene	7.21	13 ± 10	14 ± 9	22 ± 14
Isoprene	10.61	189 ± 185	364 ± 468	202 ± 213
Acetylene[c,*]	0.95	1223 ± 452	1264 ± 670	276 ± 99
		Aromatics		
Benzene	0.72	388 ± 277	454 ± 305	59 ± 27
Toluene	4.00	501 ± 270	1325 ± 1463	236 ± 320
Ethylbenzene	3.04	196 ± 160	282 ± 222	160 ± 159
m/p-Xylene	9.75	248 ± 195	538 ± 516	474 ± 596
o-Xylene	7.64	81 ± 48	164 ± 146	158 ± 232
m-Mthyltoluene	7.39	12 ± 6	26 ± 16	28 ± 34
p-Mthyltoluene	4.44	11 ± 7	16 ± 9	18 ± 16
o-Mthyltoluene	5.59	10 ± 4	15 ± 8	18 ± 20
1,3,5-Trimethylbenzene	11.76	8 ± 3	12 ± 8	17 ± 17
1,2,4-Trimethylbenzene	8.87	14 ± 7	31 ± 23	39 ± 49
1,2,3-Trimethylbenzene	11.97	9 ± 3	13 ± 8	19 ± 20
		OVOCs		

Formaldehyde	9.46	4376 ± 1444	3841 ± 793	2014 ± 670
Propionaldehyde	7.08	163 ± 61	170 ± 61	180 ± 162
Acetone	0.36	3692 ± 781	3076 ± 843	1154 ± 739
Butanal	5.97	32 ± 17	55 ± 15	81 ± 80
Valeraldehyde	5.08	12 ± 8	49 ± 13	148 ± 218
n-Hexanal	4.35	29 ± 0	29 ± 0	29 ± 0
2-Butanone	1.48	536 ± 216	1181 ± 1631	168 ± 117
Methyl tert-butyl ether	0.73	143 ± 109	287 ± 263	41 ± 15
3-Pentanone	1.24	22 ± 15	26 ± 11	60 ± 90
2-Pentanone	2.81	7 ± 2	433 ± 216	72 ± 103
Acrolein	7.45	73 ± 34	52 ± 23	69 ± 56
Methacrolein	6.01	32 ± 24	73 ± 68	35 ± 28
Methyl vinyl ketone	9.65	85 ± 54	115 ± 88	73 ± 63
		Other VOCs		
Chloroform	0.022	173 ± 52	256 ± 87	64 ± 22
Dichloromethane	0.041	1353 ± 649	1941 ± 1147	1202 ± 1357
Chloromethane	0.038	511 ± 114	834 ± 215	424 ± 97
Trichloroethylene	064	63 ± 59	98 ± 60	20 ± 13
Tetrachloroethylene	0.031	63 ± 27	88 ± 35	31 ± 15
Chloroethane	0.29	32 ± 14	70 ± 65	13 ± 7

Note: Alcohols were not measured

[a] ~~unit: g O_3/ g VOC.~~

[b] ~~the concentration units of methane are ppbv, and concentrations of other species are presented in pptv.~~

[c*] D~~d~~ue to acetylene ~~is~~ being similar in nature to alkenes, acetylene is classified into the alkenes category. It should be noted that the reactivity of acetylene with OH is far less than that of alkenes with OH.

3.2 Atmospheric oxidation capacity and OH reactivity

According to Eq. (1), AOC during the three case periods was quantified based on the OBM, as shown in Fig. 2. The calculated maximum AOC for the three Cases was ~~1.1~~1.0×10^8 molecules cm^{-3} s^{-1}, 9.1~~8.9~~×10^7 molecules cm^{-3} s^{-1} and ~~8.1~~8.8×10^7 molecules cm^{-3} s^{-1}, respectively. Comparatively, these are much lower than those computed for Santiago de Chile, Chile with a peak of 3.2×10^8 molecules cm^{-3} s^{-1} (Elshorbany et al., 2009), but much higher than that in Berlin, Germany with 1.4×10^7 molecules cm^{-3} s^{-1} (Geyer et al., 2001). It can be seen from Fig. 2 that the time profile of the AOC exhibits a diurnal variation, which is the same as the time series of the model calculated OH concentration and the observed J_{NO_2}, with a peak at noon. Daytime averaged AOC were 3.96±2.32~~4.38~~×10^7 molecules cm^{-3} s^{-1}, 3.54±2.24~~4.14~~×10^7 molecules cm^{-3} s^{-1} and 3.59±2.51~~4.06~~×10^7 molecules cm^{-3} s^{-1}, while nighttime average AOC value were 3.11±1.15~~4.54~~×10^6 molecules cm^{-3} s^{-1}, 2.38±0.57~~4.02~~×10^6 molecules cm^{-3} s^{-1} and 4.30±0.53~~7.02~~×10^5 molecules cm^{-3} s^{-1}, for the three cases respectively. These values were in line with the ozone levels, suggesting that atmospheric oxidation capacity during the ozone pollution period is greater than under clean conditions.

As expected, OH was calculated to be the main contributor to AOC. In the three cases, the average contribution of OH during the daytime accounted for over 96%. O_3, as the second important oxidant, accounted for 1~3% of the daytime AOC. The contribution of NO_3 to nighttime AOC was 1.50±0.52~~2.43~~×10^6 molecules cm^{-3} s^{-1}, 1.24±0.38~~2.35~~×10^6 molecules cm^{-3} s^{-1}

and 3.02±1.94~~1.21~~ ×-10~~5~~4 molecules cm^{-3} s^{-1}, respectively (or see Figure S3). Especially, during Case 1 and 2 with relatively polluted conditions, NO_3 became the primary oxidant in AOC, accounting for ~~53.4~~48.3% and ~~58.3~~52.3% of the nighttime AOC, respectively. It is worth noting that the chlorine atom produced by the photolysis of $ClNO_2$ may also contribute to AOC (Bannan et al., 2015) , but unfortunately it has not been quantitatively characterized in this study. In general, OH dominated AOC during daytime and NO_3 is the main oxidant at night, which is consistent with previous studies (Asaf et al., 2009; Elshorbany et al., 2009).

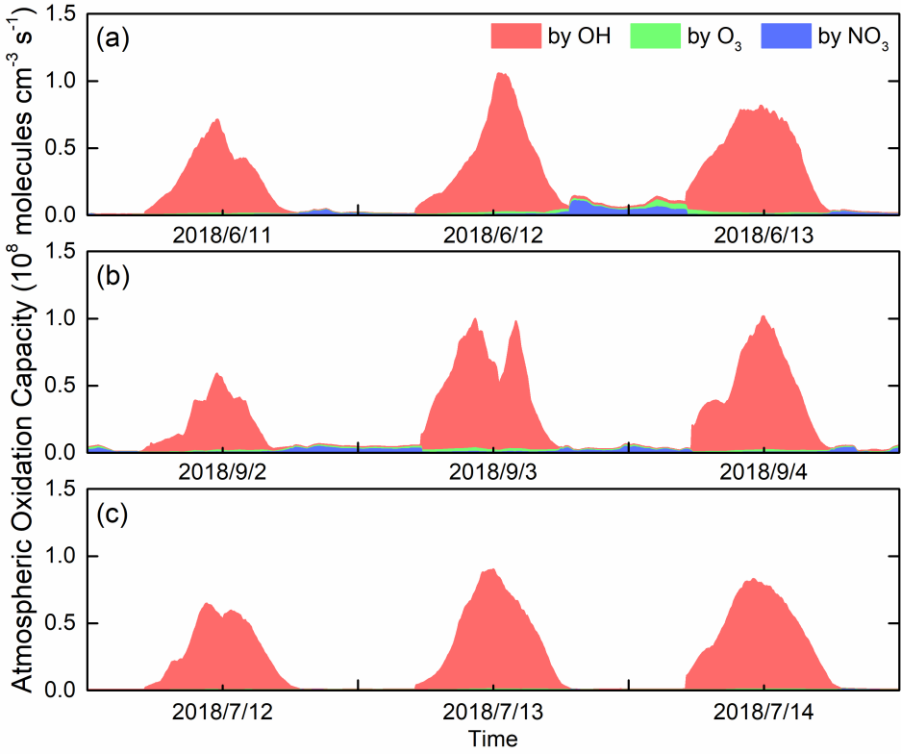

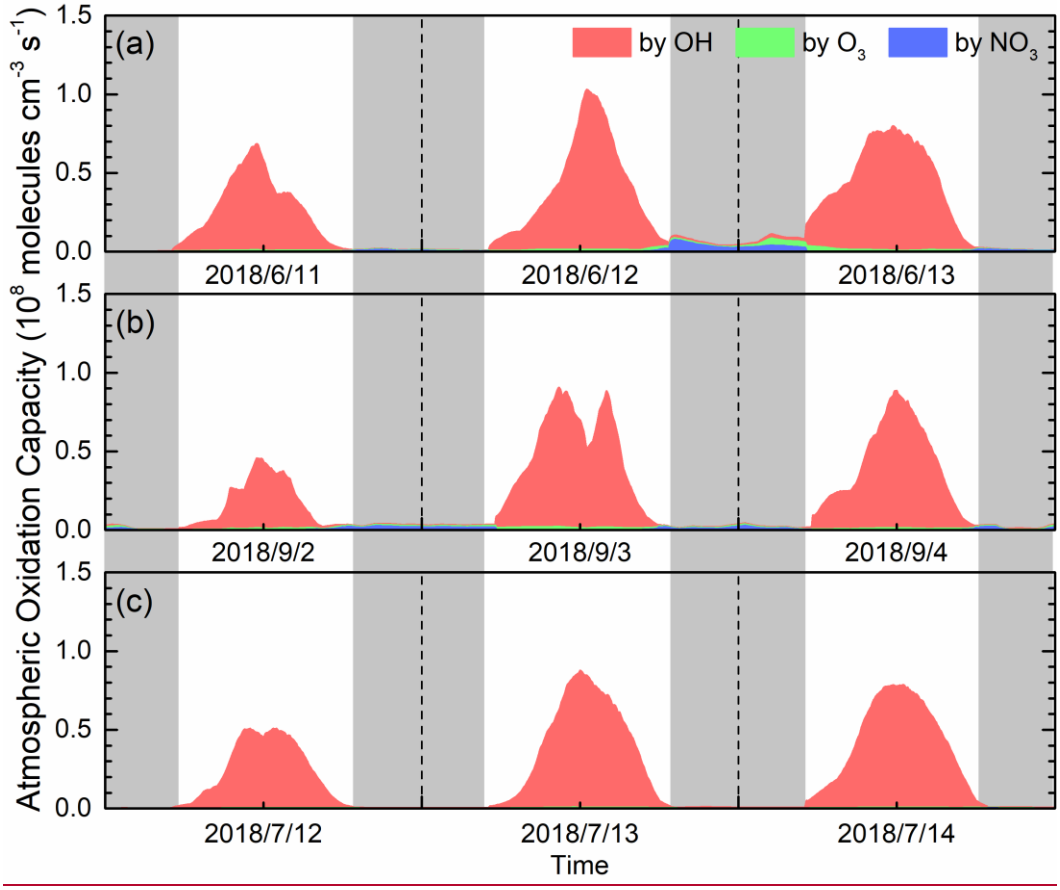

Figure 2. Modelled daytime atmospheric oxidation capacity and contributions of major oxidants at an urban site of Shanghai during (a) Case 1, (b) Case 2 and (c) Case 3. The grey areas denote the nighttime periods.

We now evaluate the loss frequency of the different reactants to OH using the indicator of OH reactivity according to Eq. (2). The diurnal variations of OH reactivity calculated via the OBM are presented in Fig. 3, including the contribution from measured VOCs, NO_x, ~~and~~ CO and model-generated intermediate species during three cases. It is evident that the OH reactivity peaked in the morning, with maximum values of 19.~~36~~ 61 s^{-1}, ~~28.71~~24.55 s^{-1} and 13.32 s^{-1} for three cases, respectively. This is due to the increased NO_x at the traffic rush hour (Sheehy et al., 2010). The average values in the three cases were 11.72~~65~~ ±2.84~~91~~ s^{-1}, 13.45~~70~~ ±4.25~~60~~ s^{-1} and 7.56~~27~~±1.52~~80~~ s^{-1}, respectively. The OH reactivity of Case 3 in the clean environment was significantly lower than that of Case ~~2~~ 1 and Case 2~~3~~, which is consistent with previous studies (Mao et al., 2010; Li et al., 2018). In general, the OH reactivity assessed in Shanghai was in the range of 4.6-~~28~~25.0 s^{-1} under different air quality conditions, which was at a relatively low level compared to that calculated for other big cities in China such as Guangzhou (20-30 s^{-1}), Chongqing (15-25 s^{-1}) and Beijing (15-25 s^{-1}) (Tan et al., 2019b), reflecting that the abundance of pollutants in Shanghai is relatively lower compared to other metropolitan areas in China .

Total OH reactivity has been measured in many urban areas over the past two decades. Compared to the studies in other regions, the estimated average OH reactivity in Shanghai was much lower than that in Paris (Dolgorouky et al., 2012), New York (Ren et al., 2003; Ren et al., 2006), and Tokyo (Yoshino et al., 2006), and was equivalent to Nashville (Kovacs et al., 2003), ~~and~~ Houston (Mao et al., 2010) and London (Whalley et al., 2018). ~~It should be noted that the OH reactivity in this study was estimated by OH oxidation of the measured species, and does not involve species that are not measured like alcohols.~~ In addition, there are some differences between the actual measured values and the estimated values of OH reactivity as mentioned in previous studies, which may be attributed to missing OH reactivity that originates from secondary products such as other OVOC and nitrate produced by photochemical reactions (Di Carlo et al., 2004; Yoshino et al., 2006; Dolgorouky et al., 2012). We also calculated the OH reactivity only considering the measured species, and the contribution of OVOCs to OH reactivity was 1.28 s^{-1}, 1.43 s^{-1}, and 0.82 s^{-1}, while the OH reactivity of OVOCs calculated by considering the simulated intermediate species was 1.77 s^{-1}, 2.05 s^{-1} and 1.26 s^{-1} in three cases, respectively. These differences indicates unmeasured species~~Unmeasured alcohols~~ and unknown secondary products contributed considerably to the actual OH reactivity~~, which indicates that the OH reactivity obtained by model calculation in this study is somewhat underestimated~~.

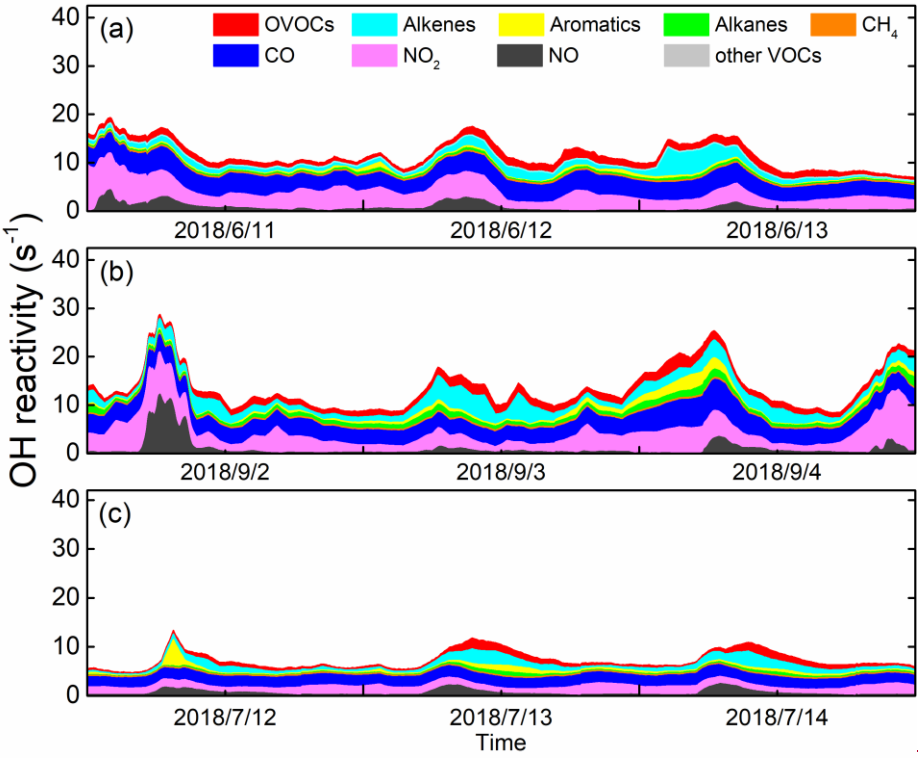

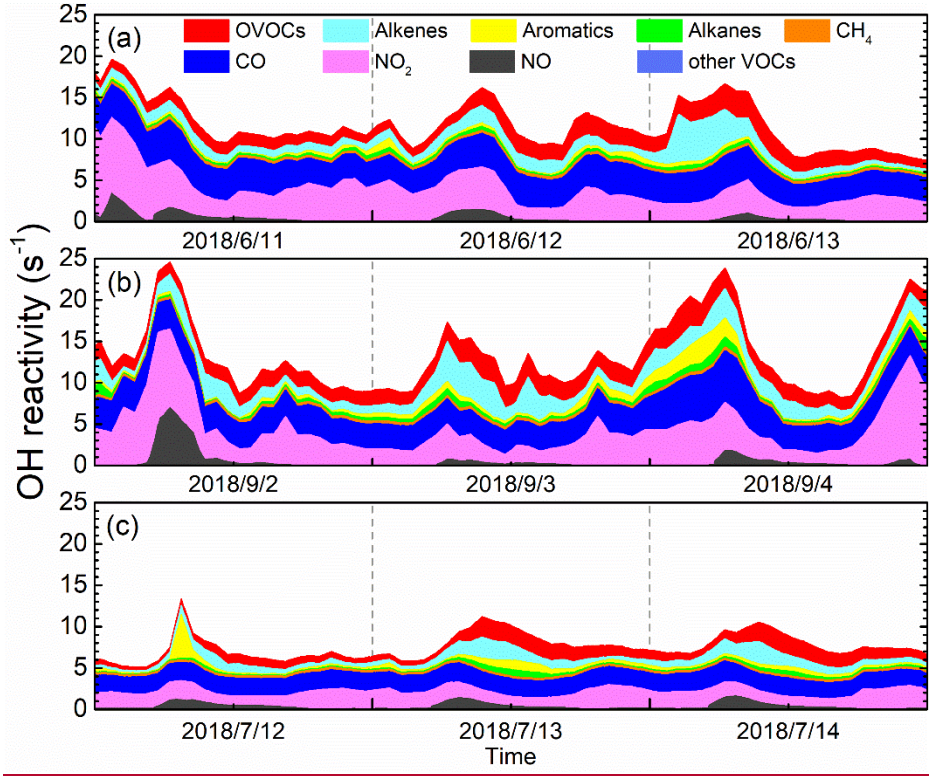

Figure 3. Diurnal profiles of OH reactivity by oxidation of all measured reactant groups at an urban site of Shanghai during (a) Case 1, (b) Case 2 and (c) Case 3.

Figure 4 (a) shows the average contribution of major groups of reactants to the total OH reactivity for three cases, including NMVOCs, NO_2, NO, CO, and CH_4. Overall, NMVOCs, CO and NO_2 are major contributors to OH reactivity, in line with past studies carried out in the urban environments (Ling et al., 2014; Gilman et al., 2009). The remarkable contribution of CO to the total OH reactivity in Case 1 points to the effective CO + OH and its significant contribution to ozone formation (Ling et al., 2014). The main difference in the composition of OH reactivity was the absolute contribution of NMVOCs in Case 1 was about 1.45 times than that of Case 2, while the absolute contributions of CO and NO_x to OH reactivity in Case 1 were comparable to those of Case 2. This ~~may be~~is caused by the higher VOCs levels of 29.73±12.10 ppbv during the Case 2 as compared to Case 1 of about 15% lower. Since the mixing ratios~~concentration~~ of pollutants in Case 3 ~~was~~ were quite low, the contribution of each reactant component to OH reactivity was much lower than the other cases.

Figure 4 (b) also presents the detailed contribution of each NMVOC group to the total OH reactivity. It can be seen that the contribution of OVOCs to OH reactivity is predominant, accounting for ~~36.86~~46.87%, ~~26.79~~40.79% and ~~30.74~~43.03% of the total OH reactivity of NMVOCs in the three cases. The contribution rate of OVOCs to OH reactivity in Case 1 was ~~6~~ 3 to ~~8~~ 6

percentage points higher than Case 2 and Case 3, illustrating the importance of OVOCs in atmospheric photochemistry and ozone generation (Fuchs et al., 2017). The contribution of alkenes to OH reactivity was importantthe largest in three cases, reaching about 4036%, which may be caused by the relatively higher contribution of alkenes emitted by motor vehicles at the urban site, indicating that ozone pollution was severely affected by vehicle emissions in Shanghai (Ling et al., 2014; Guo et al., 2013). Besides, the The contribution of aromatics and alkanes to OH reactivity wereas comparablesimilar in the three periods, both in range of 0.3~0.6 s^{-1}, accounting for 10%~20%. withAnd the contribution of other VOCs being to OH reactivity was negligible, which contribution ratio was only 0.4% or less. Since the calculation of OH reactivity did not include unmonitored alcohols, the results may underestimate the contribution of OVOCs to OH reactivity. In a previous study, Tan et al. (2019b) also reported the comparable average contribution of OVOCs to OH reactivity was about 2.9713.5 s^{-1} (k_{OH} = 13.45 s^{-1} in Case 2 this study) and similar contribution distribution of OH reactivity during summer in Shanghai. when the maximum ozone was 80 ppbv (similar to Case 2, k_{OH} = 1.43 s^{-1}) in Shanghai in August (Tan et al., 2019b). This also confirms the underestimation of atmospheric photochemical effects of OVOCs due to some missing OVOC measurements in this study.

In summary, the mixing ratiosconcentration of ozone precursors and their contribution to OH reactivity were found to be different in the three cases. To further investigate these differences, HO_x budget, OH chain length, and OFP (ozone formation potential) are discussed in depth in the following sections.

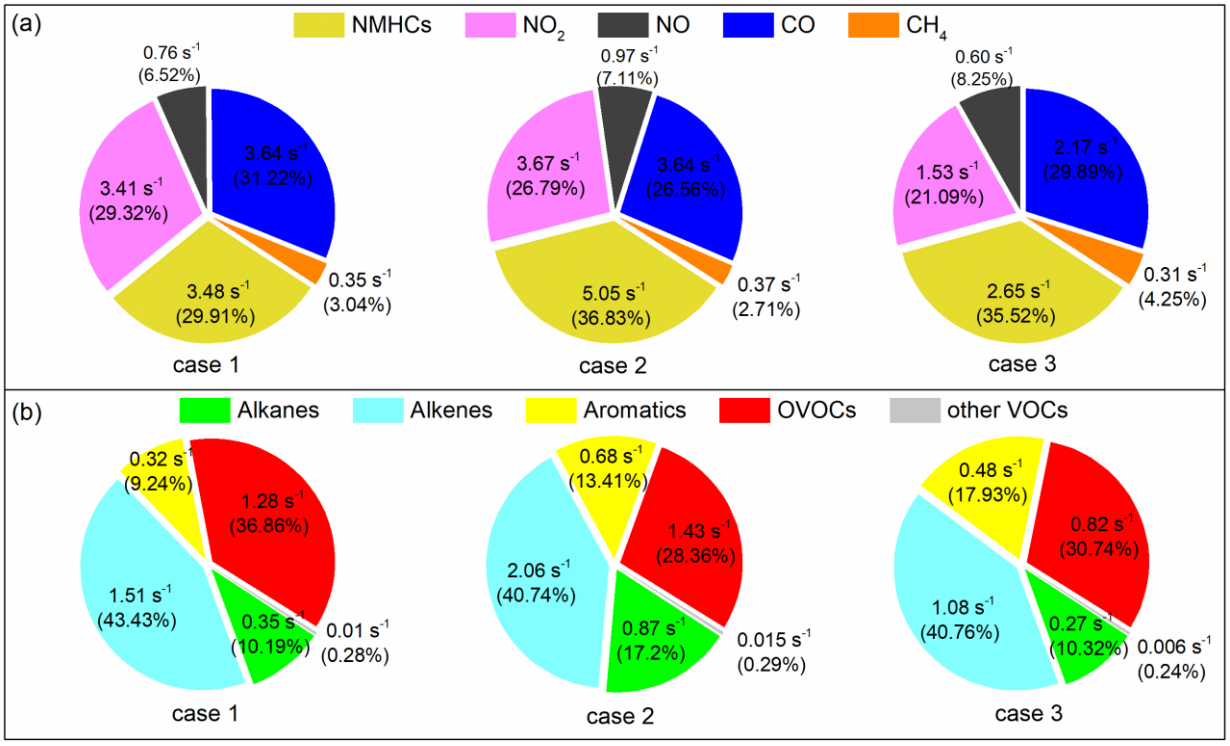

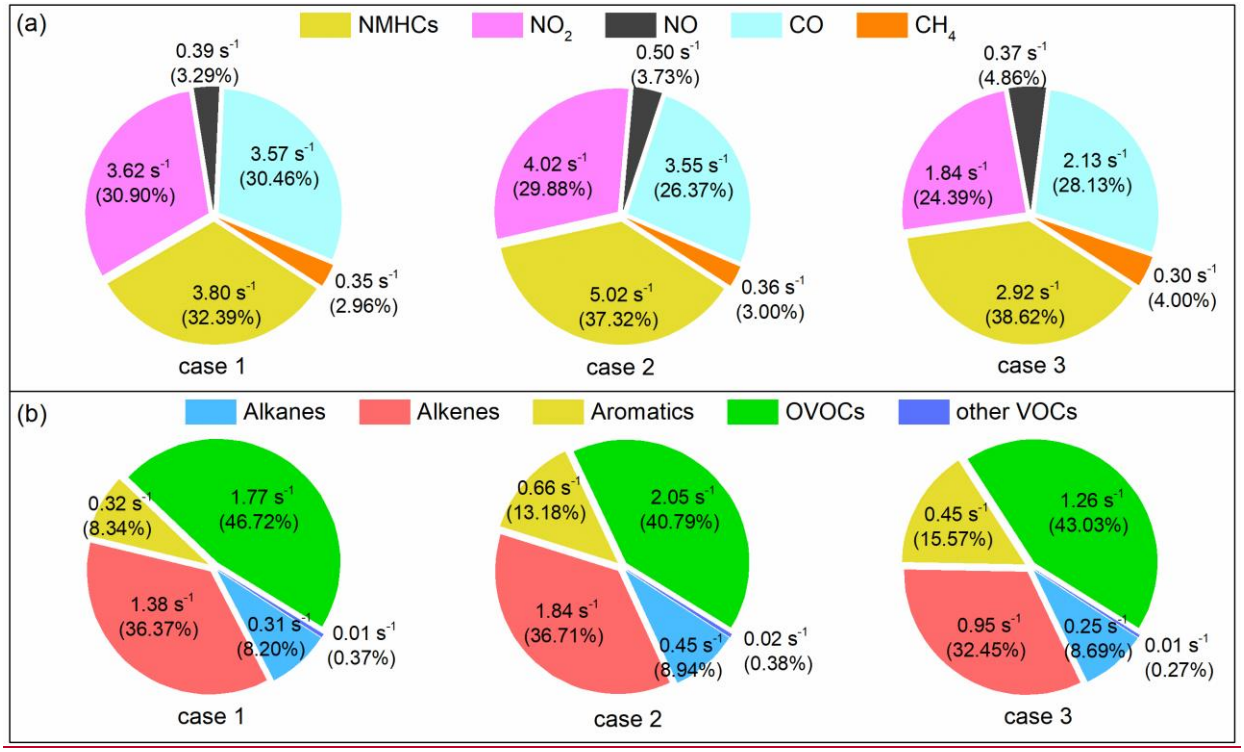

Figure 4. (a) The average contribution of major groups of reactants to the total OH reactivity during the three cases; (b) The contribution of each NMVOC group to the OH reactivity of NMVOCs during three cases.

3.3 OH chain length and HO_x budget

The OH chain length serves as an indicator for evaluating ~~the~~ HO_x cycling and is closely related to ozone production efficiency. The OH concentration and the terminal loss rate of OH by the reaction with NO_2 were simulated by the OBM. The longer chain length means that more OH radicals are generated in the HO_x cycling and more O_3 is produced before the OH terminal reaction occurs (Mao et al., 2010; Ling et al., 2014). As a previous studies showed, the OH chain length began to rise in the morning and peaked at noon (Mao et al., 2010; Ling et al., 2014; Emmerson et al., 2007). As illustrated in Fig. 5, the OH chain lengths were all ~~within 10~~less than 8, with a peak at noon. Interestingly, it was found that the OH chain length peak in Case 1 appeared around 2:00 pm, coinciding with the observed NO_x variability (see Figure~~.~~ S1). The OH chain lengths for the three cases peaked at ~~7.5~~6.3 in Case 3, followed by Case 2 (peak of ~~6.7~~5.5) and Case 1 (peak of ~~4.4~~4.1), opposite to O_3 levels (Table 1). This is ~~probably~~ due to the relatively higher NO_x level in Case 1 (see Figure S1), resulting in a relatively bigger sink of OH + NO_2. In summary, the longer OH chain length in Case 3 indicated ~~its more efficient ozone generation efficiency, followed by Case 2 and Case 1, despite the concentrations of ozone and its precursors being lower in Case 3.~~per NO_x converted into HNO_3 produces more O_3, whereas the NO_x mixing ratio in Case 3 is almost half that of Case 1 and 2 during daytime (see

Figure S1), causing ozone mixing ratio to be lower than Case 1 and 2. In addition, previous studies also found that the OH chain length was opposite to the ozone level, and gave the possible explanation also due to the lower NO_X concentrations (Mao et al., 2010; Ling et al., 2014).

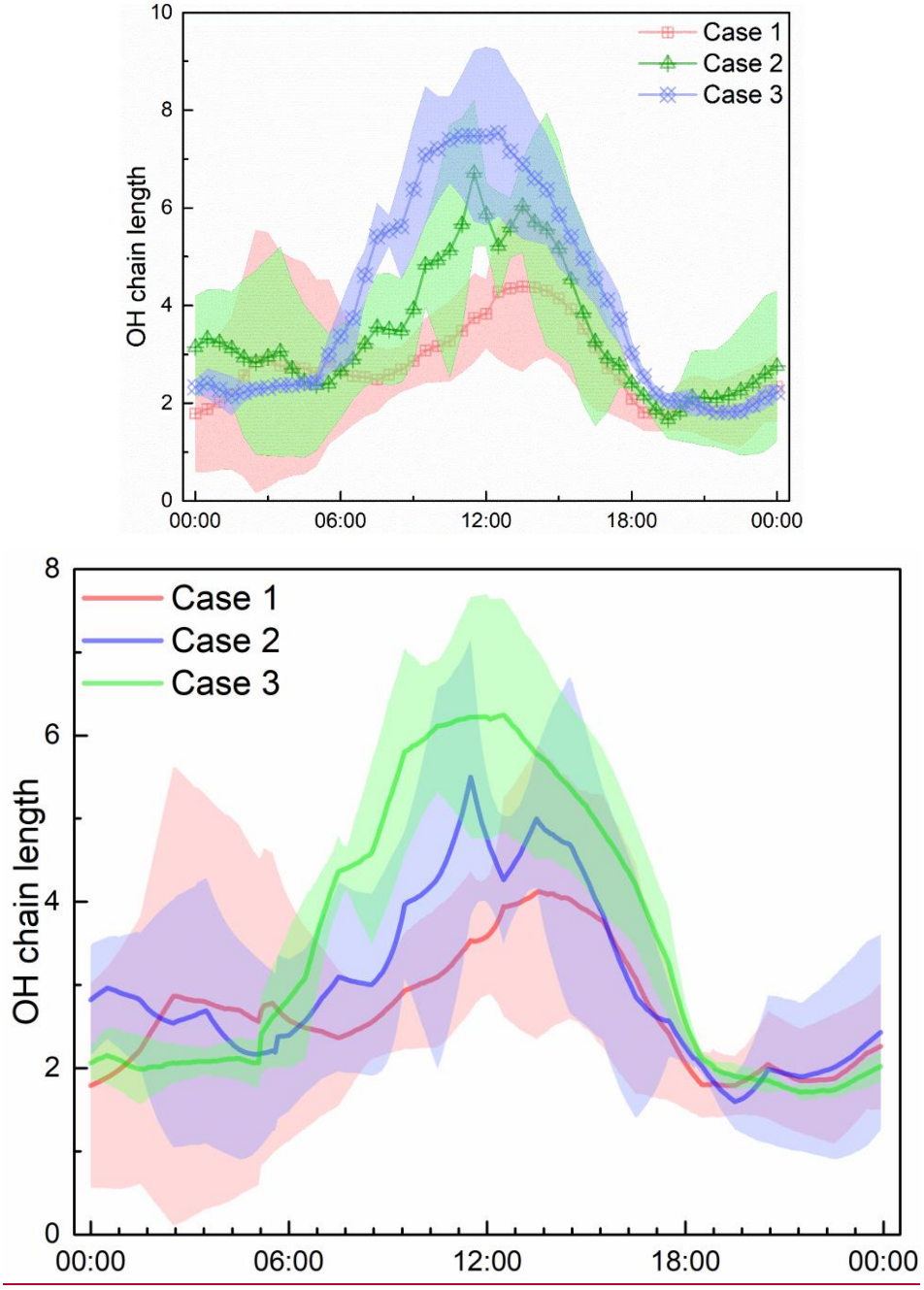

Figure 5. Average diurnal profiles of OH chain length during three cases at an urban site of Shanghai. The shaded area

indicates the standard deviation of OH chain length.

We calculated the primary sources of HO_x, including the photolysis of O_3, HONO, HCHO and other OVOCs, as well as the ozonolysis of alkenes, excluding parts (i.e. H_2O_2, CH_3OOH) that contribute less to HO_x (Mao et al., 2010; Ling et al., 2014; Sommariva et al., 2004) and any reactions in the HO_x cycling such as HO_2 + NO reaction that dominates OH generation and is just the cycling between OH and HO_2 (Mao et al., 2010). At the same time, the sinks of HO_x ~~was~~ were also simulated, including the reactions of OH + NO_2, HO_2 + HO_2 and HO_2 + RO_2, and also excluding any reactions of HO_x cycling as well as smaller contributing reactions. These HO_x production and loss pathways were considered and well investigated in other studies and locations (Mao et al., 2010; Ling et al., 2014; Wang et al., 2018).

Figure 6 shows the diurnal variability of the main generation and loss pathways of HO_x. It can be seen that the intensity of the sources and sinks of HO_x was different, but the primary contributions to HO_x budget of three cases were consistent, i.e. O_3 photolysis and reaction of OH with NO_2, respectively. The average generation rates of HO_x were~~was~~ 1.51±0.92~~1.54~~ ×10^7 molecules cm^{-3} s^{-1}, 1.10±0.70~~1.21~~ ×10^7 molecules cm^{-3} s^{-1} and 1.05±0.71~~1.10~~ ×10^7 molecules cm^{-3} s^{-1}, while the average loss rates ~~was~~ were 1.34±0.74~~1.49~~ ×10^7 molecules cm^{-3} s^{-1}, 1.00±0.55~~1.40~~ ×10^7 molecules cm^{-3} s^{-1}, and 0.8±0.52~~1.06~~×10^7 molecules cm^{-3} s^{-1}, respectively. During the daytime, the biggest contribution to HO_x production was ozone photolysis, around 40% in Case 1 and Case 2, while HONO photolysis contributed ~~39.2~~41.1% in Case 3. This indicates that ozone photolysis dominates the production of HO_x under high ozone conditions, whereas photolysis of HONO is important at lower ozone concentrations (Wang et al., 2018; Ling et al., 2014; Ren et al., 2008). Additionally~~Besides~~, the model results show that the photolysis of HCHO was also an important contributor to HO_x production in the three cases, reaching 25.9%, ~~23~~22.9~~1~~% and ~~23~~21.04%, respectively (Ling et al., 2014; Liu et al., 2012; Lu et al., 2012; Mao et al., 2010).

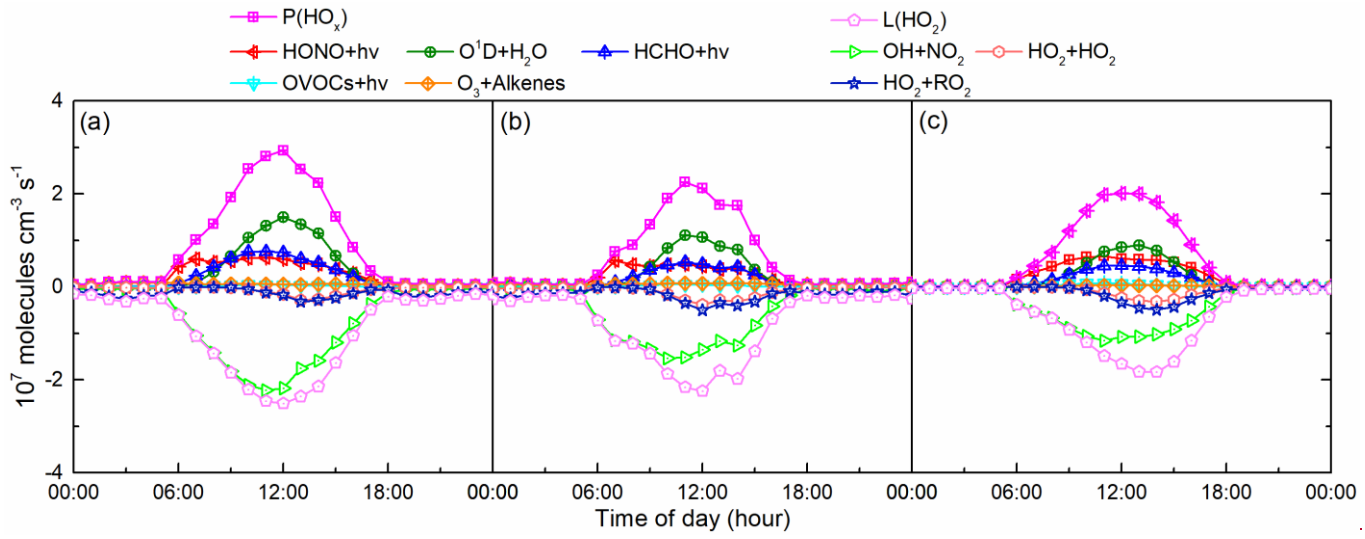

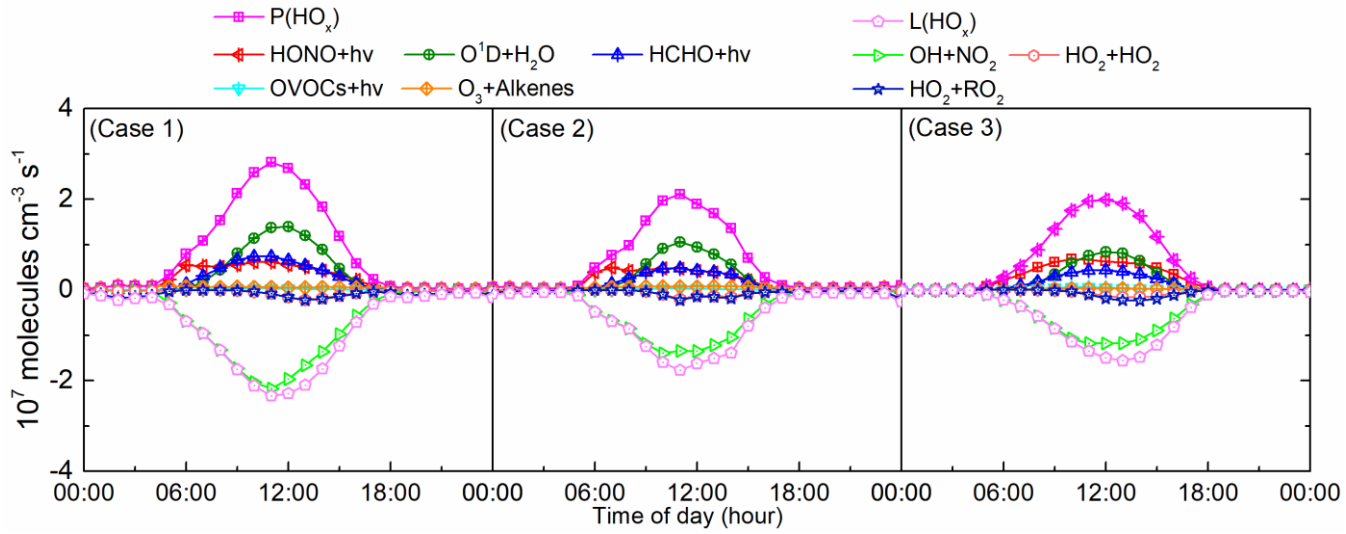

Figure 6. The average diurnal profiles of HO_x sources and sinks in (a) Case 1, (b) Case 2 and (c) Case 3 at an urban site of Shanghai.

Moreover, the diurnal profile of the HO_x budget was explored. Before 9:00 am, 9:30 am and 11:00 am during the three cases, respectively, HONO photolysis dominated the production of HO_x in the morning due to the accumulation of HONO at night. This is consistent with a previous report in Shanghai in July 2014 which found that the contribution of HONO photolysis could reach up to 80% of HO_x production in the morning (Chan et al., 2017). In addition, $ClNO_2$ photolysis is also reported to be an important source of radicals in the morning (Young et al., 2012). In the afternoon, the HONO mixing ratio~~concentration~~ decreased with photolysis, O_3 levels increased with the enhancement of photochemical intensity, and O_3 photolysis becomes the main contributor to HO_x production. Note however that the contribution of HONO and HCHO photolysis are not negligible in the afternoon. The other two HO_x formation pathways, OVOCs photolysis and alkenes ozonolysis, accounted for less than 5% in the three cases.

For the HO_x sink, the reaction of OH and NO_2 was dominant all day, and its average contribution reached 1.20±0.67~~1.27~~ ×10^7 molecules cm^{-3} s^{-1}, 0.84±0.45~~1.03~~ ×10^7 molecules cm^{-3} s^{-1} and 0.71±0.40~~0.74~~ ×10^7 molecules cm^{-3} s^{-1}, accounting for 89.11%, 84.56% and 83.29% in three cases, respectively. In Case 2 and Case 3, the reaction of OH and NO_2 dominates the sinks of HO_x before 9:00 am when NO_x was at a high level due to traffic rush hour. However, the reaction of OH and NO_2 completely dominated the HO_x sinks from 5:30 am to 11:00 am in Case 1, almost contributing all the HO_x sinks, which indicates that the traffic rush hour traffic was prolonged and the NO_x was maintained at a high concentration. This is consistent with the fact that the peak of the OH chain length appears at 2:00 pm in Case 1, as mentioned above. The reaction with NO_2 was the main sink of HO_x, confirming that equation (3) of the OH chain length chosen in this study is appropriate. The reactions between radicals themselves such as HO_2 + HO_2 and HO_2 + RO_2 became more important for the contribution of HO_x sinks in the afternoon for

the three cases, in agreement with previous studies in other regions (Guo et al., 2013; Ling et al., 2014; Mao et al., 2010).

Regarding the model-simulated concentrations of OH and HO_2, as shown in Figure S4, the maximum concentrations of OH for three cases were 9.97×10^6 molecule cm^{-3}, 8.34×10^6 molecule cm^{-3} and 10.3×10^6 molecule cm^{-3}, respectively. And the maximum concentrations of HO_2 for three cases were 4.06×10^8 molecule cm^{-3}, 3.84×10^8 molecule cm^{-3} and 3.41×10^8 molecule cm^{-3}, respectively. The previous simulated maximum concentrations of OH and HO_2 for urban site in Shanghai were 6.9×10^6 molecule cm^{-3} and 1.9×10^8 molecule cm^{-3} in summer, which lower than the simulated results here probably because of the different atmospheric conditions (Tan et al. 2019b). Due to lack of measured value of HO_x in Shanghai, we compared the measured value of other places in China. For instance, daily maximum concentrations were in the range of $(4\text{-}17)\times10^6$ molecule cm^{-3} for OH and $(2\text{–}24)\times10^8$ molecule cm^{-3} for HO_2 at the both suburban site Yufa and rural site Wangdu during summer in the North China Plain (Lu et al., 2013; Tan et al., 2017). In autumn, maximum median radical concentrations of 4.5×10^6 molecule cm^{-3} for OH at noon and 3×10^8 molecule cm^{-3} for HO_2 were reported for the Pearl River Delta in the early afternoon (Tan et al., 2019a). The simulated HO_x concentrations in this study were comparable with the measured results of other places in China, suggesting the moderate abundance of the HOx radical in Shanghai.

3.4 Ozone formation potential

Different VOC species have a wide range of reactivity and different potentials for O_3 formation, which can be calculated by the maximum incremental reactivity (MIR) (Carter, 2010). The calculated ozone formation potential (OFP) of each VOC species is used to characterize the maximum contribution of the species to ozone formation (Bufalini and Dodge, 1983). The following equation is used to calculate the OFP for each VOC species (Schmitz et al., 2000; Ma et al., 2019),

$$OFP_i = MIR_i \times [VOC_i] \times \frac{M_i}{M_{ozone}} \quad (4)$$

where OFP_i (ppbv) is the ozone formation potential of VOC species i, $[VOC_i]$ (ppbv) is the atmospheric mixing ratio~~concentration~~ of VOC species i, MIR_i (g O_3/g VOC, as listed in Table 1) is the ozone formation coefficient for VOC species i in the maximum increment reactions of ozone, M_{ozone} and M_i are the molar mass (g mol^{-1}) of O_3 and VOC species i, respectively.

In this study, OFP was introduced to estimate the photochemical reactivity of VOCs. The comparison of the average mixing ratios~~concentrations~~ of the five VOC groups and their OFP during three cases is shown in Figure 7. VOC~~s~~ mixing ratios~~concentrations~~ of Case 2 were higher than in Case 1 and Case 3, so did OFP level of Case 2. However, it is obvious that the mixing ratio~~concentration~~ of VOC group~~s~~ was not proportional to its OFP. The biggest contribution to VOCs mixing ratios~~concentration~~ here was alkanes (36.4%) and OVOCs (36.3%) in Case 1, while OVOCs (45.4%), alkenes (25.2%) and aromatics (18.6%) were the top three contributing to OFP. In Case 2, the mixing ratio~~concentration~~ of total NMVOCs reached 29.73 ppbv, the main contributors of which were alkanes (accounted for 35.5%) and OVOCs (31.6%), while the top three

contributions to total OFP (96.16 ppbv) were OVOCs (accounted for 36.1%), aromatics (30.4%) and alkenes (21.8%). Our results are consistent with those reported for Beijing in summer 2006 where OVOCs (40%), aromatics (28%) and alkenes (20%) were also the top three contributors (Duan et al., 2008). In Case 3, the NMVOCs mixing ratio~~concentration~~ (12.2 ppbv) and the corresponding OFP (53.7 ppbv) were both at a relatively lower level.

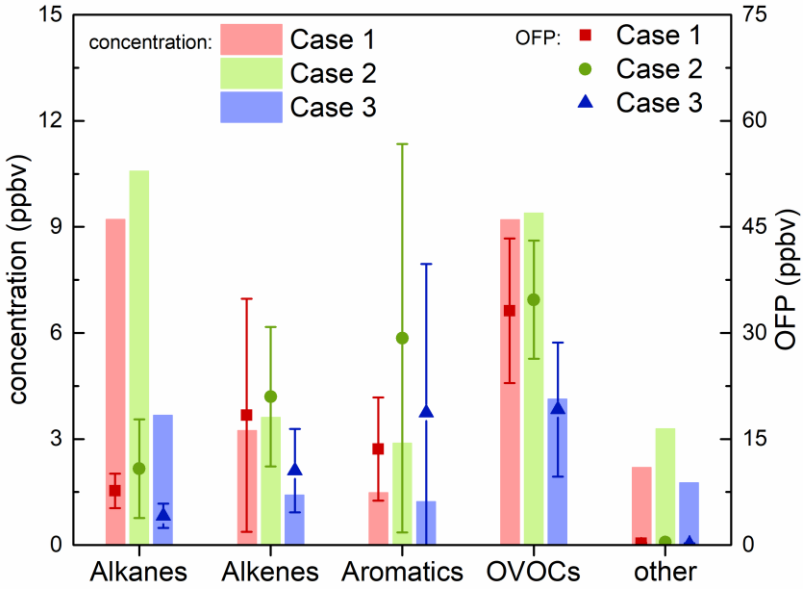

Figure 7. Average mixing ratios~~concentrations~~ and OFP (ozone formation potential) of five VOC groups for the three cases.

According to the comparison between VOC groups mixing ratios~~concentrations~~ and their OFP in Case 1 and Case 2 with relatively high ozone mixing ratios~~concentrations~~, alkanes and OVOCs were the most important contributors to NMVOCs in both cases. Although the mixing ratios~~concentrations~~ of these two groups were comparable in both Case 1 and 2, the contribution of OVOCs to OFP was about 3.5 times that of alkanes, indicating that the reactivity of alkanes is so low that it contributes less to the formation of ozone than other groups. On the contrary, OVOCs show~~s~~ ~~its~~ significant contributions to ozone formation with higher mixing ratios~~concentrations~~ leading to higher OFP. The contribution of aromatics to OFP reached 30.2% in Case 2. At the same time, the contribution of alkenes to ozone generation cannot be ignored, and for example, it reached 26.7% in Case 1. Due to the different composition profile of VOCs, the contribution of VOC to OFP is quite different in the other areas of China. For example, in Shenyang the top three contributors were aromatics (31.2%), alkenes (25.7%) and OVOCs (25.6%) (Ma et al., 2019); OVOCs (34.0-50.8%) dominated OFP in Guangzhou (Yuan et al., 2012); alkenes (48.34%) was the main contributor in Wuhan (Hui et al., 2018), while alkanes, alkenes, and aromatics accounted for 57%, 23%, and 20% in Lanzhou, respectively (Jia et al., 2016).

The top 12 NMVOCs in OFP and their average mixing ratios~~concentrations~~ during the three cases are shown in Fig. 8. These 12 species accounted for 50.90%, 41.63%, and 36.33% of the total NMVOCs observed and contributed about 79.57%, 76.55%, and 75.73% to the ozone formation in the three cases, respectively. As mentioned above, not all high-concentration species had substantial OFP contributions. As shown in Fig. 8, acetone was the third most abundant species in total NMVOCs, accounting for 14.6% of the total NMVOCs mixing ratio, but it only contributed 2.2% to total OFP in Case 1. And m/p-xylene ranked second in the contribution of OFP, accounting for 12.1%, while it represents only 1.8% of total NMVOCs mixing ratio~~concentration~~ in Case 2. The results show that HCHO was the most important OFP contributor, accounting for 35.6%, 23.6%, and 22.1% in each of the three cases, respectively. Under high ozone mixing ratios~~concentrations~~ during Case 1 and Case 2, four of the top five species contributing to OFP were the same, i.e. HCHO, toluene, ethylene and m/p-xylene, while mixing ratio~~concentration~~ and OFP of these four species were at a lower level under the clean conditions in Case 3, indicating that these four species can play a very different role in ozone formation under different chemical conditions. These results are similar to the research in the Pearl River Delta region in 2006 where the top four contributions to OFP were isoprene, m/p-xylene, ethylene and toluene (Zheng et al., 2009). Additionally~~Besides~~, it was found that the total mixing ratios~~concentrations~~ of HCHO, toluene, ethylene and m/p-xylene accounted for only 23.5%, 22.6% and 26.0% of the total NMVOCs, whereas the overall contribution of these four species to OFP was 55.7%, 55.3% and 49.8% in the three cases, respectively. This suggests that controlling different key VOC components is effective to prevent ozone pollution episodes. For instance, by controlling the concentration of these four species in Case 1 to the level of Case 3 (reduced by 2.78 ppbv), the contribution of NMVOCs to OFP would be reduced by nearly 20%.

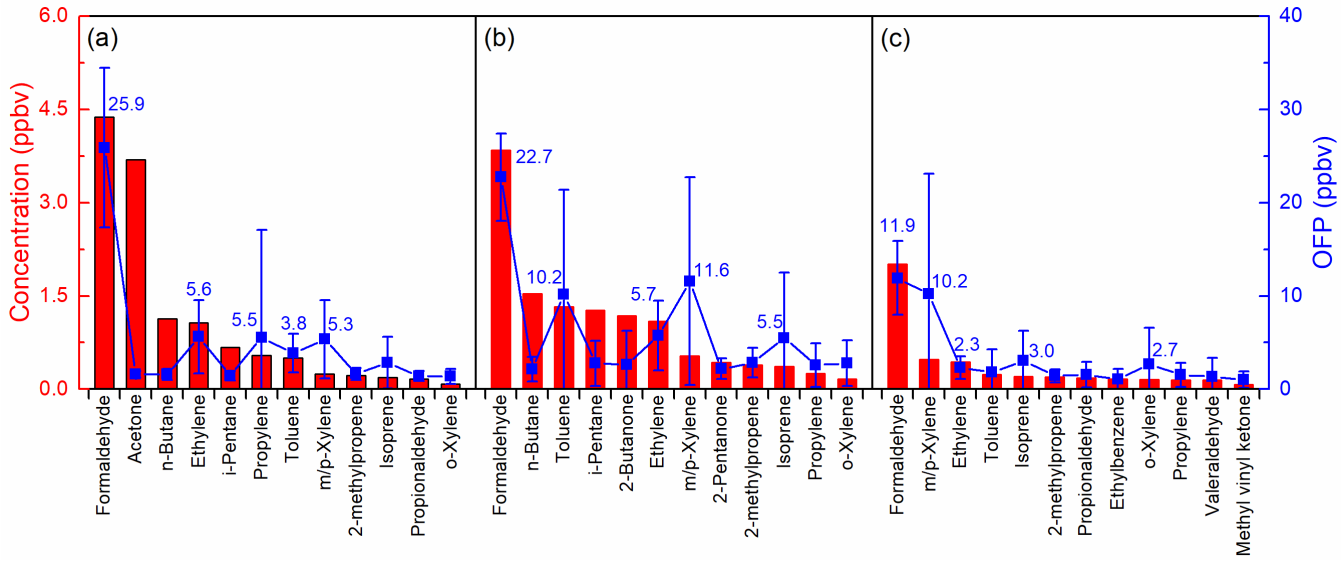

Figure 8. The top 12 NMVOCs in ozone potential formation and their average mixing ratios~~concentrations~~ during (a) Case 1, (b) Case 2 and (c) Case 3 at an urban site of Shanghai.

Summary and Conclusions

We conducted a five-month observational experiment at the Jiangwan Campus of Fudan University in Shanghai from May to September of 2018. Three cases with different ozone mixing ratios~~concentrations~~ were selected for the investigation of atmospheric oxidation capacity and photochemical reactivity. Also, the OBM constrained by a full set of measurement data is applied to evaluate atmospheric oxidation and radical chemistry during the three cases. We presented atmospheric oxidation capacity, OH reactivity, OH chain length, HO_x budget, and the ozone formation potential of observed VOCs, and compared their similarities and differences under the three different scenarios. The atmospheric oxidation capacity was related to pollution levels during the observational period. The different levels of VOCs and NO_x in the three cases resulted in differences in OH reactivity and subsequently in photochemical reactivity. The OH reactivity in Case 2 with a higher mixing ratio~~concentration~~ of ozone precursors (VOCs and NO_x) was the strongest, and CO and alkenes dominated the OH loss. HONO photolysis in the morning and O_3 photolysis in the afternoon dominated HO_x sources. For the sinks of radicals, the reaction of OH with NO_2 dominated HO_x sinks all day, and $HO_2 + HO_2$ and $HO_2 + RO_2$ became important for HO_x sinks under the increase of radical~~s~~ levels in the afternoon. ~~Regrettably, alcohol data were not available, resulting in an underestimation of the calculated contribution of OVOCs to atmospheric photochemistry in this study.~~ Moreover, a longer OH chain length, commonly used to evaluate ozone production efficiency, was found in Case 3, meaning that per NO_x converted into HNO_3 produces more O_3~~each radical generated in Case 3 could produce more ozone~~. Furthermore, according to the OFP calculated in the three cases, formaldehyde, toluene, ethylene, and m/p-xylene were significant for ozone formation in Shanghai. Finally, we conclude that to develop effective O_3 control strategies in Shanghai, the focus should be on controlling key VOC component emissions.

Data availability. Data are available for scientific purposes upon request to the corresponding author.

Author contributions. JZ and SW designed and implemented the research, as well as prepared the manuscript; HW, SJ and SL contributed to the VOCs and photolysis frequency of NO_2 measurements; AS and BZ provided constructive comments and support for the DOAS measurements and observation-based model simulation in this study.

Competing interests. The authors declare that they have no conflict of interest.

Acknowledgments

This research was supported by grants from National Key Research and Development Program of China (2017YFC0210002, 2016YFC0200401, 2018YFC0213801), National Natural Science Foundation of China (41775113, 21777026, 21607104), Shanghai Pujiang Talent Program (17PJC015) and Shanghai Rising-Star Program (18QA1403600). This work was also supported by The Program for Professor of Special Appointment (Eastern Scholar) at Shanghai Institutions of Higher Learning

and Shanghai Thousand Talents Program.

References

Alicke, B., Platt, U., and Stutz, J.: Impact of nitrous acid photolysis on the total hydroxyl radical budget during the Limitation of Oxidant Production/Pianura Padana Produzione di Ozono study in Milan, J. Geophys. Res.-Atmos., 107, 8196, https://doi.org/10.1029/2000jd000075, 2002.

Asaf, D., Pedersen, D., Matveev, V., Peleg, M., Kern, C., Zingler, J., Platt, U., and Luria, M.: Long-term measurements of NO_3 radical at a semiarid urban site: 1. Extreme concentration events and their oxidation capacity, Environ. Sci. Technol., 43, 9117-9123, https://doi.org/10.1021/es900798b, 2009.

Bannan, T. J., Booth, A. M., Bacak, A., Muller, J. B. A., Leather, K. E., Le Breton, M., Jones, B., Young, D., Coe, H., Allan, J., Visser, S., Slowik, J. G., Furger, M., Prévôt, A. S. H., Lee, J., Dunmore, R. E., Hopkins, J. R., Hamilton, J. F., Lewis, A. C., Whalley, L. K., Sharp, T., Stone, D., Heard, D. E., Fleming, Z. L., Leigh, R., Shallcross, D. E., and Percival, C. J.: The first UK measurements of nitryl chloride using a chemical ionization mass spectrometer in central London in the summer of 2012, and an investigation of the role of Cl atom oxidation, J. Geophys. Res.-Atmos., 120, 5638-5657, https://doi.org/10.1002/2014jd022629, 2015.

Bufalini, J. J., and Dodge, M. C.: Ozone-forming potential of light saturated hydrocarbons, Environ. Sci. Technol., 17, 308-311, https://doi.org/10.1021/es00111a013, 1983.

Carter, W. P.: Updated maximum incremental reactivity scale and hydrocarbon bin reactivities for regulatory applications, California Air Resources Board Contract, 07-339, 2010.

Chan, K. L., Wang, S., Liu, C., Zhou, B., Wenig, M. O., and Saiz-Lopez, A.: On the summertime air quality and related photochemical processes in the megacity Shanghai, China, Sci. Total Environ., 580, 974-983, https://doi.org/10.1016/j.scitotenv.2016.12.052, 2017.

Cheng, H., Guo, H., Wang, X., Saunders, S. M., Lam, S. H., Jiang, F., Wang, T., Ding, A., Lee, S., and Ho, K. F.: On the relationship between ozone and its precursors in the Pearl River Delta: application of an observation-based model (OBM), Environ. Sci. Pollut. Res., 17, 547-560, https://doi.org/10.1007/s11356-009-0247-9, 2010.

China, M. E. P.: Ambient air quality standards. GB 3095-2012, China Environmental Science Press, Beijing, 2012.

Coates, J., Mar, K. A., Ojha, N., and Butler, T. M.: The influence of temperature on ozone production under varying NOx conditions – a modelling study, Atmos. Chem. Phys., 16, 11601-11615, https://doi.org/10.5194/acp-16-11601-2016, 2016.

Di Carlo, P., Brune, W. H., Martinez, M., Harder, H., Lesher, R., Ren, X., Thornberry, T., Carroll, M. A., Young, V., and Shepson, P. B.: Missing OH reactivity in a forest: Evidence for unknown reactive biogenic VOCs, Science, 304, 722-725, https://doi.org/10.1126/science.1094392, 2004.

Dolgorouky, C., Gros, V., Sarda-Esteve, R., Sinha, V., Williams, J., Marchand, N., Sauvage, S., Poulain, L., Sciare, J., and Bonsang, B.: Total OH reactivity measurements in Paris during the 2010 MEGAPOLI winter campaign, Atmos. Chem. Phys., 12, 9593-9612, https://doi.org/10.5194/acp-12-9593-2012, 2012.

Duan, J., Tan, J., Yang, L., Wu, S., and Hao, J.: Concentration, sources and ozone formation potential of volatile organic compounds (VOCs) during ozone episode in Beijing, Atmos. Res., 88, 25-35, https://doi.org/10.1016/j.atmosres.2007.09.004, 2008.

Elshorbany, Y. F., Kurtenbach, R., Wiesen, P., Lissi, E., Rubio, M., Villena, G., Gramsch, E., Rickard, A. R., Pilling, M. J., and Kleffmann, J.: Oxidation capacity of the city air of Santiago, Chile, Atmos. Chem. Phys., 9, 2257-2273, https://doi.org/10.5194/acp-9-2257-2009, 2009.

Emmerson, K. M., Carslaw, N., Carslaw, D., Lee, J. D., McFiggans, G., Bloss, W. J., Gravestock, T., Heard, D. E., Hopkins, J., and Ingham, T.: Free radical modelling studies during the UK TORCH Campaign in Summer 2003, Atmos. Chem. Phys., 7, 167-181, https://doi.org/10.1016/j.atmosenv.2006.07.023, 2007.

Feng, T., Zhao, S., Bei, N., Wu, J., Liu, S., Li, X., Liu, L., Qian, Y., Yang, Q., Wang, Y., Zhou, W., Cao, J., and Li, G.: Secondary organic aerosol enhanced by increasing atmospheric oxidizing capacity in Beijing–Tianjin–Hebei (BTH), China, Atmos. Chem. Phys., 19, 7429-7443, https://doi.org/10.5194/acp-19-7429-2019, 2019.

Fuchs, H., Tan, Z., Lu, K., Bohn, B., Broch, S., Brown, S. S., Dong, H., Gomm, S., Häseler, R., He, L., Hofzumahaus, A., Holland, F., Li, X., Liu, Y., Lu, S., Min, K.-E., Rohrer, F., Shao, M., Wang, B., Wang, M., Wu, Y., Zeng, L., Zhang, Y., Wahner, A., and Zhang, Y.: OH reactivity at a rural site (Wangdu) in the North China Plain: contributions from OH reactants and experimental OH budget, Atmos. Chem. Phys., 17, 645-661, https://doi.org/10.5194/acp-17-645-2017, 2017.

Gao, W., Tie, X., Xu, J., Huang, R., Mao, X., Zhou, G., and Chang, L.: Long-term trend of O_3 in a mega City (Shanghai), China: Characteristics, causes, and interactions with precursors, Sci. Total Environ., 603, 425-433, https://doi.org/10.1016/j.scitotenv.2017.06.099, 2017.

Geng, F., Tie, X., Xu, J., Zhou, G., Peng, L., Gao, W., Tang, X., and Zhao, C.: Characterizations of ozone, NO_x, and VOCs measured in Shanghai, China, Atmos. Environ., 42, 6873-6883, https://doi.org/10.1016/j.atmosenv.2008.05.045, 2008.

Geyer, A., Alicke, B., Konrad, S., Schmitz, T., Stutz, J., and Platt, U.: Chemistry and oxidation capacity of the nitrate radical in the continental boundary layer near Berlin, J. Geophys. Res.-Atmos., 106, 8013-8025, https://doi.org/10.1029/2000jd900681, 2001.

Gilman, J. B., Kuster, W. C., Goldan, P. D., Herndon, S. C., Zahniser, M. S., Tucker, S. C., Brewer, W. A., Lerner, B. M., Williams, E. J., Harley, R. A., Fehsenfeld, F. C., Warneke, C., and de Gouw, J. A.: Measurements of volatile organic compounds during the 2006 TexAQS/GoMACCS campaign: Industrial influences, regional characteristics, and diurnal dependencies of the OH reactivity, J. Geophys. Res.-Atmos., 114, D00F06, https://doi.org/10.1029/2008jd011525, 2009.

Guo, H., Jiang, F., Cheng, H. R., Simpson, I. J., Wang, X. M., Ding, A. J., Wang, T. J., Saunders, S. M., Wang, T., Lam, S. H. M., Blake, D. R., Zhang, Y. L., and Xie, M.: Concurrent observations of air pollutants at two sites in the Pearl River Delta and the implication of regional transport, Atmos. Chem. Phys., 9, 7343-7360, https://doi.org/10.5194/acp-9-7343-2009, 2009.

Guo, H., Ling, Z. H., Cheung, K., Jiang, F., Wang, D. W., Simpson, I. J., Barletta, B., Meinardi, S., Wang, T. J., Wang, X. M., Saunders, S. M., and Blake, D. R.: Characterization of photochemical pollution at different elevations in mountainous areas in Hong Kong, Atmos. Chem. Phys., 13, 3881-3898, https://doi.org/10.5194/acp-13-3881-2013, 2013.

Hofzumahaus, A., Rohrer, F., Lu, K., Bohn, B., Brauers, T., Chang, C.-C., Fuchs, H., Holland, F., Kita, K., and Kondo, Y.: Amplified trace gas removal in the troposphere, science, 324, 1702-1704, https://doi.org/10.1126/science.1164566, 2009.

Hui, L., Liu, X., Tan, Q., Feng, M., An, J., Qu, Y., Zhang, Y., and Jiang, M.: Characteristics, source apportionment and contribution of VOCs to ozone formation in Wuhan, Central China, Atmos. Environ., 192, 55-71, https://doi.org/10.1016/j.atmosenv.2018.08.042, 2018.

Hui, L., Liu, X., Tan, Q., Feng, M., An, J., Qu, Y., Zhang, Y., and Cheng, N.: VOC characteristics, sources and contributions to SOA formation during haze events in Wuhan, Central China, Sci. Total Environ., 650, 2624-2639, https://doi.org/10.1016/j.scitotenv.2018.10.029, 2019.

Jenkin, M. E., Saunders, S. M., and Pilling, M. J.: The tropospheric degradation of volatile organic compounds: a protocol for mechanism development, Atmospheric Environment 31, 81-104, https://doi.org/10.1016/S1352-2310(96)00105-7, 1997.

Jenkin, M. E., and Clemitshaw, K. C.: Ozone and other secondary photochemical pollutants: chemical processes governing their formation in the planetary boundary layer, Atmos. Environ., 34, 2499-2527, https://doi.org/10.1016/S1352-2310(99)00478-1, 2000.

Jenkin, M. E., Saunders, S. M., Wagner, V., and Pilling, M. J.: Protocol for the development of the Master Chemical Mechanism, MCM v3 (Part B): tropospheric degradation of aromatic volatile organic compounds, Atmos. Chem. Phys., 3, 181-193, https://doi.org/10.5194/acp-3-181-2003, 2003.

Jia, C., Mao, X., Huang, T., Liang, X., Wang, Y., Shen, Y., Jiang, W., Wang, H., Bai, Z., Ma, M., Yu, Z., Ma, J., and Gao, H.: Non-methane hydrocarbons (NMHCs) and their contribution to ozone formation potential in a petrochemical industrialized city, Northwest China, Atmos. Res., 169, 225-236, https://doi.org/10.1016/j.atmosres.2015.10.006, 2016.

Kanaya, Y., Cao, R., Akimoto, H., Fukuda, M., Komazaki, Y., Yokouchi, Y., Koike, M., Tanimoto, H., Takegawa, N., and Kondo, Y. J. J. o. G. R. A.: Urban photochemistry in central Tokyo: 1. Observed and modeled OH and HO_2 radical concentrations during the winter and summer of 2004, 112, https://doi.org/10.1029/2007JD008670, 2007

Kovacs, T. A., Brune, W. H., Harder, H., Martinez, M., Simpas, J. B., Frost, G. J., Williams, E., Jobson, T., Stroud, C., Young, V., Fried, A., and Wert, B.: Direct measurements of urban OH reactivity during Nashville SOS in summer 1999, J. Environ. Monit., 5, 68-74, https://doi.org/10.1039/b204339d, 2003.

Li, L., Chen, C.-H., Huang, C., Huang, H.-Y., Li, Z.-P., Fu, J. S., Jang, C. J., and Streets, D. G.: Regional air pollution characteristics simulation of O_3 and PM10 over Yangtze River Delta Region, Chinese Environmental Science, 29, 237-245, 2008.

Li, Z., Xue, L., Yang, X., Zha, Q., Tham, Y. J., Yan, C., Louie, P. K., Luk, C. W., Wang, T., and Wang, W.: Oxidizing capacity of the rural atmosphere in Hong Kong, Southern China, Sci. Total Environ., 612, 1114-1122, https://doi.org/10.1016/j.scitotenv.2017.08.310, 2018.

Ling, Z. H., Guo, H., Lam, S. H. M., Saunders, S. M., and Wang, T.: Atmospheric photochemical reactivity and ozone production at two sites in Hong Kong: Application of a Master Chemical Mechanism-photochemical box model, J. Geophys. Res.-Atmos., 119, 10567-10582, https://doi.org/10.1002/2014jd021794, 2014.

Liu, Z., Wang, Y., Gu, D., Zhao, C., Huey, L. G., Stickel, R., Liao, J., Shao, M., Zhu, T., Zeng, L., Amoroso, A., Costabile, F., Chang, C. C., and Liu, S. C.: Summertime photochemistry during CAREBeijing-2007: RO_x budgets and O_3 formation, Atmos. Chem. Phys., 12, 7737-7752, https://doi.org/10.5194/acp-12-7737-2012, 2012.

Lu, K. D., Rohrer, F., Holland, F., Fuchs, H., Bohn, B., Brauers, T., Chang, C. C., Häseler, R., Hu, M., Kita, K., Kondo, Y., Li, X., Lou, S. R., Nehr, S., Shao, M., Zeng, L. M., Wahner, A., Zhang, Y. H., and Hofzumahaus, A.: Observation and modelling of OH and HO_2 concentrations in the Pearl River Delta 2006: a missing OH source in a VOC rich atmosphere, Atmos. Chem. Phys., 12, 1541-1569, https://doi.org/10.5194/acp-12-1541-2012, 2012.

Lu, K. D., Hofzumahaus, A., Holland, F., Bohn, B., Brauers, T., Fuchs, H., Hu, M., Häseler, R., Kita, K., Kondo, Y., Li, X., Lou, S. R., Oebel, A., Shao, M., Zeng, L. M., Wahner, A., Zhu, T., Zhang, Y. H., and Rohrer, F.: Missing OH source in a suburban environment near Beijing: observed and modelled OH and HO_2 concentrations in summer 2006, Atmos. Chem. Phys., 13, 1057-1080, https://doi.org/10.5194/acp-13-1057-2013, 2013.

Ma, J. Z., Chen, Y., Wang, W., Yan, P., Liu, H. J., Yang, S. Y., Hu, Z. J., and Lelieveld, J.: Strong air pollution causes widespread haze-clouds over China, J. Geophys. Res.-Atmos., 115, https://doi.org/10.1029/2009JD013065, 2010.

Ma, J. Z., Wang, W., Chen, Y., Liu, H. J., Yan, P., Ding, G. A., Wang, M. L., Sun, J., and Lelieveld, J.: The IPAC-NC field campaign: a pollution and oxidization pool in the lower atmosphere over Huabei, China, Atmos. Chem. Phys., 12, 3883-3908, https://doi.org/10.5194/acp-12-3883-2012, 2012.

Ma, Z., Liu, C., Zhang, C., Liu, P., Ye, C., Xue, C., Zhao, D., Sun, J., Du, Y., Chai, F., and Mu, Y.: The levels, sources and reactivity of volatile organic compounds in a typical urban area of Northeast China, J. Environ. Sci., 79, 121-134, https://doi.org/10.1016/j.jes.2018.11.015, 2019.

Mao, J., Ren, X., Shuang, C., Brune, W. H., Zhong, C., Martinez, M., Harder, H., Lefer, B., Rappenglück, B., and Flynn, J.: Atmospheric oxidation capacity in the summer of Houston 2006: Comparison with summer measurements in other metropolitan studies, Atmos. Environ., 44, 4107-4115, https://doi.org/10.1016/j.atmosenv.2009.01.013, 2010.

Martinez, M., Harder, H., Kovacs, T. A., Simpas, J. B., Bassis, J., Lesher, R., Brune, W. H., Frost, G. J., Williams, E. J., and Stroud, C. A.: OH and HO_2 concentrations, sources, and loss rates during the Southern Oxidants Study in Nashville, Tennessee, summer 1999, J. Geophys. Res.-Atmos., 108, 4617, https://doi.org/10.1029/2003JD003551, 2003.

Michoud, V., Kukui, A., Camredon, M., Colomb, A., Borbon, A., Miet, K., Aumont, B., Beekmann, M., Durand-Jolibois, R., and Perrier, S.: Radical budget analysis in a suburban European site during the MEGAPOLI summer field campaign, Atmos. Chem. Phys., 12, 11951-11974, https://doi.org/10.5194/acp-12-11951-2012, 2012.

Nan, J., Wang, S., Guo, Y., Xiang, Y., and Zhou, B.: Study on the daytime OH radical and implication for its relationship with fine particles over megacity of Shanghai, China, Atmos. Environ., 154, 167-178, https://doi.org/10.1016/j.atmosenv.2017.01.046, 2017.

National Research Council: Rethinking the ozone problem in urban and regional air pollution, Natl. Acad. Press, Washington, D. C., USA, 1992.

National Bureau of Statistics: China Statistical Yearbook, China Stat. Press, Beijing, 2018.

Prinn, R. G.: The cleansing capacity of the atmosphere, Annu. Rev. Environ. Resour., 28, 29-57, https://doi.org/10.1146/annurev.energy.28.011503.163425, 2003.

Ren, X., Harder, H., Martinez, M., Lesher, R. L., Oliger, A., Shirley, T., Adams, J., Simpas, J. B., and Brune, W. H.: HO_x

concentrations and OH reactivity observations in New York City during PMTACS-NY2001, Atmos. Environ., 37, 3627-3637, https://doi.org/10.1016/S1352-2310(03)00460-6, 2003.

Ren, X., Brune, W. H., Mao, J., Mitchell, M. J., Lesher, R. L., Simpas, J. B., Metcalf, A. R., Schwab, J. J., Cai, C., and Li, Y.: Behavior of OH and HO_2 in the winter atmosphere in New York City, Atmos. Environ., 40, 252-263, https://doi.org/10.1016/j.atmosenv.2005.11.073, 2006.

Ren, X., Olson, J. R., Crawford, J. H., Brune, W. H., Mao, J., Long, R. B., Chen, Z., Chen, G., Avery, M. A., Sachse, G. W., Barrick, J. D., Diskin, G. S., Huey, L. G., Fried, A., Cohen, R. C., Heikes, B., Wennberg, P. O., Singh, H. B., Blake, D. R., and Shetter, R. E.: HO_x chemistry during INTEX-A 2004: Observation, model calculation, and comparison with previous studies, J. Geophys. Res.-Atmos., 113, 2156–2202, https://doi.org/10.1029/2007jd009166, 2008.

Santiago, J.-L., Martilli, A., and Martin, F.: On dry deposition modelling of atmospheric pollutants on vegetation at the microscale: Application to the impact of street vegetation on air quality, Boundary Layer Meteorol., 162, 451-474, https://doi.org/10.1007/s10546-016-0210-5, 2016.

Saunders, S. M., Jenkin, M. E., Derwent, R. G., and Pilling, M. J.: Protocol for the development of the Master Chemical Mechanism, MCM v3 (Part A): tropospheric degradation of non-aromatic volatile organic compounds, Atmos. Chem. Phys., 3, 161-180, https://doi.org/10.5194/acp-3-161-2003, 2003.

Schmitz, T., Hassel, D., and Weber, F.-J.: Determination of VOC-components in the exhaust of gasoline and diesel passenger cars, Atmos. Environ., 34, 4639-4647, https://doi.org/10.1016/s1352-2310(00)00303-4, 2000.

Seinfeld, J. H., and Pandis, S. N.: Atmospheric chemistry and physics: from air pollution to climate change, John Wiley & Sons, 2016.

Sheehy, P. M., Volkamer, R., Molina, L. T., and Molina, M. J.: Oxidative capacity of the Mexico City atmosphere – Part 2: A RO_x radical cycling perspective, Atmos. Chem. Phys., 10, 6993-7008, https://doi.org/10.5194/acp-10-6993-2010, 2010.

Shen, S., Wang, S., and Zhou, B.: Investigation of Atmospheric Formaldehyde and Glyoxal Based on Differential Optical Absorption Spectroscopy, Spectroscopy and Spectral Analysis, 36, 2384-2390, 2016.

Shi, C., Wang, S., Liu, R., Zhou, R., Li, D., Wang, W., Li, Z., Cheng, T., and Zhou, B.: A study of aerosol optical properties during ozone pollution episodes in 2013 over Shanghai, China, Atmos. Res., 153, 235-249, https://doi.org/10.1016/j.atmosres.2014.09.002, 2015.

Sommariva, R., Haggerstone, A. L., Carpenter, L. J., Carslaw, N., Creasey, D. J., Heard, D. E., Lee, J. D., Lewis, A. C., Pilling, M. J., and Zádor, J.: OH and HO_2 chemistry in clean marine air during SOAPEX-2, Atmos. Chem. Phys., 4, 839-856, https://doi.org/10.5194/acp-4-839-2004, 2004.

Tan, Z., Fuchs, H., Lu, K., Hofzumahaus, A., Bohn, B., Broch, S., Dong, H., Gomm, S., Häseler, R., He, L., Holland, F., Li, X., Liu, Y., Lu, S., Rohrer, F., Shao, M., Wang, B., Wang, M., Wu, Y., Zeng, L., Zhang, Y., Wahner, A., and Zhang, Y.: Radical chemistry at a rural site (Wangdu) in the North China Plain: observation and model calculations of OH, HO2 and RO2 radicals, Atmos. Chem. Phys., 17, 663-690, https://doi.org/10.5194/acp-17-663-2017, 2017.

Tan, Z., Lu, K., Hofzumahaus, A., Fuchs, H., Bohn, B., Holland, F., Liu, Y., Rohrer, F., Shao, M., Sun, K., Wu, Y., Zeng, L., Zhang, Y., Zou, Q., Kiendler-Scharr, A., Wahner, A., and Zhang, Y.: Experimental budgets of OH, HO_2, and RO_2 radicals and implications for ozone formation in the Pearl River Delta in China 2014, Atmos. Chem. Phys., 19, 7129-

7150, https://doi.org/10.5194/acp-19-7129-2019, 2019a.

Tan, Z., Lu, K., Jiang, M., Su, R., Wang, H., Lou, S., Fu, Q., Zhai, C., Tan, Q., Yue, D., Chen, D., Wang, Z., Xie, S., Zeng, L., and Zhang, Y.: Daytime atmospheric oxidation capacity in four Chinese megacities during the photochemically polluted season: a case study based on box model simulation, Atmos. Chem. Phys., 19, 3493-3513, https://doi.org/10.5194/acp-19-3493-2019, 2019b.

Tie, X., Geng, F., Peng, L., Gao, W., and Zhao, C.: Measurement and modeling of O_3 variability in Shanghai, China: Application of the WRF-Chem model, Atmos. Environ., 43, 4289-4302, https://doi.org/10.1016/j.atmosenv.2009.06.008, 2009.

Tie, X., Geng, F., Guenther, A., Cao, J., Greenberg, J., Zhang, R., Apel, E., Li, G., Weinheimer, A., Chen, J., and Cai, C.: Megacity impacts on regional ozone formation: observations and WRF-Chem modeling for the MIRAGE-Shanghai field campaign, Atmos. Chem. Phys., 13, 5655-5669, https://doi.org/10.5194/acp-13-5655-2013, 2013.

Wang, S., Nan, J., Shi, C., Fu, Q., Gao, S., Wang, D., Cui, H., Saiz-Lopez, A., and Zhou, B.: Atmospheric ammonia and its impacts on regional air quality over the megacity of Shanghai, China, Sci. Rep., 5, 15842, https://doi.org/10.1038/srep15842, 2015.

Wang, T., Ding, A., Gao, J., and Wu, W. S.: Strong ozone production in urban plumes from Beijing, China, Geophys. Res. Lett., 33, L21806, https://doi.org/10.1029/2006gl027689, 2006.

Wang, T., Nie, W., Gao, J., Xue, L. K., Gao, X. M., Wang, X. F., Qiu, J., Poon, C. N., Meinardi, S., Blake, D., Wang, S. L., Ding, A. J., Chai, F. H., Zhang, Q. Z., and Wang, W. X.: Air quality during the 2008 Beijing Olympics: secondary pollutants and regional impact, Atmos. Chem. Phys., 10, 7603-7615, https://doi.org/10.5194/acp-10-7603-2010, 2010.

Wang, T., Xue, L., Brimblecombe, P., Lam, Y. F., Li, L., and Zhang, L.: Ozone pollution in China: A review of concentrations, meteorological influences, chemical precursors, and effects, Sci. Total Environ., 575, 1582-1596, https://doi.org/10.1016/j.scitotenv.2016.10.081, 2017.

Wang, Y., Guo, H., Zou, S., Lyu, X., Ling, Z., Cheng, H., and Zeren, Y.: Surface O3 photochemistry over the South China Sea: Application of a near-explicit chemical mechanism box model, Environ. Pollut., 234, 155-166, https://doi.org/10.1016/j.envpol.2017.11.001, 2018.

Wood, E. C., Herndon, S. C., Onasch, T. B., Kroll, J. H., Canagaratna, M. R., Kolb, C. E., Worsnop, D. R., Neuman, J. A., Seila, R., and Zavala, M.: A case study of ozone production, nitrogen oxides, and the radical budget in Mexico City, Atmos. Chem. Phys., 9, 2499-2516, https://doi.org/10.5194/acp-9-2499-2009, 2009.

Whalley, L. K., Stone, D., Bandy, B., Dunmore, R., Hamilton, J. F., Hopkins, J., Lee, J. D., Lewis, A. C., and Heard, D. E.: Atmospheric OH reactivity in central London: observations, model predictions and estimates of in situ ozone production, Atmos. Chem. Phys., 16, 2109-2122, https://doi.org/10.5194/acp-16-2109-2016, 2016.

Whalley, L. K., Stone, D., Dunmore, R., Hamilton, J., Hopkins, J. R., Lee, J. D., Lewis, A. C., Williams, P., Kleffmann, J., Laufs, S., Woodward-Massey, R., and Heard, D. E.: Understanding in situ ozone production in the summertime through radical observations and modelling studies during the Clean air for London project (ClearfLo), Atmos. Chem. Phys., 18, 2547-2571, https://doi.org/10.5194/acp-18-2547-2018, 2018.

~~Wood, E. C., Herndon, S. C., Onasch, T. B., Kroll, J. H., Canagaratna, M. R., Kolb, C. E., Worsnop, D. R., Neuman, J. A., Seila, R., and Zavala, M.: A case study of ozone production, nitrogen oxides, and the radical budget in Mexico City,~~

Atmos. Chem. Phys., 9, 2499-2516, https://doi.org/10.5194/acp-9-2499-2009, 2009.

Xing, J., Wang, J., Mathur, R., Wang, S., Sarwar, G., Pleim, J., Hogrefe, C., Zhang, Y., Jiang, J., Wong, D. C., and Hao, J.: Impacts of aerosol direct effects on tropospheric ozone through changes in atmospheric dynamics and photolysis rates, Atmos Chem Phys, 17, 9869-9883, https://doi.org/10.5194/acp-17-9869-2017, 2017.

Xu, J., Tie, X., Gao, W., Lin, Y., and Fu, Q.: Measurement and model analyses of the ozone variation during 2006 to 2015 and its response to emission change in megacity Shanghai, China, Atmos. Chem. Phys., 19, 9017-9035, https://doi.org/10.5194/acp-19-9017-2019, 2019.

Xue, L., Gu, R., Wang, T., Wang, X., Saunders, S., Blake, D., Louie, P. K. K., Luk, C. W. Y., Simpson, I., and Xu, Z.: Oxidative capacity and radical chemistry in the polluted atmosphere of Hong Kong and Pearl River Delta region: analysis of a severe photochemical smog episode, Atmos. Chem. Phys., 9891-9903, https://doi.org/10.5194/acp-16-9891-2016, 2016.

Yoshino, A., Sadanaga, Y., Watanabe, K., Kato, S., Miyakawa, Y., Matsumoto, J., and Kajii, Y.: Measurement of total OH reactivity by laser-induced pump and probe technique—comprehensive observations in the urban atmosphere of Tokyo, Atmos. Environ., 40, 7869-7881, https://doi.org/10.1016/j.atmosenv.2006.07.023, 2006.

Yuan, B., Chen, W., Shao, M., Wang, M., Lu, S., Wang, B., Liu, Y., Chang, C.-C., and Wang, B.: Measurements of ambient hydrocarbons and carbonyls in the Pearl River Delta (PRD), China, Atmos. Res., 116, 93-104, https://doi.org/10.1016/j.atmosres.2012.03.006, 2012.

Zhang, J., Wang, T., Chameides, W. L., Cardelino, C., Kwok, J., Blake, D. R., Ding, A., and So, K. L.: Ozone production and hydrocarbon reactivity in Hong Kong, Southern China, Atmos. Chem. Phys., 7, 557-573, https://doi.org/10.5194/acp-7-557-2007, 2007.

Zhang, L., Wang, T., Zhang, Q., Zheng, J., Xu, Z., and Lv, M.: Potential sources of nitrous acid (HONO) and their impacts on ozone: A WRF-Chem study in a polluted subtropical region, J. Geophys. Res.-Atmos., 121, 3645-3662, https://doi.org/10.1002/2015jd024468, 2016.

Zhao, H., Wang, S., Wang, W., Liu, R., and Zhou, B.: Investigation of Ground-Level Ozone and High-Pollution Episodes in a Megacity of Eastern China, PLoS One, 10, e0131878, https://doi.org/10.1371/journal.pone.0131878, 2015.

Zheng, J., Shao, M., Che, W., Zhang, L., Zhong, L., Zhang, Y., and Streets, D.: Speciated VOC emission inventory and spatial patterns of ozone formation potential in the Pearl River Delta, China, Environ. Sci. Technol., 43, 8580-8586, https://doi.org/10.1021/es901688e, 2009.